



Pipe Wall Condition Assessment and Leak  
Detection using Paired Pressure Sensors with  
Hydraulic Transient Analysis

He Shi

B.Eng., M.Eng.

March 2019

Thesis submitted in fulfilment of the requirements for the degree  
of Doctor of Philosophy

The University of Adelaide

Faculty of Engineering, Computer and Mathematical Sciences  
School of Civil, Environmental and Mining Engineering

Copyright© 2019



# Abstract

This PhD research has developed new measurement strategies and analysis techniques to enable hydraulic transient-based condition assessment of targeted pipe sections in complex pipe systems. The conventional practice of hydraulic transient-based pipeline condition assessment involves analysis of signals from a single pressure sensor located at each measurement site. Although multiple measurement sites can be used, they are typically far apart from each other since the access points (e.g. air valves or fire hydrants) are usually sparsely located. The pressure measurement obtained from a single sensor is a superposition of reflections coming from both upstream and downstream of the sensor. This superposition makes the measured wave reflections often too complex to analyse, especially in complex pipe systems where multiple features (e.g. deteriorated sections, branches and cross-connections, and other unknown features) often exist in the pipe section of interest.

The research presented in this thesis has proposed a dual-sensor measurement strategy that uses two closely placed pressure sensors at a measurement site, and has developed a wave separation algorithm that enables the extraction of the two directional pressure waves travelling upstream and downstream. The wave separation can significantly simplify the signal to be analysed, and the unprecedented directional information enables advanced condition assessment techniques to be developed. Numerical and experimental verification has been conducted, with an application to pipe wall condition assessment.

In the experimental verification, conventional flush-mounted pressure transducers have been used by connecting through closely located tapping points on the pipe wall. In addition, a customised in-pipe fibre optic pressure sensor array has been developed and tested in the laboratory, as a step towards real-world implementation. The sensor array cable can be inserted into a pipe through a single access point, avoiding the use of multiple tapping points. Complexities introduced by the in-pipe cable have been investigated, and accordingly, adjustments to the wave separation and wall condition assessment techniques have been made.

The wave separation technique has been further developed by using a two-source-four-sensor transient testing configuration to enable the virtual isolation of a targeted pipe section in complex systems. Two dual-sensor units (i.e. two pairs of pressure sensors) are used to bracket the targeted pipe section, with the two sensors in each pair being located in close proximity. Two transient pressure wave generators are used, which bracket the four sensors and the “virtually” isolated pipe section. This measurement strategy enables the extraction of the transfer matrix of the “virtually” isolated pipe section, which is a full representation of the characteristics of this section independent from any complexities outside the section bounded by the sensors. A novel leak detection technique has been developed based on the analysis of the extracted transfer matrix, and has been validated by numerical simulation. The technique determines the leak location and impedance (related to the leak size), and it is applicable to the detection of multiple leaks.

# Statement of Originality

I certify that this work contains no material which has been accepted for the award of any other degree or diploma in my name, in any university or other tertiary institution and, to the best of my knowledge and belief, contains no material previously published or written by another person, except where due reference has been made in the text. In addition, I certify that no part of this work will, in the future, be used in a submission in my name, for any other degree or diploma in any university or other tertiary institution without the prior approval of the University of Adelaide and where applicable, any partner institution responsible for the joint-award of this degree.

I acknowledge that copyright of published works contained within this thesis resides with the copyright holder(s) of those works.

I also give permission for the digital version of my thesis to be made available on the web, via the University's digital research repository, the Library Search and also through web search engines, unless permission has been granted by the University to restrict access for a period of time.

I acknowledge the support I have received for my research through the provision of an Australian Government Research Training Program Scholarship.

Signed: ..... Date: *26/03/2019* .....

This page is intentionally left blank.

# **Acknowledgments**

I first express my gratitude to my supervisors, Prof. Martin Lambert, Prof. Angus Simpson and Dr. Aaron Zecchin for their supervision and mentoring during my PhD study. They have always been supportive and caring. I also appreciate the academic guidance and help provided by senior research fellow Dr. Jinzhe Gong.

I thank my research collaborators Prof. John Arkwright, Mr Anthony Papageorgiou and Mr Peter Cook at Flinders University for their support on the development of the in-pipe fibre optic sensor array used in my research. I also thank Dr Gretel M. Png, Mr Brenton Howie and Mr Simon Golding at the University of Adelaide for their support on some of my laboratory work.

I thank my fellow postgraduate students in the School of Civil, Environmental and Mining Engineering for the friendship and accompany. I also thank all the staff in the School for their support and help.

I thank my husband and my parents for their support and encouragement. My PhD journey has been challenging due to family and work commitments. Their support and understanding have been critical to the completion of my study. I also thank my son Keming for bringing joy and happiness during my PhD period.

This page is intentionally left blank



# Table of Contents

Abstract.....	I
Statement of Originality.....	III
Acknowledgments .....	V
Table of Contents.....	VII
List of Publications .....	XI
List of Tables .....	XIII
List of Figures.....	XV
<b>Chapter 1</b> .....	<b>1</b>
Introduction.....	1
1.1    Structural deterioration of water supply systems and associated challenges	1
1.2    Conventional techniques for pipeline condition assessment.....	3
1.2.1    Acoustic and ultrasonic methods .....	3
1.2.2    Electromagnetic methods.....	5
1.2.3    Optical methods .....	6
1.3    Hydraulic transient-based techniques for pipeline condition assessment ....	6
1.3.1    Transient-based techniques for pipe leak detection .....	7
1.4    Transient-based technique for pipe wall condition assessment .....	11
1.4.1    Detection of thinner-walled pipe sections.....	11
1.4.2    Detection of extended blockages .....	13

1.5	Key challenges to address .....	14
1.6	Research objectives .....	16
1.7	Organisation of the thesis .....	18
<b>Chapter 2</b>	.....	<b>23</b>
Hydraulic Transient Wave Separation Algorithm using a Dual-sensor with Applications to Pipeline Condition Assessment..... 23		
2.1	Introduction .....	29
2.2	Wave separation algorithm using a dual-sensor .....	33
2.2.1	Hydraulic wave propagation theory .....	33
2.2.2	Determination of the transfer function $H(s)$ .....	37
2.2.3	The wave separation algorithm.....	40
2.3	Numerical verification.....	43
2.3.1	System layout and procedure.....	43
2.3.2	Wave separation results .....	47
2.4	Experimental verification .....	50
2.4.1	System layout and procedure.....	51
2.4.2	Wave separation results .....	53
2.4.3	Application to pipeline condition assessment.....	57
2.5	Discussion.....	60
2.5.1	Detection resolution.....	60
2.5.2	Detection range.....	61
2.5.3	Non-uniform deterioration.....	61
2.5.4	Other sources of reflections .....	62

2.5.5	Accuracy of transfer function .....	62
2.6	Conclusions.....	62
<b>Chapter 3</b>	.....	<b>65</b>
Leak detection in virtually isolated pipe sections within a complex pipe system using a two-source-four-sensor transient testing configuration..... 65		
3.1	Introduction.....	71
3.2	Transfer matrix extraction for a targeted pipe section .....	76
3.2.1	Transfer matrix of a uniform pipe section .....	76
3.2.2	Two-source-four-sensor testing strategy for water pipes.....	77
3.2.3	Determination of the transfer matrix using pressure measurements ..	79
3.3	Leak detection for a targeted pipe section using transfer matrix .....	81
3.3.1	Transfer matrix for a pipe section with leaks.....	81
3.3.2	Extraction of the leak-induced feature.....	83
3.3.3	Determination of the leak location and size.....	86
3.4	Numerical simulations .....	88
3.4.1	Case 1: A single pipe with two leaks .....	88
3.4.2	Case 2: A pipe section in a pipe network.....	94
3.5	Discussion.....	99
3.5.1	Effect of friction.....	99
3.5.2	Challenges in field application.....	100
3.6	Conclusions.....	102
<b>Chapter 4</b>	.....	<b>105</b>

Wave separation and pipeline condition assessment using in-pipe fibre optic pressure sensors .....	105
4.1    Introduction .....	111
4.2    In-pipe fibre optic transient pressure sensor array.....	114
4.3    Laboratory experiments.....	115
4.3.1    Experimental apparatus .....	115
4.3.2    Pressure measurements and simulations.....	118
4.4    Wave Separation.....	121
4.4.1    Directional pressure waves .....	121
4.4.2    Discussion.....	125
4.5    Pipe wall condition assessment .....	126
4.5.1    Methodology.....	126
4.5.2    Application and verification .....	128
4.6    Conclusions .....	130
<b>Chapter 5</b> .....	133
Conclusions .....	133
5.1    Research outcomes .....	133
5.2    Research contributions .....	135
5.3    Future work .....	137
<b>References</b> .....	139

# List of Publications

The following journal papers and conference papers are the outcomes of this research.

## Journal papers

- 1) Shi, H., Gong, J., Zecchin, A. C., Lambert, M. F., and Simpson, A. R. (2017). "Hydraulic transient wave separation algorithm using a dual-sensor with applications to pipeline condition assessment." *Journal of Hydroinformatics*, 19(5), 752-765, [10.2166/hydro.2017.146](https://doi.org/10.2166/hydro.2017.146).
- 2) Shi, H., Gong, J., Simpson, A. R., Zecchin, A. C., and Lambert, M. F. (2019). "Leak detection in virtually isolated pipe sections within a complex pipe system using a two-source-four-sensor transient testing configuration." *Journal of Hydraulic Engineering*, under review.
- 3) Shi, H., Gong, J., Cook, P. R., Arkwright, J. W., Png, G. M., Lambert, M. F., Zecchin, A. C., and Simpson, A. R. (2019). "Wave separation and pipeline condition assessment using in-pipe fibre optic pressure sensors." *Journal of Hydroinformatics*, 21(2), 371-379, [10.2166/hydro.2019.051](https://doi.org/10.2166/hydro.2019.051).

**Conference paper**

- 4) Shi, H., Gong, J., Arkwright, J. W., Papageorgiou, A. W., Lambert, M. F., Simpson, A. R., and Zecchin, A. C. (2015). "Transient pressure measurement in pipelines using optical fibre sensor." *Proceedings of the 40th Australian Conference on Optical Fibre Technology*, Engineers Australia, Barton, ACT, Australia.

# List of Tables

Table 2.1 Physical details of the pipe sections used in the numerical simulations...	45
Table 2.2 Physical details of the pipeline system used in the laboratory experiments. .....	52
Table 3.1 System information for Case 1.....	89
Table 3.2 System information for Case 2.....	95
Table 4.1 Physical details of the pipeline system used in the laboratory experiments. .....	117
Table 4.2 Pipe impedance determined from the directional pressure wave coming from the upstream side of the dual-sensor and propagating towards the dead-end [Figure 4.6(a)].....	129

This page is intentionally left blank



# List of Figures

Figure 1.1 Schematic diagram showing the current transient pressure measurement strategy used in the field..... 15

Figure 2.1 (a) Proposed configuration for the pressure transient test with a dual-sensor in a pipeline; and (b) corresponding block diagram in the frequency domain illustrating the wave propagation. (Note, LTI System = Linear Time Invariant System)..... 35

Figure 2.2 Layout of the pipeline system used in the numerical simulations (not to scale). See Table 2.1 for physical details. .... 45

Figure 2.3 (a) Numerical pressure traces measured at  $T_1$  and  $T_2$ ; and (b) Enlarged view of the wave reflections from deteriorated sections in the numerical study. .... 47

Figure 2.4 (a) Directional reflected pressure waves travelling from upstream to downstream; and (b) Directional reflected pressure waves travelling from downstream to upstream..... 50

Figure 2.5 System layout of the experimental pipeline system. .... 51

Figure 2.6 (a) Original pressure traces measured in the laboratory experiments; and (b) pressure oscillations before the first boundary reflection. .... 54

Figure 2.7 Amplitude spectrum of the reflected waves. .... 55

Figure 2.8 (a) Directional reflected pressure waves travelling towards the closed in-line valve; and (b) directional reflected pressure waves travelling towards the tank. .... 56

Figure 2.9 Comparison between the original wave reflections measured at  $T_1$  (the solid line) and the superimposed result of the determined directional wave reflections (the dashed line). .....57

Figure 2.10 Relationship between the normalized wave reflection ( $p_n$ ) and the relative change in the wall thickness ( $e_{rc}$ ) for the experimental pipeline. ....58

Figure 3.1 Test configuration for extracting the transfer matrix of a targeted pipe section with  $N$  leaks. ....78

Figure 3.2 Layout of the single pipeline system in Case 1. ....88

Figure 3.3 Pressure responses at  $T_A$  and  $T_D$  as obtained from transient test 1 (using generator G1) in Case 1. ....90

Figure 3.4 Imaginary part of transfer matrix element  $U_{22}$  as obtained from numerical simulations and the transfer matrix extraction technique for the pipe section with two leaks in Case 1 (solid line), compared with the theoretical result for the same pipe section with two leaks (dotted line), and the theoretical result for the pipe section when it is intact (dashed line). ....92

Figure 3.5 Imaginary part of  $(U_{22} - U_{11})$  as obtained from numerical simulations and the transfer matrix extraction technique for the pipe section with two leaks in Case 1 (solid line), and the theoretical result for the same pipe section with two leaks (dotted line). ....93

Figure 3.6 Results from the proposed leak detection technique showing the existence of two leaks (indicated by the two spikes), their normalised locations and the corresponding values of impedance ratio (pipe to leak). ....94

Figure 3.7 Layout of the simple pipe network in Case 2. ....95

Figure 3.8 Pressure responses at  $T_A$  as obtained from transient test 1 (using generator G1) in Case 2. ....97

Figure 3.9 Imaginary part of  $(U_{22} - U_{11})$  as obtained from numerical simulations and the proposed transfer matrix extraction technique for the pipe section with one leak in Case 2 (solid line), and the theoretical result for the same pipe section with one leak (dotted line). ..... 98

Figure 3.10 Results from the proposed leak detection technique showing the existence of one leaks (indicated by the single spike), the normalised leak location and the corresponding value of impedance ratio (pipe to leak). 98

Figure 4.1 Schematic of the in-pipe fibre optic sensor cable. .... 115

Figure 4.2 Schematic of the Fibre Bragg Grating (FBG) pressure sensor..... 115

Figure 4.3 Layout of the experimental pipeline system. .... 116

Figure 4.4 Transient pressure responses from conventional sensor T2 (laboratory results with and without the present of fibre sensor cable, and numerical results) and from fibre optic sensor FBG3 (fibre sensor cable in pipe).. 120

Figure 4.5 Transient pressure measurements from FBG2 and FBG3. .... 123

Figure 4.6 Wave separation results obtained from numerical simulations, fibre optic sensors (FBG2 and FBG3) and conventional sensors (T1 and T2): (a) wave reflections from the upstream side of the dual-sensor and propagating towards the dead-end; and (b) wave reflections from the downstream side of the dual-sensor and propagating towards the tank. .... 124

This page is intentionally left blank

# Chapter 1

## Introduction

### 1.1 Structural deterioration of water supply systems and associated challenges

Water distribution systems (WDS) are fundamental to modern civilisation; however, the sustainable management of large scale WDSs is a global challenge. In Australia, despite the fact that water authorities spend about AU\$4 billion in capital expenditure every year, an estimated 19,000 breaks in water mains occur annually, resulting in the loss of more than 265 GL of potable water (Bureau of Meteorology 2016). Almost all developed countries face the same problem due to the ageing of their water infrastructure. For example, in the US, it is estimated that more than US\$1 trillion will be required between 2011 to 2035 to replace ageing water mains and address projected growth (American Water Works Association 2012).

The majority of a water distribution system (WDS) infrastructure consists of pipelines that form complex networks. During construction, the structural integrity of pipeline systems can be compromised due to improper handling and poor workmanship (Gould et al. 2016). After commissioning, pipelines suffer from structural deterioration due to various sources such as traffic loading

(Rakitin and Xu 2015), ground movement (Tucker 2010), corrosion (Świetlik et al. 2012), biological activity (Beech and Sunner 2004), and excessive hydraulic transient activity (Rezaei et al. 2015).

Leakage in WDSs is a global issue, and the leakage rate ranges from about 10% in well-maintained WDSs (Beuken et al. 2006) to above 50% in poorly managed systems (Mutikanga et al. 2009). The annual potable water loss in Australia (265 GL) is equivalent to the annual consumption of 1.5 million homes and represents a value over \$700 million. Leaking water pipes also impose risks to public health, since polluted water with harmful bacteria may enter into the system through the leak openings during low pressure events (Mora-Rodríguez et al. 2014). Structurally deteriorated pipe sections will also result in pipe bursts, which damage properties and interrupt traffic. The economic cost of pipe bursts is staggering. As shown by an investigation in the US, the average cost of a single large diameter (greater than 500 mm) water main failure is about US\$1.7 million (Gaewski and Blaha 2007).

The deterioration of water pipelines is not uniform, and faults are difficult to detect due to the sheer scale of the pipe network and the fact that most pipes are buried underground. Due to a lack of information on the actual condition of pipes, current asset management practice is often reactive and on the basis of standard economic life: typically remedial actions are taken only after pipe bursts or service interruptions have occurred; and pipeline replacement programs are often guided by indicative surrogate factors, such the age of the pipe and the number of historical pipe bursts. The current practice is not sustainable. For example, Water Corporation of Western Australia predicts that

the potential cost for replacing water pipes in the metropolitan area of Perth alone will reach almost AU\$1 billion in 2050-59, which is an increase of more than a factor of 12 compared to the cost of AU\$76.5 million in 2010-19 (Water Corporation WA 2014).

Better and more sustainable strategies for pipe asset management are urgently needed, which has to be guided by the actual pipe condition and the risk of pipe failure, such that high-risk pipes are replaced in time while the useful life of pipes in reasonable condition is extended. Cost-effective pipeline condition assessment is essential to obtain the critical information of pipe condition and failure risk. However, current technologies all have limitations, and more advanced pipeline condition assessment technologies need to be developed.

## **1.2 Conventional techniques for pipeline condition assessment**

There are several pipe leak detection and wall condition assessment techniques available in the market; however, none of them can achieve cost-effective condition assessment for long distance pipe systems or pipe networks. The conventional techniques can be categorised into three groups: *acoustic and ultrasonic methods*, *electromagnetic methods* and *optical methods*.

### **1.2.1 Acoustic and ultrasonic methods**

Acoustic methods are traditionally used for leak detection in pipelines. Two acoustic sensors (e.g. hydrophones or accelerometers) placed in different locations are used to measure leak-induced acoustic signals, then a software algorithm is used to calculate the cross-correlation function of the two leak

signals to determine the location of the leak (Fuchs and Riehle 1991). Leak detection using acoustic correlators can only cover a limited distance in one test (typically less than 100 m), and is ineffective in plastic pipes, where acoustic signals attenuate much more quickly than in metallic pipes (Muggleton and Brennan 2004).

Acoustic measurement and correlation analysis have also been used for pipeline condition assessment through wave speed analysis. The acoustic wave speed analysis uses a correlation method to calculate the average wave speed in a pipe section bounded by two acoustic sensors, from which the average pipe wall thickness is then calculated (Bracken et al. 2010). However, the average wave speed can be misleading if the section of pipe includes unregistered reaches with a much lower wave speed. For example, a polyvinyl chloride (PVC) pipe has a much lower wave speed than that of a metal or asbestos cement (AC) pipe, and the existence of an undocumented PVC replacement would result in a low average wave speed even though the metal or AC parts are in good condition.

Ultrasonic-based pipeline condition assessment methods involve generating ultrasonic waves and measuring the wave reflections. For localised pipe wall thickness detection, an ultrasonic transmitter sends an ultrasonic ping and the signals reflected from the external and internal surfaces of the pipe wall are measured. The time between the two reflections is used to compute the thickness of the pipe wall (Liu and Kleiner 2012). For extended detection, guided wave ultrasound methods, in which the ultrasonic waves propagate along the axial direction of a pipe and the propagation and reflection are guided by the pipe wall, have been developed for detecting cracks along the pipe wall



(Lowe et al. 1998; Demma et al. 2004). However, the range of detection is typically very limited due to fast signal dissipation and the complexities in the wave reflection, especially for pipes buried underground (Liu and Kleiner 2013).

### **1.2.2 Electromagnetic methods**

Electromagnetic pipeline condition assessment methods include techniques using magnetic flux leakage (MFL), remote field eddy current (RFEC), broadband electromagnetic (BEM) and ground penetrating radar (GPR) (Liu and Kleiner 2012). The MFL method uses strong magnets to induce a saturated magnetic field around a short section of ferrous pipe wall. If the pipe section contains damaged areas, a magnetic sensor detects the flux leakage from the air.

The RFEC and BEM both use eddy current based techniques. A transmitter coil creates a current to the pipe surface, which generates a magnetic field. Flux lines from the magnetic field pass through the metallic pipe wall, and generate a voltage across it. The voltage produces eddy currents in the pipe wall, which induce a secondary magnetic field. Wall thickness is indirectly estimated by measuring signal attenuation and phase delay of the secondary magnetic field. RFEC methods use relatively low frequencies for testing, and the BEM techniques transmit a signal that covers a broad frequency spectrum.

The MFL, RFEC and BEM can only be used for fault detection in ferrous pipes. They require excavation and pipe wall cleaning, and each test can only cover a few metres of pipe. For practical applications, the limited spatial extent of these methods means that only a few spatial points along a pipeline can be tested. As

a result, highly approximate statistical inference methods are used to estimate the condition of a pipe based on these few points. GPR methods (Costello et al. 2007; Donazzolo and Yelf 2010) use electromagnetic wave pulses and their reflections to identify the interface between different material layers. The GRP technique can locate water pipe of all types of materials, but for buried pipes the resolution is not enough for pipe wall condition assessment.

### **1.2.3 Optical methods**

Closed-circuit television (CCTV) (Jo et al. 2010) inspection and the laser scanning (Duran et al. 2003) technique are two well-adopted optical methods for the inspection of a pipe's inner surface. These methods introduce a carrier with the CCTV camera or laser sensors into the pipe via an access point. The moving velocity and sampling rate of the carrier determine the resolution and affect the accuracy of the scanning. The inspection is complicated by the roughness as well as the colour of the pipe surface. Currently, available optical inspection systems are intrusive, costly and only used in de-watered pipes (Tur and Garthwaite 2010).

## **1.3 Hydraulic transient-based techniques for pipeline condition assessment**

Research in the past three decades has demonstrated that controlled hydraulic transient pressure waves, also known as water hammer waves, can be used as a tool for pipeline condition assessment. This process is similar to the use of sonar waves to detect remote objects within marine environments. As a pressure wave propagates along a pressurised water pipeline at a high speed (typically 1000 to

1200 m/s in water-filled metallic pipes, and 800 to 1000 m/s in asbestos cement pipes), part of the wave energy is reflected at pipe sections where the structural properties of the pipe cross-section changes (e.g. due to leaks, spalling of cement-mortar lining, or internal and/or external corrosion). This results in the creation of wave reflections that can be observed by appropriately placed pressure sensors, and then analysed by appropriate computer algorithms. Measurement and analysis of these reflections enables a diagnosis of the pipeline condition. A number of hydraulic transient based techniques have been developed and those for leak detection and pipe wall condition assessment are reviewed in the following sub-sections.

### **1.3.1 Transient-based techniques for pipe leak detection**

Transient based pipeline leak detection methods can be generally divided into three categories: *time-domain-reflectometry (TDR) methods*, *inverse transient analysis (ITA) methods* and *frequency domain methods*.

#### ***Leak detection using time-domain-reflectometry***

TDR-based leak detection techniques analyse leak-induced wave reflections directly in their raw form, or analyse the transformed impulse response function (IRF). The direct wave reflection analysis uses the magnitude of a pressure wave reflection to determine the leak size and uses the arrival time to estimate its location (Brunone 1999; Lee et al. 2007a). However, the leak-induced reflections can be difficult to identify when the pressure response is complex due to background noise or the existence of multiple features.

The use of IRFs is an improvement over the direct wave reflection analysis. The pipe system's IRF is independent of the waveform of the input signal, and leak-induced reflections are represented by spikes in the IRF response (Liou 1998; Vítkovský et al. 2003; Kim 2005; Lee et al. 2007b). This help to enhance the accuracy in localisation. Recent work has shown that the use of pseudo random sequences and advanced signal processing techniques can enhance the robustness and accuracy of pipeline IRF extraction (Nguyen et al. 2018). However, the leak-induced spikes are typically rather small in the IRF, and the method may still encounter challenges when applied to real pipelines with multiple features and complex wave responses.

### ***Leak detection using inverse transient analysis***

Pudar and Liggett (1992) first proposed that leaks may be detected by solving an inverse problem to match the measurement of steady-state pressure and flow at multiple locations. Liggett and Chen (1994) extended the steady-state work to transient measurement and analysis, and the technique is known as the inverse transient analysis (ITA) method. ITA methods inversely calibrate a numerical pipeline model by minimising the calculated and measured transient pressure responses, and the pipe numerical model providing the best match is considered as the most likely representation of the real pipe system (Vítkovský et al. 2000; Kapelan et al. 2004; Jung and Karney 2008; Covas and Ramos 2010). ITA based pipeline leak detection has been extended to simple pipe networks (Shamloo and Haghghi 2010).

The implementation of ITA can be very time-consuming, because it iteratively calibrates the pipeline parameters by comparing the measured transient pressure

trace with the numerical results from the pipeline in the forward model. The forward modelling is typically conducted in the time domain and by using the Method of Characteristics (MOC) (Wylie and Streeter 1993; Chaudhry 2014). Recently development of frequency-domain inverse analysis has the potential to enhance the computational efficiency, where the forward modelling is conducted in the frequency domain using the impedance method (Kim 2014) or the admittance matrix method (Capponi et al. 2017). The successful calibration of a pipeline system relies on accurate forward simulation. However, varying boundary conditions, parameter uncertainties in real pipelines, and the difficulty in accurately simulating transient behaviour make errors in the forward modelling almost inevitable (Vítkovský et al. 2007). In addition, when the parameters to be calibrated are significant in number the results may be non-unique (Vítkovský et al. 2007; Zhang et al. 2018a).

### ***Leak detection using frequency-domain analysis***

Frequency domain leak detection techniques have been studied extensively (Colombo et al. 2009). One innovation in this area has been that steady oscillatory flow can be adopted to extract a system's response to signals of different frequencies, which is known as the system's frequency response function (FRF) or transfer function and can be used for leak detection. In this approach, both the head and flow are assumed to be composed of the steady-state average and oscillatory components. Impedance or transfer matrix methods (Wylie and Streeter 1993; Chaudhry 2014) are commonly used to solve the frequency response of a pipeline system.

Jönsson and Larson (1992) first proposed that the spectral analysis of a measured pressure trace could be used for leak detection. (Mpesha et al. 2001) proposed that leaks would introduce extra resonant peaks in the frequency response diagram (FRD) of a system. However, research by Ferrante and Brunone (2003) demonstrated that extra peaks would not be observed unless leak size is larger than a critical value. Covas et al. (2005) proposed a standing wave difference method, which uses the spectral analysis of an FRD to determine the leak location. Lee et al. (2005b) observed that a leak in a single pipeline would introduce a sinusoidal pattern on the resonant responses, and the location and size of the leak can be determined from the period and amplitude of this pattern. Sattar and Chaudhry (2008) found that the leak-induced sinusoidal pattern could be observed on the anti-resonant responses in some situations. The factors that decide whether the leak-induced sinusoidal pattern would appear at the resonant or at the anti-resonant frequencies have been explained by Gong et al. (2014a). Gong et al. (2013a) developed a leak detection technique that only uses the first three resonant peaks, which significantly reduces the requirement on the bandwidth of the excitation signal. A customised solenoid valve that generates pseudorandom binary sequences (PRBS) was developed and numerical and laboratory experiments confirmed its usefulness in pipeline FRD extraction (Gong et al. 2013b; Gong et al. 2016b).

Frequency response-based leak detection methods have much better computational efficiency compared to the time-domain ITA. However, the successful implementation of these techniques relies on accurate measurement of the FRF of a pipeline system, which is difficult in the field due to the

complexities of the pipeline configuration and the limitation in the bandwidth of the transient input signal (Gong et al. 2013b; Lee et al. 2013).

## **1.4 Transient-based technique for pipe wall condition assessment**

Research of transient-based pipe wall condition assessment has been focused on the detection of thinner-walled pipe sections (e.g. sections with extended internal/external corrosion or the spalling of cement-mortar lining), and on sections with extended blockages (e.g. sections with extended tuberculation).

### **1.4.1 Detection of thinner-walled pipe sections**

Stephens et al. (2008; 2013) were the first to investigate transient analysis applied to the detection of changes in pipe wall thicknesses. Stephens et al. (2013) studied a mild steel cement-mortar lined (MSCL) water transmission main in the field, and calibrated the wave speed along the pipe for the detection of sections with extended spalling of cement-mortar lining and/or internal corrosion by using time-domain ITA. The calibrated remaining pipe wall thicknesses (as derived from the wave speed) were consistent with those from ultrasonic pipe wall thickness inspection. However, due to the structural complexity and parametric uncertainties of real pipelines, the efficiency and accuracy of the ITA-based pipe wall condition assessment techniques need to be improved. Zhang et al. (2018b) proposed a head-based MOC technique with flexible computational grids to speed up the forward modelling part of an ITA analysis. Associated research by Zhang et al. (2018a) confirmed that the ITA-based pipe wall condition assessment technique suffers from the problem of

multiple solutions, since different combinations of the pipe wave speed distributions can result in very similar transient pressure responses at some locations.

Hachem and Schleiss (2012) proposed a technique for detecting a structurally weak section in single pipelines using a steep transient pressure wave and TDR analysis. The wave speed in the deteriorated section was estimated by comparing the measured wave speed with that of an intact pipe. This technique would have difficulties in determining the wave speeds should multiple deteriorated sections exist. Gong et al. (2013c) developed a technique for detecting deteriorated pipe sections based on direct analysis of the magnitude and the TDR principle. The magnitude of the wave reflection induced by a section with wall thickness changes is indicative of the impedance of that section, which can then be directly used to calculate the wall thickness and wave speed in that section. The technique is efficient and effective for single pipelines with only a few deteriorated pipe sections, and it has been verified in field trials on a MSCL water main (Gong et al. 2015) and an asbestos cement (AC) water main (Gong et al. 2016c) in regional Australia.

A further development based on the direct reflection analysis-based condition assessment technique is the reconstructive method of characteristic (RMOC) technique (Gong et al. 2014b). The RMOC technique enables the reconstruction of the impedance continuously along a pipe by using a measured transient response trace and by calculating along the characteristic lines of MOC backward in time. However, the original RMOC technique is only applicable to reservoir-pipeline-valve (R-P-V) systems, where the valve closure is used to



generate a step transient wave and pressure response is measured at the upstream face of the valve. Zeng et al. (2018b) has developed a technique to reconstruct the pipeline impedance of an R-P-V system using a modified layer-peeling method, which analyses the IRF instead of the response from a step incident wave. Zhang et al. (2019) has generalised the RMOC technique to be independent of the boundary conditions of the pipeline system. This is achieved by using two pressure transducers in close proximity – an inspiration from the sensor array measurement strategy used in the PhD research presented here.

In the frequency domain, Zecchin et al. (2009) developed a mathematical framework for transient simulation in arbitrary pipe networks using the admittance matrix method. The framework was used in general calibration of pipeline parameters in a network environment (Zecchin et al. 2014a). The principle is to find an optimal pipe model whose response matches the measured response, which is similar to that of conventional ITA but in the frequency domain. However, the work so far has been limited to numerical studies, and applications to real pipeline networks will be challenging.

### **1.4.2 Detection of extended blockages**

Duan et al. (2012) proposed a technique to detect extended blockages (pipe sections with larger wall thicknesses but the same external diameter as the intact part) using the FRD of single pipe systems. The principle is that extended blockages could cause the resonant frequencies of a single pipeline system to shift, and the frequency shift can be used to determine the properties of the extended blockage. Although the concept of the technique has been validated in the laboratory (Duan et al. 2013); however, many challenges are expected in

real applications (Duan 2016b). As acknowledged by the same authors, the shifts of the resonant peaks due to extended blockages are typically insignificant (Duan et al. 2011) therefore difficult to determine accurately.

Zeng et al. (2018a) developed a technique for extended blockage detection using a modified layer-peeling method. It was found through numerical simulations that the wave speed and internal diameter can be reconstructed even for non-uniform extended blockages. The technique requires an R-P-V system configuration with the generation and measurement points at the valve end.

## **1.5 Key challenges to address**

A common limitation to all the conventional transient-based pipeline defect detection and wall condition assessment techniques is that they are difficult to be extended to applications involving complex pipe systems or pipe networks. This is because conventional single pipe transient based methods make explicit assumptions about boundary conditions that are incompatible with network junction interactions. That is, the boundary conditions imposed on a single pipe section from the surrounding network lead to measured transient responses that can be too complex to analyse with conventional methods. The most common measurement strategy used in the field is illustrated in Figure 1.1. Multiple single pressure transducers are sparsely placed along a pipeline at existing access points, such as air valves or fire hydrants. Pressure waves travel along a pressurised pipeline in two directions – towards both the upstream and the downstream directions. For a single pressure transducer, the measurement is always a superimposed signal of both the waves travelling in the two directions. When multiple deteriorated sections exist on both sides of a transducer, which

is the most common scenario in real pipeline systems, reflections are complex in waveform due to the wave superposition. In water distribution systems, where pipe branches are significant in number and size (compared to the size of the main pipe), the measured pressure signal can be very complex and difficult to interpret.

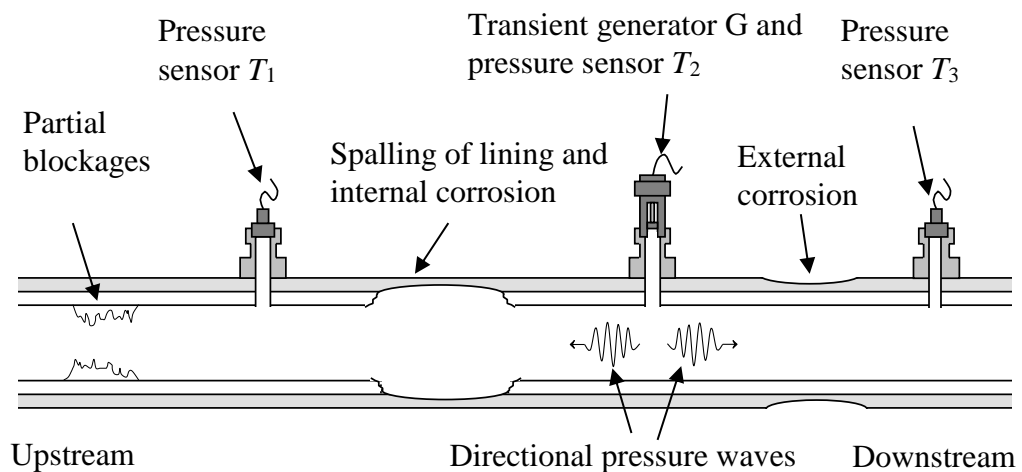


Figure 1.1 Schematic diagram showing the current transient pressure measurement strategy used in the field.

To avoid the complexity, many conventional transient-based techniques use a single pressure transducer at a dead-end, such that pressure waves can only come from one direction. Additionally, the FRD-based techniques also require the whole pipe system to be simple in configuration (e.g. reservoir-pipeline-valve or reservoir-pipeline-reservoir). However, these requirements are difficult to achieve in field pipelines, which are typically buried underground with limited access and can also be embedded in a complex network environment.

Gong et al. (2012b) proposed that the use of the transient pressure measurements from two pressure transducers installed at different locations along a pipe could separate the pressure waves travelling upstream and downstream. In a following study, Gong et al. (2012a) found that arranging the two pressure transducers in close proximity can facilitate the wave separation. Zecchin et al. (2014b) found that the use of a pair of pressure transducers can enable the determination of the system IRF. While these preliminary numerical studies have proven the concept that the directional pressure waves can be separated to facilitate pipeline condition assessment, it is envisaged that many challenges exist in real applications due to the uncertainties in the pressure measurement and pipeline parameters. Similar applications can be found in acoustic research, where two or more microphones are used to separate the travelling acoustic waves in ducts filled with air (De Sanctis and Van Walstijn 2009; Kemp et al. 2013). However, these acoustic techniques cannot be directly applied to transient pressure analysis in water pipelines due to the difference in the dominant physical processes, and associated modelling paradigms, for acoustic waves versus hydraulic transient waves.

## **1.6 Research objectives**

The overall objective of this PhD research is to address the complexity in the interpretation and analysis of transient pressure data associated with the supposition of the two directional waves underlying any pressure measurement. The research here proposes to use paired pressure sensors (two pressure transducers in close proximity) to measure the pipeline transient pressure response at each station, instead of just using a single pressure sensor, as is the

conventional approach. New and practical techniques are developed to extract the directional information of travelling pressure waves, which then enables the development of advanced pipeline leak detection and wall condition assessment techniques for targeted pipe sections in complex pipeline systems. The specific aims of this research are as follows:

**Aim 1:** To develop a robust wave separation algorithm that can extract the two directional travelling pressure waves in a pipeline from the pressure traces measured by a pair of pressure transducers located in close proximity (a dual-sensor unit). This separation of the measurement of pressure into its respective wave components allows for the directional attribution of observed pressure fluctuations. That is, the wave reflections induced by anomalies located on either side of the dual-sensor unit are able to be separated, through the reconstruction of the directional travelling waves. This enables a significant reduction in the complexity of the wave form, and the wave reflections will be attributable to their source.

**Aim 2:** This twofold aim is to develop: (i) a system identification algorithm that can determine the system transfer matrix of a section of pipe bounded by two dual-sensor units; and (ii) an associated technique for detecting leaks in the pipe section to utilise this system transfer matrix. The two dual-sensor units provide information about the pressure waves travelling into, and out of, the section of interest, even if the section is part of a complex network. Given a linear systems framework, this complete acquisition of the input/output signals enables the determination of the associated system transfer matrix, which is a full representation of the physical characteristics of the section of interest. As an

outcome of this aim, this specific section of pipeline can be isolated from a complex pipeline network for independent analysis (e.g. leak detection).

**Aim 3:** To develop and assess the utility of a fibre optic dual-sensor array. The in-pipe fibre optic pressure sensor will enable distributed measurement of transient pressure through a single access point on the pipe. This restriction to a single access point is a critical limitation for the practical implementation of dual-sensor approaches in the field. Laboratory experiments will be conducted to validate the approach and explore its utility for condition assessment..

## **1.7 Organisation and overview of the thesis**

This PhD thesis contains five chapters. Chapter 1 (this current chapter) is an introduction of the research project, with a literature review, a summary of the research challenges, a statement of the research aims, and an outline of the organisation of the thesis. The main body of this thesis – Chapters 2 to 4 – constitutes the three journal manuscripts arising from the research. The final chapter contains the conclusions and recommendations for future work.

Chapter 2 presents an advanced wave separation algorithm for transient analysis in pipelines. The technique enables the extraction of directional travelling pressure waves by using two closely placed pressure sensors at one measurement site (referred to as a dual-sensor). The dynamic relationship between the two pressure transducers can be calibrated in-situ to enhance the robustness of the wave separation. In addition to numerical simulations, the research has also conducted the first experimental verification of transient wave separation on a copper pipeline in the laboratory, where a step wave generated

by a side-discharge valve was used as the excitation and two adjacent pressure sensors flush mounted on the experimental pipe were used for transient measurements. Comparison of the wave separation results with their numerically predicted counterparts has shown that the wave separation algorithm is successful. The results have also shown that the proposed wave separation technique facilitates transient-based pipeline condition assessment by reducing the complexity of the wave form. The research findings have been published in the *Journal of Hydroinformatics* (DOI: 10.2166/hydro.2017.146).

Chapter 3 presents an innovative approach for leak detection in a targeted pipe section using hydraulic transient waves and the dual-sensor measurement strategy. The new concept is to utilize a special transient pressure generation and sensing configuration, combined with custom developed signal processing algorithms, to “virtually” break any complex pipeline system down to its simplest form – a single pipe section – for independent condition diagnosis. The virtual isolation of a pipe section is achieved by a *two-source-four-sensor* transient testing strategy: two dual-sensor units are used to bracket the targeted pipe section (with the two sensors in each unit being in close proximity); and two transient pressure wave generators are used, which bracket the four sensors and the targeted pipe section. This testing strategy enables the extraction of the transfer matrix of the in-bracket pipe section, independent from any hydraulic components outside of the two transient generators.

A transfer matrix of a pipe section is a full representation of the wave propagation characteristics (in the format of frequency response functions) as governed by the physical properties of the pipe section. Given this, the extracted

transfer matrix can be used for leak detection. It has been found that a linear combination of two elements in the extracted transfer matrix is sensitive to leaks, where a leak will introduce a sinusoidal with the period and the magnitude of the pattern related to the location and impedance of the leak, respectively. Multiple leaks introduce multiple sinusoidal patterns. An algorithm has been developed to extract the leak information from the extracted transfer matrix of the “virtually” isolated pipe section, and the technique has been validated by numerical simulations. Note that the technique and the findings are different from that of conventional FRD-based leak detection techniques, in which the boundary conditions of the pipe system need to be known and the entire system needs to be simple (e.g. reservoir-pipe-reservoir or reservoir-pipe-valve). The work presented in this thesis is the first to utilise the *two-source-four-sensor* transient generation and measurement strategy for leak detection in targeted pipe sections embedded in complex systems. This concept is also useful for other applications such as blockage detection and pipe wall condition assessment. The research findings have been submitted to the *Journal of Hydraulic Engineering* for peer review.

Chapter 4 presents a customised in-pipe fibre optic pressure sensor array and its application to transient wave separation and pipe wall condition assessment in the laboratory. The sensor array consists of five fibre Bragg grating (FBG)-based pressure sensors in close proximity (~0.5 m apart). The cable that protects the optical fibre is made from a plastic material, and has a diameter of approximately 4 mm. At each FBG pressure sensor, a 10 mm window is open in the protective cable, and a flexible elastomeric sleeve is used to cover the FBG. This fibre optic sensor array represents a second generation of



development and is especially designed for high-speed pressure measurement under relatively large pressure conditions (2 bar to 10 bar). The sensors have a wider pressure applicable range and a better linearity compared to the first generation of the fibre optic pressure sensors tested in 2014 (which is reported in a conference paper itemised in the *List of Publications*, but this work is not included in this PhD thesis).

Extensive laboratory experiments have been conducted in the Robin Hydraulics Laboratory at the University of Adelaide on this fibre optic pressure sensor array. The sensor array was inserted into the pipeline through a single entrance point. Pressure response data were successfully collected from the fibre optic sensor array with a sampling rate up to 20 kHz. The previously developed wave separation algorithm was adapted to analyse the transient pressure measurement from the FBG sensors. The resultant directional pressure waves were then used to detect pipe sections with a thinner wall thickness. A challenge is the influence of the in-pipe fibre optic sensing cable on the transient pressure measurement. The impact was analysed and adjustments to the pipeline condition assessment algorithm were undertaken to resolve the issue. The successful experimental application has provided a verification of the usefulness of the in-pipe fibre optic sensor array, which can facilitate transient-based pipeline condition assessment for buried water pipes with limited access points. The results of the research have been published in the *Journal of Hydroinformatics* (DOI: 10.2166/hydro.2019.051).

Chapter 5 presents the conclusions from this PhD research. It summarises the key findings from and the key contributions of the research. It also briefly discusses the direction for future work.

## **Chapter 2**

### **Hydraulic Transient Wave**

### **Separation Algorithm using a Dual- sensor with Applications to Pipeline**

### **Condition Assessment**

### **(Journal Paper 1)**

Publication details:

Shi, H., Gong, J., Zecchin, A. C., Lambert, M. F., and Simpson, A. R. (2017).  
"Hydraulic transient wave separation algorithm using a dual-sensor with  
applications to pipeline condition assessment." *Journal of Hydroinformatics*,  
19(5), 752-765, 10.2166/hydro.2017.146.

This page is intentionally left blank

## Statement of Authorship

Title of Paper	Hydraulic transient wave separation algorithm using a dual-sensor with applications to pipeline condition assessment
Publication Status	<input checked="" type="checkbox"/> Published <input type="checkbox"/> Accepted for Publication <input type="checkbox"/> Submitted for Publication <input type="checkbox"/> Unpublished and Unsubmitted work written in manuscript style
Publication Details	Shi, H., Gong, J., Zecchin, A. C., Lambert, M. F., and Simpson, A. R. (2017). "Hydraulic transient wave separation algorithm using a dual-sensor with applications to pipeline condition assessment." <i>Journal of Hydroinformatics</i> , 19(5), 752-765, <a href="https://doi.org/10.2166/hydro.2017.146">10.2166/hydro.2017.146</a> .

### Principal Author

Name of Principal Author (Candidate)	He Shi		
Contribution to the Paper	Conception and design of the project; Analysis and interpretation of the research data; Drafting the manuscript.		
Overall percentage (%)	75%		
Certification:	This paper reports on original research I conducted during the period of my Higher Degree by Research candidature and is not subject to any obligations or contractual agreements with a third party that would constrain its inclusion in this thesis. I am the primary author of this paper.		
Signature		Date	14/03/2019

### Co-Author Contributions

By signing the Statement of Authorship, each author certifies that:

- i. the candidate's stated contribution to the publication is accurate (as detailed above);
- ii. permission is granted for the candidate to include the publication in the thesis; and
- iii. the sum of all co-author contributions is equal to 100% less the candidate's stated contribution.

Name of Co-Author	Jinzhe Gong		
Contribution to the Paper	Conception and design of the project; Analysis and interpretation of the research data; Critically reviewing the manuscript.		
Signature		Date	15/3/2019

Name of Co-Author	Aaron Zecchin		
Contribution to the Paper	Conception and design of the project; Analysis and interpretation of the research data; Critically reviewing the manuscript.		
Signature		Date	15/3/19

Name of Co-Author	Martin Lambert		
Contribution to the Paper	Conception and design of the project; Analysis and interpretation of the research data; Critically reviewing the manuscript.		
Signature		Date	15/3/19

Name of Co-Author	Angus Simpson		
Contribution to the Paper	Conception and design of the project; Analysis and interpretation of the research data; Critically reviewing the manuscript.		
Signature		Date	15/3/19

## **Abstract**

Over the past two decades, techniques have been developed for pipeline leak detection and condition assessment using hydraulic transient waves (i.e. water hammer waves). A common measurement strategy for applications involves analysis of signals from a single pressure sensor located at each measurement site. The measured pressure trace from a single sensor is a superposition of reflections coming from upstream, and downstream, of the sensor. This superposition brings complexities for signal processing applications for fault detection analysis. This paper presents a wave separation algorithm, accounting for transmission dynamics, which enables the extraction of directional travelling waves by using two closely placed pressure sensors at one measurement site (referred as a dual-sensor). Two typical transient incident pressure waves, a pulse wave and a step wave, are investigated in numerical simulations and laboratory experiments. Comparison of the wave separation results with their predicted counterparts shows the wave separation algorithm is successful. The results also show that the proposed wave separation technique facilitates transient-based pipeline condition assessment.

This page is intentionally left blank



## **2.1 Introduction**

The aging of water distribution systems worldwide has brought many issues, ranging from significant water and energy losses (Colombo and Karney 2002) to risks to public health due to possible pathogen intrusion (Karim et al. 2003). Over the past two decades, hydraulic transients (water hammer waves) have been identified as a useful tool for non-invasive pipeline leak detection (Mpesha et al. 2002; Ferrante and Brunone 2003; Covas et al. 2005; Lee et al. 2005a; Soares et al. 2010; Ferrante et al. 2012; Duan 2016a), blockage detection (Sattar et al. 2008; Meniconi et al. 2013; Massari et al. 2014), wall condition assessment (Gong et al. 2013c; Stephens et al. 2013) and general system parameter identification (Zecchin et al. 2013; Zecchin et al. 2014a). When undertaking a hydraulic transient analysis of a pipeline system, a transient disturbance (a pulse or a step pressure wave) is typically introduced by abruptly operating a valve. Then the transient pressure wave propagates along the pipe in both upstream and downstream directions. Any physical changes or anomalies in a pipeline will affect the propagation of transient pressure waves, resulting in specific reflections. These reflections can be analysed in either the time or frequency domain, in order to diagnose the anomalies in the pipeline system.

Most existing studies are based on the analysis of the transient pressure measured by a single sensor, or by multiple sensors usually separated by a significant distance along pipes. However, there are often simultaneous waves travelling in opposite directions. The hydraulic pressure at any single point in a

pipeline can be expressed as the sum of a travelling pressure wave coming from upstream of the measurement point and a travelling pressure wave coming from downstream. As a consequence, for a single pressure sensor, the measured signal is always a superimposed signal of waveforms propagating upstream and downstream. One measurement strategy to avoid a superposition problem is by placing the measurement point at a dead end to ensure the reflection comes only from one direction (Gong et al. 2014b). However, when investigating transmission mains, which may be tens of kilometres long, it is not always practical to find an ideal measurement point at a dead end. Moreover, when multiple anomalies exist on both sides of a sensor, which is the common case in most pipelines, the measured pressure signal can be very complex and difficult to interpret, even when multiple measurement sites are used (Gong et al. 2016c).

To investigate and extract the directional information of travelling transient pressure waves, Gong et al. (2012b) proposed a technique that uses two pressure sensors (100 m spaced in a pipe with an internal diameter 600 mm) to separate the pressure waves travelling downstream from those travelling upstream along a pipeline. In a subsequent study by Gong et al. (2012a), a new measurement strategy, which involved the use of two pressure sensors in close proximity (1 m spaced in a pipe with an internal diameter 600 mm), was proposed to facilitate the wave separation. However, these preliminary studies were limited to numerical simulations with ideal conditions where the pipeline between two sensors is assumed to be lossless and the incident wave is a sharp step signal.

Zecchin et al. (2014b) proposed a technique for extracting the impulse response of a single pipeline using a pair of sensors (10 m spaced in a pipe with an internal diameter of 200 mm) for measurement, and using hydraulic noise as the excitation. The hydraulic noise is in the form of wide-sense stationary pressure signals (the mean function and correlation function do not change over time). In that study, a theoretical propagation loss between two sensors was considered. However, the directional travelling waves were not extracted from the measurements. The wide-sense stationary pressure signals are difficult to achieve in practice, and only a numerical case study was conducted in that paper.

It should be noted that the use of two pressure sensors in close proximity (referred to as a “dual-sensor” in the following) for wave separation has been studied in the acoustics research area, where acoustic waves in ducts measured by two (or more) microphones are analysed (Chung and Blaser 1980). However, hydraulic transient waves in water-filled pipes have many differences from acoustic waves propagating in the air, namely, they have a different signal bandwidth, wave magnitude and wave propagation properties where wall friction plays a much more significant role. Moreover, the research in acoustic ducts focuses on calculating the reflection and transmission coefficients, rather than splitting the directional travelling waves explicitly, which is the focus of the wave separation method developed in the current paper. In the field of pipeline transient analysis, the use of two pressure sensors in close proximity has been used for unsteady flow measurement (Washio et al. 1996a; Kashima et al. 2013) However, except for the preliminary numerical work reported in Gong *et al.* (2012b; 2012a) and Zecchin et al. (2014b), to the knowledge of the

authors, there is no study on the separation of hydraulic transient waves using a dual-sensor in pressurised pipelines.

The research reported in the current paper develops a systematic wave separation algorithm that can extract the two directional travelling hydraulic transient waves from pressure traces as measured by two closely spaced pressure sensors. Compared to the preliminary numerical work in Gong *et al.* (2012b; 2012a) and Zecchin *et al.* (2014b), the new developments include: (1) an experimental data-driven approach to estimate the transfer function between the two sensors, which enables wave separation without the knowledge of the specific pipe parameters (e.g. flow rate, friction factor, and diameter of the pipe); (2) the extraction and removal of the incident waves, making the algorithm applicable to real incident waves with curved wave fronts rather than the theoretical sharp incident waves used in previous studies; and (3) the first experimental verification of the wave separation technique.

To validate the wave separation algorithm, a pulse incident wave is used in a numerical study and a step wave is considered in a laboratory study. In both studies, as presented in this paper, the comparison between the extracted directional reflection trace with its counterpart, which has a reflection from one direction only, shows the wave separation algorithm is successful. The wave separation algorithm provides the directional information of travelling transient pressure waves in pipelines and simplifies the interpretation of the signals. The directional waves, as obtained in the laboratory study, are then used to determine the properties of two deteriorated pipe sections in the experimental system (simulated by short pipe sections with thinner wall thicknesses). The

results demonstrate that the proposed wave separation technique can adequately facilitate transient-based pipeline condition assessment. Limitations of the technique and practical challenges are discussed before drawing the conclusions.

## **2.2 Wave separation algorithm using a dual-sensor**

### **2.2.1 Hydraulic wave propagation theory**

The transient behaviour of pressurised fluid within a closed conduit pipeline system is governed by the so called water hammer equations, which are a series of two one-dimensional (1-D) quasi-linear hyperbolic differential equations describing mass and momentum conservation (Wylie and Streeter 1993; Chaudhry 2014). The solution of the water hammer equations can be expressed in terms of pressure waves travelling upstream and downstream (Wylie and Streeter 1993; Chaudhry 2014). This is a consequence of the mathematical properties of the hyperbolic equations, but also reflects the physics of the fluid, that is, the fluid pressure at any single point in a pipeline can be expressed as the sum of a pressure wave travelling in the positive direction and a pressure wave travelling in the negative direction, i.e.:

$$p(x,t) = p^+(x,t) + p^-(x,t) \quad (2.1)$$

where  $p$  is the total pressure as measured by a sensor,  $p^+$  is the positive pressure wave coming from the upstream,  $p^-$  is the negative pressure wave travelling from the downstream to the upstream,  $x$  is the axial coordinate along the pipe and  $t$  is time.

Applying the Laplace transform to Equation (2.1) to transform the signals into the Laplace (or frequency) domain, the pressure signal is then described as:

$$P(x, s) = P^+(x, s) + P^-(x, s) \quad (2.2)$$

where  $s$  is the complex valued frequency (the Laplace variable), and the capital  $P$  represents pressure signals in the frequency domain.

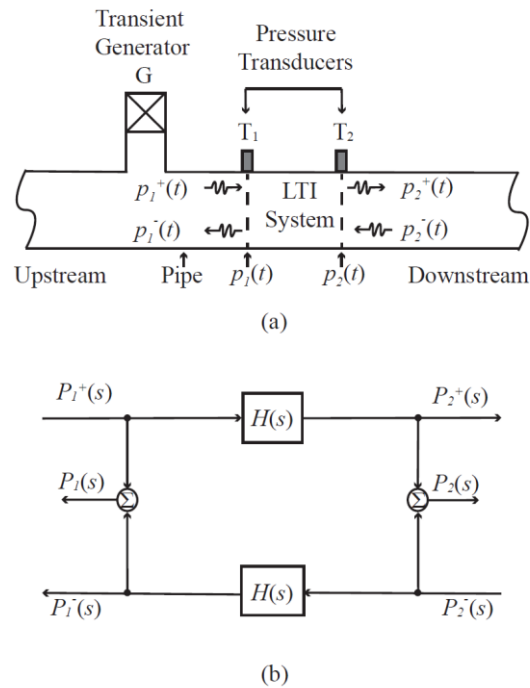


Figure 2.1 (a) Proposed configuration for the pressure transient test with a dual-sensor in a pipeline; and (b) corresponding block diagram in the frequency domain illustrating the wave propagation. (Note, LTI System = Linear Time Invariant System).

A typical configuration for transient pressure measurement using a dual-sensor in a pipeline is given in Figure 2.1(a): a side discharge valve  $G$  is used as the transient generator,  $T_1$  and  $T_2$  are the pressure sensors, and  $p_1(t)$  and  $p_2(t)$  are the measured pressure traces by  $T_1$  and  $T_2$ , respectively. The pipe section between  $T_1$  and  $T_2$  is assumed to act as a linear time-invariant (LTI) system (Ljung 1999), where the pressures  $p_1^+(t)$  and  $p_2^+(t)$  are the positive travelling waves at  $T_1$  and  $T_2$ , respectively, and  $p_1^-(t)$  and  $p_2^-(t)$  are the negative travelling waves at  $T_1$  and  $T_2$ , respectively.

The configuration can be described by a block diagram as shown in Figure 1(b). A transfer function  $H(s)$  is the representation of the wave propagation dynamics between sensor  $T_1$  and  $T_2$ , where  $P_1(s)$  and  $P_2(s)$  are the Laplace transforms of  $p_1(t)$  and  $p_2(t)$  respectively (as for all other capitalised symbols). Based on Equation (2),  $P_1(s)$  and  $P_2(s)$  can be written as the sum of the positive and the negative travelling waves as in Equations (2.3) and (2.4):

$$P_1(s) = P_1^+(s) + P_1^-(s) \quad (2.3)$$

$$P_2(s) = P_2^+(s) + P_2^-(s) \quad (2.4)$$

The outputs of the system [ $P_1^-(s)$  and  $P_2^+(s)$ ] and the inputs of the system [ $P_2^-(s)$  and  $P_1^+(s)$ ] are related by the transfer function  $H(s)$  and written as:

$$P_1^-(s) = P_2^-(s)H(s) \quad (2.5)$$

$$P_2^+(s) = P_1^+(s)H(s) \quad (2.6)$$

Substituting Equations (2.5) and (2.6) into Equations (2.3) and (2.4), respectively, yields:

$$P_1(s) = P_1^+(s) + P_2^-(s)H(s) \quad (2.7)$$

$$P_2(s) = P_1^+(s)H(s) + P_2^-(s) \quad (2.8)$$

$P_2^-(s)$  can be eliminated by multiplying Equation (2.8) by  $H(s)$  and then subtracting Equation (2.7) from the resulting equation, yielding the final result:



$$P_1^+(s) = \frac{P_1(s) - P_2(s)H(s)}{1 - H^2(s)} \quad (2.9)$$

Substituting Equation (2.9) into Equation (2.3) and rearranging gives:

$$P_1^-(s) = \frac{P_2(s)H(s) - P_1(s)H^2(s)}{1 - H^2(s)} \quad (2.10)$$

From Equations (2.9) and (2.10), the positive travelling wave  $P_1^+(s)$  and negative travelling wave  $P_1^-(s)$  can be extracted from the original pressure measurements [  $P_1(s)$  and  $P_2(s)$  ] using the transfer function  $H(s)$  in the transform domain.

## 2.2.2 Determination of the transfer function $H(s)$

### *Analytic representation*

The transfer function  $H(s)$  is a characterisation of the physical wave propagation dynamics of the pipe section. In 1-D water hammer analysis, the transfer function  $H(s)$  for the pipe between two sensors can be expressed analytically as:

$$H(s) = e^{-\Gamma(s)l} \quad (2.11)$$

where  $l$  is the length between two sensors,  $\Gamma(s)$  is the propagation operator or propagation constant that describes the frequency dependent attenuation and phase change per unit length (Wylie and Streeter 1993).  $\Gamma(s)$  can be expressed in a general form by (Zecchin 2010):

$$\Gamma(s) = \frac{1}{a} \sqrt{[s + R(s)][s + C(s)]} \quad (2.12)$$

where  $a$  is the wave speed,  $R(s)$  and  $C(s)$  represent the resistance and compliance terms, respectively.

Specific expressions of the propagation operator  $\Gamma(s)$  can be derived from the general form for specific hydraulic conditions (e.g. for laminar or turbulent flow, for elastic or viscoelastic pipes) (Zecchin 2010; Gong et al. 2016a). If only steady friction and elastic pipe behaviour are considered, as is the case in this research, then  $C(s) = 0$  and  $R(s) = R$ . The resistance term can be given by (Zecchin 2010):

$$R = \frac{f |\bar{Q}|}{DA} \quad (2.13)$$

where  $f$  is the Darcy–Weisbach friction factor,  $|\bar{Q}|$  is the absolute value of the steady-state flow,  $D$  is the internal diameter of the pipe, and  $A$  is the cross-sectional area of the pipe.

From a practical perspective, using the analytic form (2.11),  $H(s)$  can be completely specified using measured values of  $l$ ,  $a$ , and a calibrated value of  $R$  (or known  $D$  with estimates of  $\bar{Q}$  and  $f$ ).

### ***Experimental representation***

As an alternative to the analytic expression for  $H(s)$ , the properties of the transfer function can also be determined experimentally. In hydraulic transient analysis, a pipeline system is typically excited by abruptly opening or closing a valve, which results in a discrete wave with a short duration as an incident pressure wave (e.g. a sharp step or pulse wave). Under these conditions, an assumption can be made that during the time of the incident wave entering into the system at  $T_1$  then exiting the system at  $T_2$ , there are no transient waves entering the system from  $T_2$  (i.e.  $p_2^-(t) = 0$  in Figure 2.1). This assumption is often valid when the incident wave is short, and the system is excited from a steady state condition. Therefore, the LTI system in Figure 1(a) can be temporarily treated as a single-input and single-output system for this short time period. The input is the incident wave  $p_1^+(t) = p_{1i}(t)$  at  $T_1$ , and the output is the incident wave  $p_2^+(t) = p_{2i}(t)$  at  $T_2$ . The incident waves  $p_{1i}(t)$  and  $p_{2i}(t)$  can be extracted from the original measured pressure trace  $p_1(t)$  and  $p_2(t)$  by applying a rectangular time window (i.e. truncating the short signal section that includes the wave front out of the whole pressure trace).

The transfer function  $H(s)$  is the linear mapping from an input to an output in the Laplace domain, and can be given by:

$$H(s) = \frac{P_{2i}(s)}{P_{1i}(s)} \quad (2.14)$$

where  $P_{1i}(s)$  and  $P_{2i}(s)$  are the Laplace transforms of the incident waves at  $T_1$  and  $T_2$ , respectively. Note that the experimental approach does not require any flow rate information except that there is no wave (or relatively very small wave) in one direction, which is an advantage over the analytical approach.

### 2.2.3 The wave separation algorithm

In Figure 2.1(a), when an incident pressure wave is generated at G and arrives at sensor  $T_1$ , the positive travelling pressure wave at  $T_1$  contains the incident wave and the reflected wave coming from upstream of  $T_1$ . The reflected wave is the focus because it carries the pipeline information that can be used for pipeline condition assessment. However, compared to the incident wave, the reflections due to wall deterioration are usually small (Gong et al. 2015). Given this, removing the dependence of the incident wave from the wave separation results leads to clearer separated directional travelling waves, and the method is described below.

In Figure 2.1(a), the positive travelling waves can be written as the sum of the incident wave and the reflected wave coming from upstream:

$$p_1^+(t) = p_{1i}(t) + p_{1r}^+(t) \quad (2.15)$$

$$p_2^+(t) = p_{2i}(t) + p_{2r}^+(t) \quad (2.16)$$

where  $p_{1r}^+(t)$  and  $p_{2r}^+(t)$  are the reflected waves coming from upstream of the measurement points  $T_1$  and  $T_2$  respectively. The negative travelling waves

$p_1^-(t)$  and  $p_2^-(t)$  can be written as the negative travelling reflected waves

$p_{1r}^-(t)$  and  $p_{2r}^-(t)$ :

$$p_1^-(t) = p_{1r}^-(t) \quad (2.17)$$

$$p_2^-(t) = p_{2r}^-(t) \quad (2.18)$$

As a result, the pressure waves as measured by the sensors at points  $T_1$  and  $T_2$  can be described by:

$$p_1(t) = p_{1i}(t) + p_{1r}(t) \quad (2.17)$$

$$p_2(t) = p_{2i}(t) + p_{2r}(t) \quad (2.18)$$

where  $p_{1r}(t) = p_{1r}^+(t) + p_{1r}^-(t)$  and  $p_{2r}(t) = p_{2r}^+(t) + p_{2r}^-(t)$ . As a sharp step or pulse wave is usually used as an incident wave, and in the time domain the incident waves  $p_{1i}(t)$  and  $p_{2i}(t)$  can be easily identified and extracted from the measured pressure traces using a time-windowing procedure as for Equation (2.14). Similarly the reflections  $p_{1r}(t)$  and  $p_{2r}(t)$  can also be extracted by applying an appropriate rectangular time window.

Transforming Equations (2.15)–(2.20), and then substituting the transformed equations and Equation (2.14) into Equations (2.9) and (2.10), rearrangement of the final result yields the following wave forms for the two reflected wave components:

$$P_{1r}^+(s) = \frac{P_{1r}(s) - P_{2r}(s)H(s)}{1 - H^2(s)} \quad (2.17)$$

$$P_{1r}^-(s) = \frac{P_{2r}(s)H(s) - P_{1r}(s)H^2(s)}{1 - H^2(s)} \quad (2.18)$$

The inverse Laplace transforms of Equations (2.21) and (2.22) will give the positive travelling reflected waves and the negative travelling reflected waves in the time domain.

For analysis of real pipeline systems where the pressure signals measured by sensors are used, the value of the Laplace variable is restricted to the imaginary axis, i.e.  $s = i\omega$ , where  $i$  is the imaginary unit, and  $\omega$  is the radial frequency. Consequently, the Fourier transform can be used instead of the Laplace transform.

To apply the wave separation algorithm to pressure traces  $[p_1(t)$  and  $p_2(t)]$  measured by a dual-sensor as in Figure 2.1(a), the following steps will be performed:

1. Time-windowing to separate incident waves and reflections in the original pressure traces measured by a dual-sensor using Equations (2.19) and (2.20).
2. Transfer incident waves and reflections into the frequency domain by using the Fourier transform.
3. Determine the transfer function between two sensors using the analytic Equation (2.11) or using the experimental Equation (2.14).

4. Extract the directional reflection waves in the frequency domain using Equations (2.21) and (2.22).
5. Transfer wave separation results into the time domain using an Inverse Fourier Transform, or using the results directly in the frequency domain for further analysis, e.g. determine the frequency response of the pipe section.

It should be noted that, when other incident waves are used in place of discrete waves with a short duration, step 1 can be ignored and Equations (2.9) and (2.10) in step 4 used instead. Before the wave separation algorithm is applied to real data, pre-processing may be needed, including determining the effective frequency range to minimise the impact of high frequency noise on the time domain reconstruction of the separated reflected waves. Because the analysis is built on linear systems theory, the incident waves should be small perturbations to limit the effect of linearization (Lee and Vitkovsky 2010).

## **2.3 Numerical verification**

To verify the dual-sensor wave separation algorithm, numerical simulations have been conducted. A single pulse hydraulic pressure wave is used as the incident wave in the numerical investigations since it has never been studied previously for wave separation.

### **2.3.1 System layout and procedure**

For the numerical study, a metallic pipeline system with two short deteriorated sections and one relatively long section with a change of pipe class is considered. The layout of the numerical pipeline system is given in Figure 2.2. The physical

details of the pipe sections are summarised in Table 2.1. The length of each reach is carefully designed to satisfy the Courant condition for MOC simulations (with a time step of 0.05 ms). The system is a reservoir-pipeline-reservoir (R-P-R) system. Reservoir 1 has a constant head of 60 m, and the constant head for Reservoir 2 is 57 m. The total length of the pipeline is 1 km. The steady-state flow is calculated as 0.264 m<sup>3</sup>/s, corresponding to a velocity of 1.34 m/s. For the normal pipe sections, the internal diameter is 500 mm, the wall thickness is 8 mm, the Reynolds number is  $4.75 \times 10^5$  (indicating turbulent flow) and the wave speed is 1154 m/s. Two pipe sections L<sub>2</sub> and L<sub>9</sub> which have thinner wall thicknesses (6 and 5 mm), larger internal pipe diameters (504 and 506 mm) and smaller wave speeds (1083 and 1036 m/s) are placed in the system to simulate the deteriorated sections (e.g. extended internal corrosion). Pipe section L<sub>7</sub> with a length of approximately 150 m, the same internal diameter as the majority of the pipe, but a thinner wall thickness (7 mm) and thus a lower wave speed (1123 m/s), is placed in the system to simulate a section of a lesser pipe class. A significantly higher Darcy-Weisbach friction factor (0.03) has been assigned to sections L<sub>2</sub> and L<sub>9</sub> to represent the effect of a much higher wall surface roughness as would result from a pipe that has experienced corrosion. The dual sensor (with a sensor spacing of 0.9809 m) is placed in the middle of the pipeline system at  $T_1$  and  $T_2$ , respectively. A side-discharge valve which is located at 0.9809 m upstream from  $T_1$  is used as the transient generator. The steady-state discharge through the side-discharge valve is set as 0.01 m<sup>3</sup>/s. The length of each pipe section has been selected to satisfy the Courant condition for the time domain method of characteristics (MOC) simulations so that no interpolation scheme is required (Chaudhry 2014).



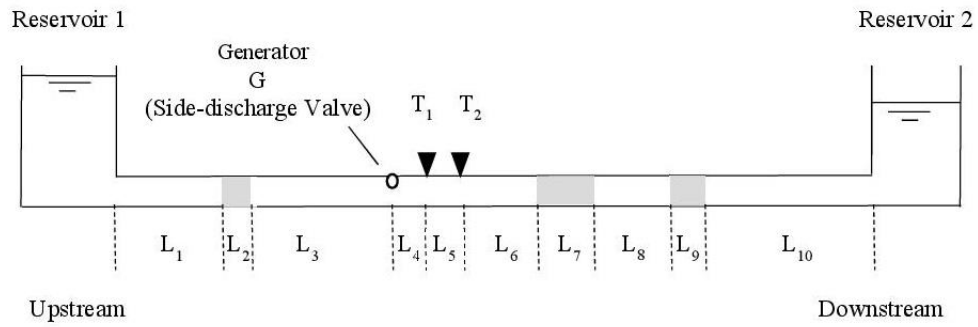


Figure 2.2 Layout of the pipeline system used in the numerical simulations (not to scale). See Table 2.1 for physical details.

Table 2.1 Physical details of the pipe sections used in the numerical simulations.

Link	Length (m)	Internal diameter (mm)	Wall thickness (mm)	Wave speed (m/s)	Friction factor (-)
L1	415.9593	500	8	1154	0.017
L2	12.0213	504	6	1083	0.030
L3	72.0096	500	8	1154	0.017
L4	0.9809	500	8	1154	0.017
L5	0.9809	500	8	1154	0.017
L6	69.9901	500	8	1154	0.017
L7	150.1451	500	7	1123	0.017
L8	60.0080	500	8	1154	0.017
L9	11.9944	506	5	1036	0.030
L10	205.9890	500	8	1154	0.017

An incident pressure wave is generated at time  $t = 0.1$  s by manoeuvring the side-discharge valve. The incident wave is a pulse wave with 20 ms duration, generated by fully closing the side discharge valve then fully opening it again (the manoeuvre is designed numerically that the incident pulse pressure wave as generated has a shape similar to a cosine function changing from 0 to  $\pi$ , to make the signal more realistic than a sharp instantaneous rise). The response of the pipeline system is simulated by MOC with steady friction only.

### 2.3.2 Wave separation results

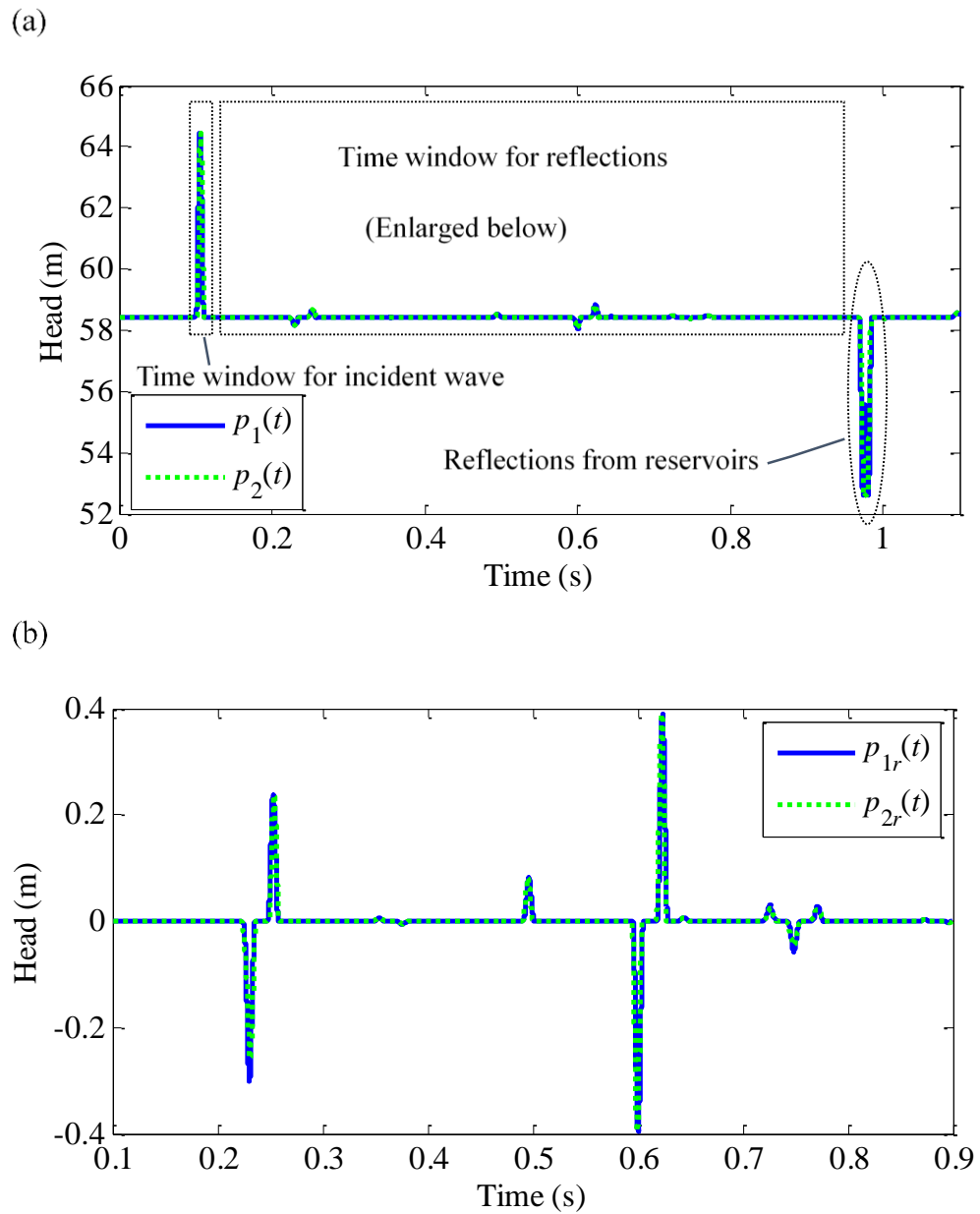


Figure 2.3 (a) Numerical pressure traces measured at  $T_1$  and  $T_2$ ; and (b) Enlarged view of the wave reflections from deteriorated sections in the numerical study.

The pressure traces at  $T_1$  and  $T_2$  are used as the measurements  $p_1(t)$  and  $p_2(t)$ , which are shown in Figure 2.3(a). The wave separation algorithm is applied to the measurements  $p_1(t)$  and  $p_2(t)$  by following the steps which were outlined

previously. The reflected waves  $p_{1r}(t)$  and  $p_{2r}(t)$  are shown in Figure 2.3(b). It can be seen from Figure 2.3(b) that the pressure reflections as recorded by the dual-sensor possess a complex form of pressure wave fluctuations, although only three uniform sections with lower wave speeds are considered. This complexity is due to the superimposition of the reflections from the three thinner-walled sections.

Figure 2.4(a) shows the reflections from upstream of  $T_1$  and Figure 2.4(b) gives the reflections from downstream. The pressure waves  $p_{1r\_A}^+(t)$  and  $p_{1r\_A}^-(t)$  are obtained by using the analytic expression of the transfer function between two sensors according to Equations (2.11) and (2.12), while  $p_{1r\_E}^+(t)$  and  $p_{1r\_E}^-(t)$  are calculated from the experimental transfer function which is estimated by using the extracted incident waves according to Equation (2.14). The analytically and experimentally determined transfer functions are consistent within the bandwidth of the incident wave.

For a comprehensive comparison, the wave separation results are compared with predicted results as computed directly from the MOC. The predicted results for upstream reflections ( $p_{1r\_P}^+(t)$ ) as shown in Figure 2.4(a)) are obtained from MOC modelling the system similar to that depicted in Figure 2.2, but only with one deteriorated section  $L_2$  existing on the upstream side of the sensors. On the downstream side of the sensors, there are just uniform intact pipes (i.e.  $L_7$  and  $L_9$  are set as the same as the intact sections). Hence, the simulated reflections only come from upstream and are a result of section  $L_2$ .

Similarly, the predicted results for downstream reflections ( $p_{1r\_p}^-(t)$  as shown in Figure 2.4(b)) are acquired by MOC modelling with no defective sections existing on the upstream side of the sensors. So that reflections only happen on the downstream side of the sensors and include reflections from sections L<sub>7</sub> and L<sub>9</sub>.

It can be seen in Figure 2.4 that the reflections from the three thinner-walled pipe sections are separated and clearly shown in the directional waves  $p_{1r}^+(t)$  and  $p_{1r}^-(t)$  respectively. The separation results from two different transfer function calculation methods (analytical and experimental) are almost identical, and both of them have an excellent match with the MOC predictions. It should be noted that the separated results of directional waves include multiple reflections while the predicted results do not. The multiple reflections are due to secondary reflections between anomalous sections on the two sides of sensors. For example, when all three thinner-walled sections are considered in the simulation, the major wave reflections from sections L<sub>7</sub> and L<sub>9</sub> (as shown in Figure 2.4(b)) will propagate from downstream to upstream, pass the dual-sensor and then be reflected by section L<sub>2</sub> as secondary reflections. These secondary reflections will then propagate downstream as part of  $p_{1r}^+(t)$ . Nevertheless, the numerical simulation demonstrates that the proposed wave separation approach is valid for pipelines excited by single pulse incident pressure waves.

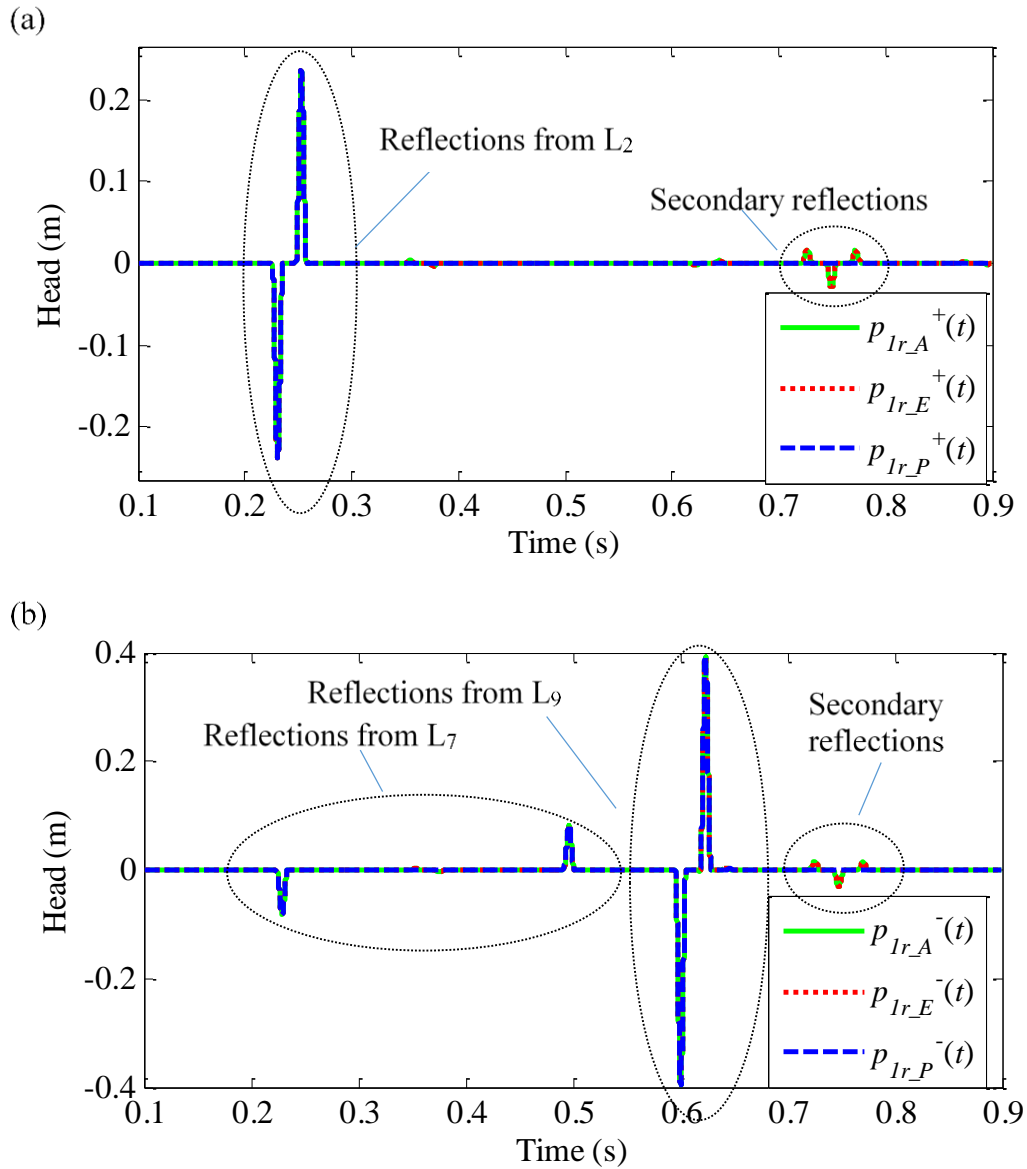


Figure 2.4 (a) Directional reflected pressure waves travelling from upstream to downstream; and (b) Directional reflected pressure waves travelling from downstream to upstream.

## 2.4 Experimental verification

Laboratory experiments have been conducted in a single copper pipeline in the Robin Hydraulics Laboratory at the University of Adelaide. The laboratory system is a copper pipe (internal diameter 22.14 mm, total length 37.43 m)

bounded by two pressurised tanks. The pressurised tanks can be isolated by an in-line valve to make the system a reservoir-pipeline-valve (R-P-V) configuration. A step incident pressure wave is used to avoid repetition from the numerical study and it better represents the incident waves used in the field.

### 2.4.1 System layout and procedure

The layout of the pipeline system used in the experiments is shown in Figure 2.5 and the physical details are given in Table 2.2. The wave speeds are calculated using the theoretical wave speed formula (Wylie and Streeter 1993). The following parameter values are used: Young's modulus of a copper pipe  $E = 124.1$  GPa, restraint factor for thick-walled copper pipe anchored throughout  $c_1 = 1.006$ , bulk modulus of elasticity of water at  $15^\circ\text{C}$  is  $K = 2.149$  GPa, and density of water at  $15^\circ\text{C}$  is  $\rho = 999.1$  kg/m<sup>3</sup>. The restraint factor is a dimensionless parameter that depends on the elastic properties and the constraint condition of the pipe (Wylie and Streeter 1993).

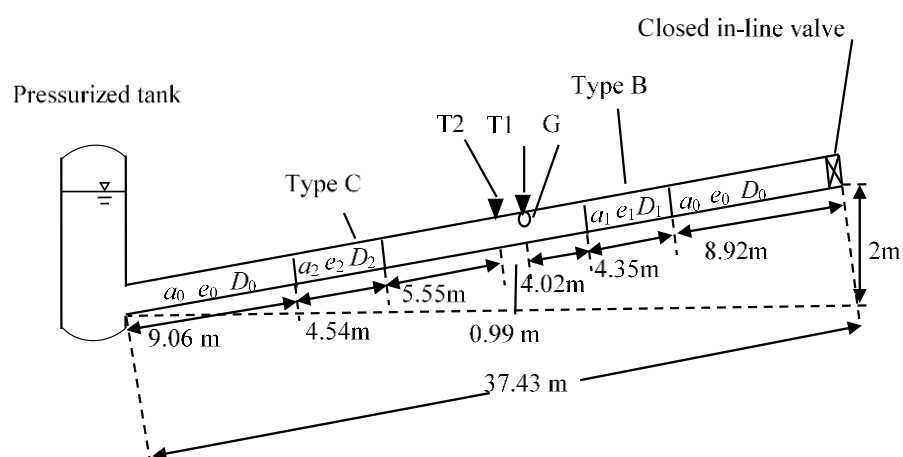


Figure 2.5 System layout of the experimental pipeline system.

Table 2.2 Physical details of the pipeline system used in the laboratory experiments.

Pipe class	Internal diameter (symbol = value (mm))	Wall thickness (symbol = value (mm))	Wave speed (symbol = value (m/s))
A	$D_0 = 22.14$	$e_0 = 1.63$	$a_0 = 1319$
B	$D_1 = 22.96$	$e_1 = 1.22$	$a_1 = 1273$
C	$D_2 = 23.58$	$e_2 = 0.91$	$a_2 = 1217$

The majority of the pipeline is in Class A. Two short pipe sections of Class B and C, respectively, which have thinner wall thicknesses than that of Class A, are placed in the system to simulate pipe sections with wall deterioration. The head in the pressurised tank was controlled at approximately 31 m during the experiments. The in-line valve at the other end was kept closed during the experiments.

A solenoid side-discharge valve was used as the transient generator (G) and placed at the same location as pressure sensor  $T_1$ . The other pressure sensor ( $T_2$ ) was located upstream (on the left) of the transient generator separated by a distance of 0.99 m. A step pressure wave was generated by abruptly closing the solenoid valve in approximately 3 ms. The pressure responses were measured by the two sensors with a sampling frequency of 20 kHz.



### **2.4.2 Wave separation results**

The original head responses as measured by the dual-sensor are shown in Figure 2.6(a). The pressure oscillations before the first boundary reflection are the focus and shown in Figure 2.6(b). The steady-state head is determined by averaging a period of measurement before the incident wave and then subtracting from the raw measurements. The start time of the incident wave is set to zero, and the pressure traces are truncated before the boundary reflections (the reflection from the tank and the closed in-line valve). It can be seen that the reflections from the Class B and Class C pipe sections are superimposed in the two measured traces, resulting in complex reflections that are difficult to interpret.

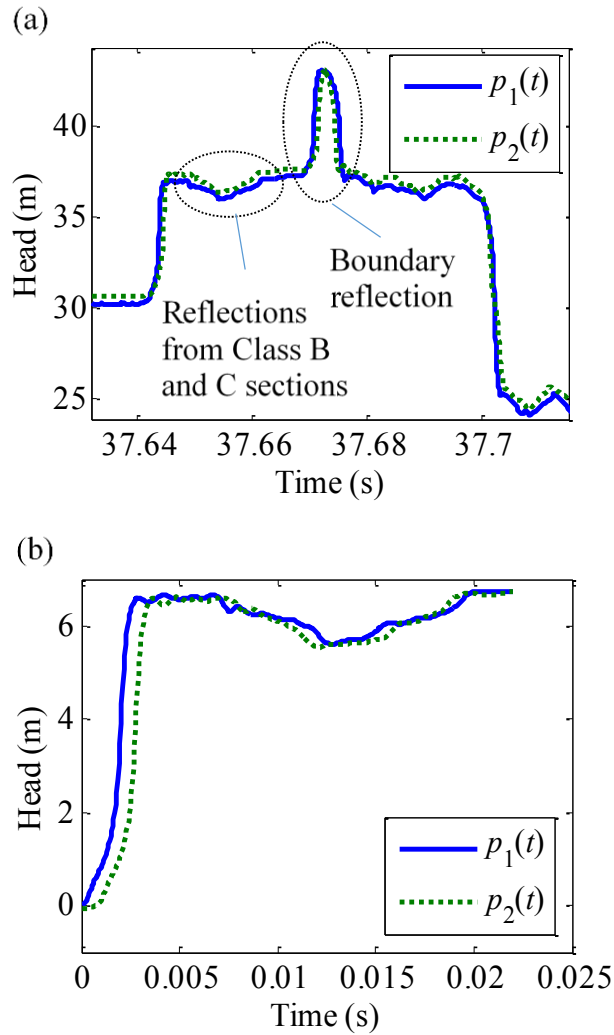


Figure 2.6 (a) Original pressure traces measured in the laboratory experiments; and (b) pressure oscillations before the first boundary reflection.

The incident waves and the wave reflections are then extracted as outlined previously in Step 1 in the analysis methodology. The measured incident waves are used to determine the experimental transfer function  $H(s)$  using Equation (2.14) in Step 3. The amplitude spectrums of the measured wave reflections are checked to investigate the effective frequency range (the bandwidth) as depicted in Figure 2.7. It is found that most energy of the reflected signals is in frequencies less than 300 Hz, which represents the useful bandwidth of the pressure waves. Given this, an upper frequency bound of 600 Hz was adopted

to avoid effects of noise in the high frequency range and also to cover the effective bandwidth of the reflected waves.

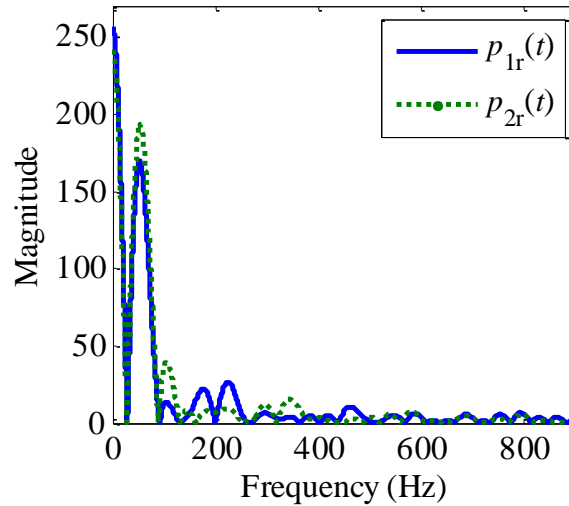


Figure 2.7 Amplitude spectrum of the reflected waves.

The positive and negative travelling pressure reflection waves  $p_{1r}^+(t)$  (propagating towards the closed in-line valve) and  $p_{1r}^-(t)$  (propagating towards the tank) are determined by Equations (2.21) and (2.22) for frequencies up to 600 Hz in Step 4. The results are given in Figure 2.8 and compared with the predicted results generated by MOC simulations (the procedure is the same as that used in the numerical study, i.e. only deterioration on one side is considered when generating the predicted results). The steady-state pressure in the MOC model is set equal to the measured steady-state pressure in the laboratory. The step incident wave in the MOC model is designed according to the measured incident step wave with a rise time of 3 ms and a pressure head magnitude of 6.60 m. The shape of a cosine function changing from  $\pi$  to  $2\pi$  is adopted to simulate the curved wave front.

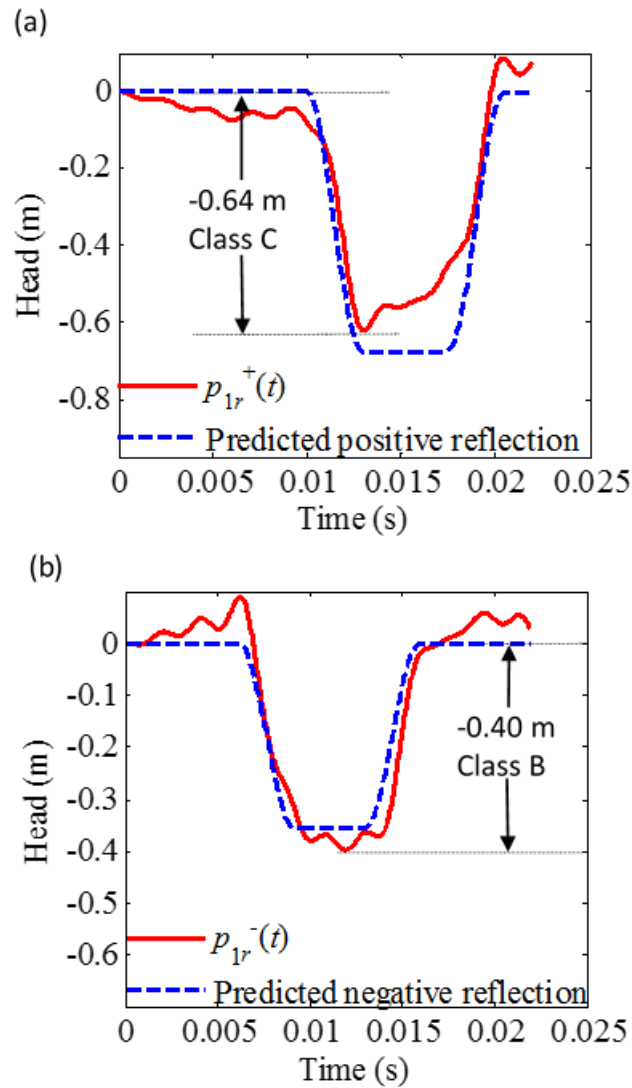


Figure 2.8 (a) Directional reflected pressure waves travelling towards the closed in-line valve; and (b) directional reflected pressure waves travelling towards the tank.

It can be seen that in the directional waves, reflections from the two thinner-walled sections are separated, and the determined directional wave reflections are consistent with the numerically generated predicted results. The superimposed reflection is reconstructed by adding  $p_A^+(t)$  and  $p_A^-(t)$  together and then comparing them with the original measured wave reflection  $p_{1r}(t)$  in

Figure 2.9. The reconstructed reflection trace is generally consistent with the original measured reflection trace, with small differences due to the exclusion of the frequency components above 600 Hz in the wave separation. Overall, the experimental results have illustrated the feasibility of the separation of directional travelling pressure waves in pipelines using a dual-sensor.

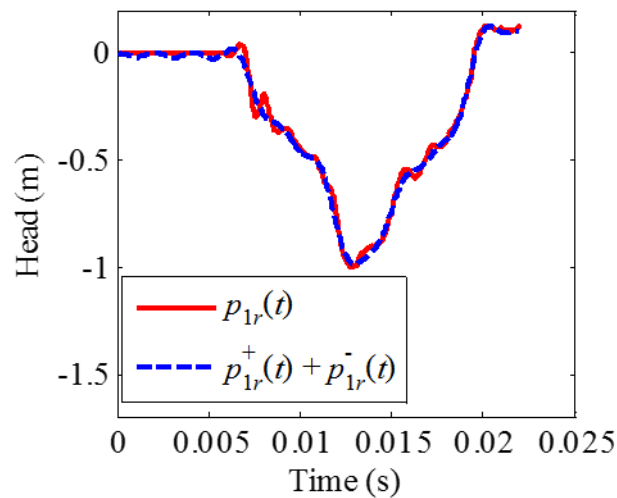


Figure 2.9 Comparison between the original wave reflections measured at  $T_1$  (the solid line) and the superimposed result of the determined directional wave reflections (the dashed line).

### 2.4.3 Application to pipeline condition assessment

The time domain condition assessment technique as outlined in Gong *et al.* (2013) is now applied to the resultant directional reflection waves [ $p_{1r}^+(t)$  and  $p_{1r}^-(t)$  as shown in Figure 2.8] to determine the wall thickness of the thinner-walled sections (the Class B and C sections). It is known that the external diameter of the experimental pipeline is uniform and the change in class affects the internal diameter. For this scenario, the relationship between the relative

size of a wave reflection and the relative change in the wall thickness is derived as:

$$p_n = \frac{\sqrt{\frac{(K/\rho)(1+e_{rc})}{K/\rho+e_{rc}a_0^2}} - \left[1 - 2e_{rc} \frac{(K/E)a_0^2c_1}{K/\rho - a_0^2}\right]^2}{\sqrt{\frac{(K/\rho)(1+e_{rc})}{K/\rho+e_{rc}a_0^2}} + \left[1 - 2e_{rc} \frac{(K/E)a_0^2c_1}{K/\rho - a_0^2}\right]^2} \quad (2.23)$$

where  $p_n$  represents the normalized head perturbation of the reflected wave and is defined as  $p_n = (p_r - p_i)/p_i$ , where  $p_r$  and  $p_i$  are the sizes of reflected wave and incident wave respectively;  $e_{rc}$  is the relative change in wall thickness and is defined as  $e_{rc} = (e_d - e_0)/e_0$ , where  $e_0$  and  $e_d$  represent the wall thickness in the intact and deteriorated section respectively;  $a_0$  is the wave speed in the intact pipe. Note that Equation (2.23) is derived under an assumption for lossless elastic pipelines.

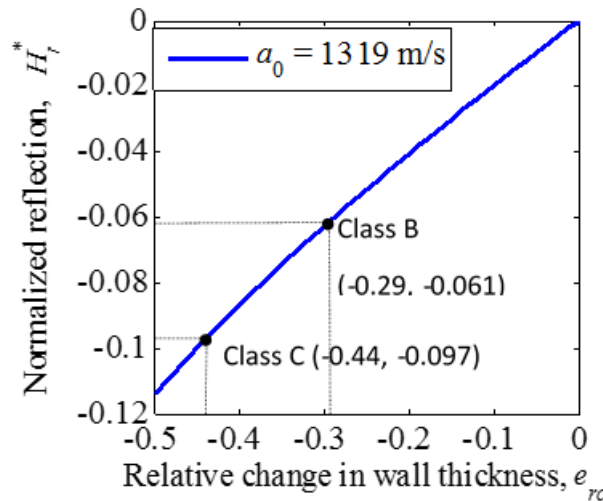


Figure 2.10 Relationship between the normalized wave reflection ( $p_n$ ) and the relative change in the wall thickness ( $e_{rc}$ ) for the experimental pipeline.

The plot of Equation (2.23) is given in Figure 2.10. The theoretical wave speed in the intact (Class A) pipe is considered, which is  $a_0 = 1319$  m/s as in Table 2.2. The range of  $e_{rc}$  used is from  $e_{rc} = -0.5$  to  $e_{rc} = 0$ , which represents wall thickness variation from half the original wall thickness to the original wall thickness. The plot can serve as a look-up chart for condition assessment for pipes with internal changes in wall thickness.

It is obvious that the original pressure measurements as shown in Figure 2.9 cannot be directly used for condition assessment because the reflections from the Class B and the Class C sections are superimposed. In contrast, the separated directional wave reflections as shown in Figure 2.8 show the wave reflections from the two sections separately and clearly, and they can easily be used for further analysis.

The values of the relative wave reflections ( $p_r - p_i$ ) from the Class C and Class B sections are determined from the minima of  $p_{1r}^+(t)$  and  $p_{1r}^-(t)$  respectively as shown in Figure 2.8, for which the results are  $p_{1r}^+ - p_i = -0.64$  m and  $p_{1r}^- - p_i = -0.40$  m respectively. The magnitude of the incident step wave is determined as  $p_i = 6.60$  m from the measured trace shown in Figure 2.6(b). As a result, the normalized reflections for the Class C and Class B sections are  $p_n^+ = -0.097$  and  $p_n^- = -0.061$ , respectively. Referring to the look-up chart in Figure 2.10, the relative change in wall thickness corresponding to these two wave reflections are  $e_{rc}^+ = -0.44$  and  $e_{rc}^- = -0.29$ , respectively. Finally, using the wall thickness of the Class A pipe of  $e_0 = 1.63$  mm, the wall thicknesses in the

Class C and Class B sections are determined by the reflection analysis as  $e^+ = 0.91$  mm and  $e^- = 1.16$  mm, respectively. Compared with the wall thicknesses as given by the manufacturer ( $e_2 = 0.92$  mm and  $e_1 = 1.22$  mm as shown in Table 2.2), the wall thicknesses are estimated with relatively high accuracy.

These results have demonstrated that the wave separation algorithm as developed in this research can significantly facilitate pipeline condition assessment by resolving the complexity due to wave superposition.

## 2.5 Discussion

Some practical issues related to real applications of transient-based pipeline condition assessment are discussed in this section. Recommended future work is also presented.

### 2.5.1 Detection resolution

The spatial resolution of detection is limited by the effective bandwidth of the pressure waves, which is itself related to the sharpness of the wave front. For a ramp incident wave, theoretically one can accurately diagnose deteriorated sections only with a length longer than  $T_i a_d / 2$ , where  $T_i$  is the rise time of the ramp wave front and  $a_d$  is the wave speed in the deteriorated pipe section (Gong et al. 2013c). Sections shorter than that may still be detectable but will not give a full-sized reflection, therefore the change in wall thickness will be underestimated. In the experimental study, the rise time of the incident step was about 3 ms. Using a wave speed of 1,300 m/s, the threshold is calculated as approximately 2 m.



### **2.5.2 Detection range**

The length of pipe that can be assessed reliably mainly depends on the signal-to-noise ratio (SNR). It is expected that measurements in the field can have stronger noise than in the laboratory (e.g. due to pump operations). The frequency range to include in the analysis should be selected carefully to balance the SNR and detection resolution (as discussed above). Usually low frequency waves have better SNR than high frequency components, because the latter typically have less initial energy and suffer higher damping rates. A spectrum analysis for the wave reflections (as described in the Experimental verification section) will help to determine the useful bandwidth. Nevertheless, field trials by the authors confirmed that a step transient pressure wave can travel many kilometres with insignificant attenuation in water transmission mains (diameter 600 mm) (Stephens et al. 2013; Gong et al. 2015; Gong et al. 2016c). However, the sharpness of the wavefront decreases over the distance of propagation.

### **2.5.3 Non-uniform deterioration**

In real pipelines, deteriorated sections most likely have non-uniform wall thickness variations. As a result, the wave reflections may not have sharp edges as shown in the laboratory study. In such cases, the extrema of the reflections should be used to calculate the normalized head perturbation. The determined wall thickness represents the general condition of the deteriorated section.

### **2.5.4 Other sources of reflections**

In addition to deteriorated pipe sections, wave reflections can be induced by other sources, which typically include changes in pipe material and class, leaks, blocks, branches and air pockets. Prior information of pipeline systems (e.g. as constructed drawings) will be helpful in identifying the source of wave reflections. The characteristics of the wave form can also facilitate the categorisation (e.g. discrete blocks introduce extended positive reflections while leaks introduce extended negative reflections). Note that pipe joints typically do not introduce noticeable reflections, since the dimension of joints is much smaller than the effective wavelength.

### **2.5.5 Accuracy of transfer function**

A topic for future work is to enhance the accuracy in the determination of the transfer function between the two pressure sensors. Error in the transfer function will affect the wave separation and therefore the condition assessment. It can be induced by background noise and the inconsistency among pressure transducers (i.e. for the same pressure condition, different sensors may give slightly different readings). The use of sensor arrays to provide redundant information may be helpful in enhancing the accuracy.

## **2.6 Conclusions**

A wave separation algorithm has been developed for extracting the directional hydraulic transient pressure waves that travel along a pipeline in the downstream and upstream directions, respectively. Discrete incident transient waves, such as a single pulse or a step wave which are commonly used in

transient-based pipeline fault detection, are used to excite a pipeline system and induce reflections from deteriorated pipe sections. The wave separation is achieved by analysing the pressure responses of the pipeline as measured by a proximity dual-sensor setup. The wave separation resolves the complexity of the superposition of travelling pressure waves in a pipeline, providing directional information of wave reflections and simplifying the wave forms. The key contributions of the research include: (1) the development of an experimental technique for estimating the transfer function between two sensors that is more practical than analytical estimation for real pipelines with parameter uncertainties; (2) the further development of the wave separation algorithm to enhance the accuracy for the separation of the relatively small wave reflections by removing the dependence of the relatively large incident wave; and (3) the verification of the wave separation technique by numerical and laboratory experiments.

In the numerical simulations, a discrete pulse pressure wave is considered as the incident wave, which has not been studied previously for hydraulic transient wave separation in pipelines. Three thinner-walled pipe sections are placed in the numerical pipeline system, with two of them simulating deteriorated sections due to internal corrosion and one simulating a section with a lower pipe class. The wave separation algorithm has been successfully implemented, with the resultant directional reflection waves consistent with the predicted results.

Experimental verification of the hydraulic transient wave separation algorithm has been conducted. A step transient pressure wave generated by a fast closure of a side-discharge valve is considered as the incident wave. The original

pressure responses as measured by the dual-sensor spaced at 0.99 m include the superimposed wave reflections from two thinner-walled pipe sections. The directional reflection waves are extracted by the wave separation algorithm and the results are generally consistent with the numerically generated predicted results. An existing pipeline condition assessment technique that is based on direct time domain analysis of wave reflections is adopted and applied to the extracted directional waves. The wall thicknesses of the two thinner-walled pipe sections are estimated from the reflected waves by using the pipe wall thickness change look-up chart and the results are consistent with the specifications provided by the manufacturer. The experimental study has validated the proposed wave separation algorithm, and confirmed the usefulness of the algorithm in transient-based pipeline condition assessment and fault detection.

## **Chapter 3**

# **Leak detection in virtually isolated pipe sections within a complex pipe system using a two-source-four-sensor transient testing configuration**

## **(Journal Paper 2)**

Publication details:

Shi, H., Gong, J., Simpson, A. R., Zecchin, A. C., and Lambert, M. F. (2019). "Leak detection in virtually isolated pipe sections within a complex pipe system using a two-source-four-sensor transient testing configuration." *Journal of Hydraulic Engineering*, submitted on 9 Oct 2018, under review.

This page is intentionally left blank

## Statement of Authorship

Title of Paper	Leak detection in virtually isolated pipe sections within a complex pipe system using a two-source-four-sensor transient testing configuration
Publication Status	<input type="checkbox"/> Published <input type="checkbox"/> Accepted for Publication <input checked="" type="checkbox"/> Submitted for Publication <input type="checkbox"/> Unpublished and Unsubmitted work written in manuscript style
Publication Details	Shi, H., Gong, J., Simpson, A. R., Zecchin, A. C., and Lambert, M. F. (2019). "Leak detection in virtually isolated pipe sections within a complex pipe system using a two-source-four-sensor transient testing configuration." <i>Journal of Hydraulic Engineering</i> , submitted on 9 Oct 2018, under review.

### Principal Author

Name of Principal Author (Candidate)	He Shi		
Contribution to the Paper	Conception and design of the project; Analysis and interpretation of the research data; Drafting the manuscript.		
Overall percentage (%)	75%		
Certification:	This paper reports on original research I conducted during the period of my Higher Degree by Research candidature and is not subject to any obligations or contractual agreements with a third party that would constrain its inclusion in this thesis. I am the primary author of this paper.		
Signature		Date	14/03/2019

### Co-Author Contributions

By signing the Statement of Authorship, each author certifies that:

- i. the candidate's stated contribution to the publication is accurate (as detailed above);
- ii. permission is granted for the candidate to include the publication in the thesis; and
- iii. the sum of all co-author contributions is equal to 100% less the candidate's stated contribution.

Name of Co-Author	Jinzhe Gong		
Contribution to the Paper	Conception and design of the project; Analysis and interpretation of the research data; Critically reviewing the manuscript.		
Signature		Date	15/3/2019

Name of Co-Author	Angus Simpson		
Contribution to the Paper	Conception and design of the project; Analysis and interpretation of the research data; Critically reviewing the manuscript.		
Signature		Date	15/3/2019

Name of Co-Author	Aaron Zecchin		
Contribution to the Paper	Conception and design of the project; Analysis and interpretation of the research data; Critically reviewing the manuscript.		
Signature		Date	15/3/19

Name of Co-Author	Martin Lambert		
Contribution to the Paper	Conception and design of the project; Analysis and interpretation of the research data; Critically reviewing the manuscript.		
Signature		Date	15/3/19



## **Abstract**

Leak detection in complex pipeline systems is challenging due to complex wave reflections. This research proposes a new technique for leak detection in targeted pipe sections within complex water supply pipe systems using controlled hydraulic transient pressure waves and a two-source-four-sensor transient testing configuration. To “virtually” isolate a targeted pipe section for independent analysis, a two-source-four-sensor transient testing configuration is used to extract the transfer matrix of the targeted pipe section. Two pairs of pressure sensors are used to bracket the targeted pipe section by “virtually” isolating it, with the two sensors in each pair being in close proximity. Two transient pressure wave generators are used, which bracket the four sensors and the “virtually” isolated pipe section. It is found that the imaginary part of the difference between two elements in the transfer matrix is sensitive to leaks. The result should be zero if no leak is present, while a leak will introduce a sinusoidal pattern. The period and the magnitude of the pattern are related to the location and impedance of the leak, respectively. An algorithm is developed to extract the leak information, which is applicable to multiple leaks. Two numerical case studies are conducted to validate the new leak detection technique. Case 1 is on a single pipe system with two leaks and deteriorated pipe sections, and pulse pressure waves are used as the excitation. Case 2 is on a simple pipe network with one leak and pseudo-random binary signals are used as the excitation. The successful determination of the leak location and impedance proves the concept. Challenges in field applications are also discussed.

This page is intentionally left blank

### **3.1 Introduction**

Pressurized pipeline systems are used globally to transmit and distribute all types of fluids, such as water, gas and oil. Leakages in pipeline systems can cause economic loss and sometimes environmental hazards. Leakage in water distribution systems (WDSs) is a global issue, and the leakage rate ranges from about 10% in well-maintained WDSs (Beuken et al. 2006) to above 50% in poorly managed systems (Mutikanga et al. 2009). In Australia, every year an estimated 19,000 breaks in water transmission mains occur, resulting in the loss of 265 GL of potable water (Bureau of Meteorology 2016). This water loss is equivalent to the annual consumption of 1.5 million homes and represents a value over \$700m. Leak detection in WDSs, however, is challenging due to the sheer size of the pipe network and the fact that most pipes are buried underground.

Acoustic correlation analysis is the most commonly used technique for leak detection in water pipelines at present (Li et al. 2015). Two acoustic sensors are attached to two separate fittings on a pipeline and record the vibration on the pipe fittings (using accelerometers) or the acoustic pressure in water (using hydrophones). Cross-correlation of the two measured signals can indicate whether there is a common acoustic source (a leak) in the pipe, and also the time difference for the acoustic wave to travel from the source to the two sensors (Muggleton et al. 2006). The time difference, together with the known distance and wave speed between the two sensors, can be used to calculate the leak location. The acoustic correlation-based leak detection techniques are relatively easy to implement since only passive listening is required. However,

leak-induced acoustic waves are prone to interference from water network background noise and environmental noise, also the propagation is sensitive to the pipe material (Butterfield et al. 2018).

An alternative is the hydraulic transient-based leak detection approach (Puust et al. 2010). Controlled hydraulic transient pressure waves can be generated in pipelines by transient wave generators. Usable devices include valves (Meniconi et al. 2011b; Shucksmith et al. 2012; Gong et al. 2016b), portable pressure tanks (Brunone et al. 2008), and spark plugs (Gong et al. 2018a). The incident wave typically has a magnitude of a few meters of pressure head, and propagates along the pipe under test at high speed (around 1200 m/s in metallic pipes). Wave reflections occur at physical discontinuities (e.g. a leak), and can be measured by pressure transducers. Over the past two decades, a number of transient-based leak detection techniques have been developed, and they can be generally allocated into the following categories: (1) techniques that analyse wave reflections (either from the raw data or pre-processed data) using principles of time-domain reflectometry (TDR) (Shucksmith et al. 2012; Nguyen et al. 2018); (2) techniques that analyse the frequency response function (FRF) of a pipe system (Covas et al. 2005; Lee et al. 2005b; Gong et al. 2013a); (3) techniques that focus on the damping of transient pressure responses in a pipeline system (Wang et al. 2002); and (4) inverse transient analysis (ITA)-based techniques that search for an optimal numerical pipe model whose response matches the pressure measurements (Kapelan et al. 2003; Covas and Ramos 2010; Capponi et al. 2017). The transient-based techniques are attractive because a single test can cover up to kilometres of pipe length,

and the active testing approach can reveal other information such as blockages (Meniconi et al. 2013) and pipe wall condition (Gong et al. 2016c).

Despite that many transient-based leak detection techniques have been proposed, applications in real water pipeline systems are limited. A significant challenge to all the transient-based techniques is the complexity of real water pipeline systems. For the TDR-based techniques, leak-induced reflections can be difficult to distinguish from other reflections, such as those from cross-connections and unknown wall thickness changes. The FRF of a single pipe system is more sensitive to leaks than extended wall thickness changes (Duan et al. 2011), therefore the FRF-based techniques are advantageous over the TDR-based techniques in detecting small leaks. However, most FRF-based techniques are only applicable to reservoir-pipeline-reservoir (R-P-R) or reservoir-pipeline-valve (R-P-V) systems. Duan (2016a) has recently extended the FRF-based leak detection to simple pipe systems with a branch or a loop. The conventional FRF-based approach is difficult to be further extended to more complex pipe systems, because the FRF considered in all previous studies is a representation of the overall system, and complex systems will produce FRFs that too complex to analyse. The transient-damping-based technique is also difficult to apply to complex pipe systems, in which the damping can be related to many factors (Nixon and Ghidaoui 2006). The ITA-based techniques require iterative parameter calibration using optimization algorithms. The process is computationally costly and not robust if the number of parameters to calibrate is large (Vítkovský et al. 2007).

The current research presented here proposes a new frequency-domain technique for leak detection in targeted pipe sections. A key innovation of the new technique is the concept of utilizing a special transient pressure generation and sensing configuration, combined with custom developed signal processing algorithms, to “virtually” break any complex pipeline systems down to its simplest form – a single pipe section – for independent condition diagnosis. To the authors’ knowledge, this work is the first to utilize this approach for leak detection in targeted pipe sections embedded in complex systems. The proposed approach is opposite to the conventional research idea of gradually adapting the transient-based leak detection techniques developed for simple pipeline systems (e.g. reservoir-pipeline-valve or reservoir-pipeline-reservoir systems) to more complex pipe systems and networks (Ghazali et al. 2012; Duan 2016a; Capponi et al. 2017).

The virtual isolation of a pipe section is achieved by a two-source-four-sensor transient testing strategy, which enables the extraction of the transfer matrix of a selected pipe section out of any complex pipe system. A transfer matrix of a pipe section is a full representation of the wave propagation characteristics as defined by the physical properties of the section (Wylie and Streeter 1993; Chaudhry 2014). This testing strategy was originally developed and used in the field of acoustic analysis of ducts (Munjal and Doige 1990; Salissou and Panneton 2010), and recently it was validated using a short water pipeline in the laboratory by Yamamoto et al. (2015) for studying the transfer matrix of resistance (orifices) and compliance (trapped air). Note that the focus of Yamamoto et al. (2015) was purely on the individual components, and not on long pipe sub-systems. The current research adapts this technique to the transfer

matrix extraction of long sections in complex water pipe systems, with significantly more complex wave interaction phenomena. Different from the sine-sweep approach for system excitation as used in Yamamoto et al. (2015), the current research numerically tests pulse pressure waves that are easy to generate and pseudo-random binary signals that are tolerant to interference.

A major contribution of the current research is the development of a new leak detection algorithm based on the analysis of the transfer matrix of a “virtually” isolated pipe section. This transfer matrix is related to the “virtually” isolated pipe section only, and is independent from any complexities of the rest of the pipe system (e.g. boundary conditions and other network connectivity). As a result, the extracted transfer matrix is much simpler than the transfer matrix of the overall pipe system, and the analysis is more straightforward. In contrast, conventional FRF-based leak detection algorithms use the transfer matrix of the overall pipe system to derive the frequency-domain pressure response at particular locations, which is system specific and can be difficult to analyse for complex pipe systems. In this research, it has been found that the imaginary part of the difference between two elements in the transfer matrix is sensitive to leaks. The result should be zero if no leak is present, while a leak will introduce a sinusoidal pattern. The period and the magnitude of the pattern are related to the location and impedance of the leak, respectively. Multiple leaks will introduce multiple sinusoidal patterns. An algorithm is developed to extract the leak information, including the number of leaks as well as their locations and impedance (which relates to the size of the leak).

In the following, the technique for extracting the transfer matrix of a targeted pipe section and the new algorithm for leak detection of a “virtually” isolated pipe section are described. Two numerical case studies (a simple pipeline system and a simple pipe network) are conducted to validate the transfer matrix extraction technique and the proposed leak detection algorithm. Challenges in real world applications are also discussed.

## 3.2 Transfer matrix extraction for a targeted pipe section

### 3.2.1 Transfer matrix of a uniform pipe section

For a uniform single pipe section, the relation between the two sets of pressure and flow as observed at the two ends of the section can be written as (Wylie and Streeter 1993; Chaudhry 2014)

$$\begin{Bmatrix} Q \\ H \end{Bmatrix}_D = \begin{bmatrix} \cosh(\mu L) & -\frac{1}{Z_p} \sinh(\mu L) \\ -Z_p \sinh(\mu L) & \cosh(\mu L) \end{bmatrix} \begin{Bmatrix} Q \\ H \end{Bmatrix}_U \quad (3.1)$$

where  $H$  and  $Q$  are complex pressure head and flow in the frequency domain; the footnotes  $D$  and  $U$  represent the downstream and the upstream boundary of the pipe section respectively;  $L$  is the length of the pipe;  $Z_p$  is the characteristic impedance of the pipe section; and  $\mu$  is the propagation factor.

The propagation factor is described by (Wylie and Streeter 1993; Chaudhry 2014)



$$\mu = \frac{\sqrt{-\omega^2 + j\omega gAR}}{a} \quad (3.2)$$

where  $\omega$  is the angular frequency;  $j = \sqrt{-1}$  is the imaginary unit;  $g$  is the gravitational acceleration;  $A$  is the cross sectional area of the pipe;  $a$  is the wave speed; and  $R$  is the frictional resistance term. For turbulent and laminar flows,  $R = fQ_0 / (gDA^2)$  and  $R = 32\nu / (gD^2A)$  respectively, in which  $f$  is the Darcy-Weisbach friction factor;  $Q_0$  is the steady-state flow rate;  $D$  is the diameter of the pipe; and  $\nu$  is the kinematic viscosity of the fluid.

The characteristic impedance is (Wylie and Streeter 1993; Chaudhry 2014)

$$Z_p = \frac{\mu a^2}{j\omega gA} \quad (3.3)$$

### 3.2.2 Two-source-four-sensor testing strategy for water pipes

The proposed configuration for extracting the transfer matrix of a targeted pipeline section using the two-source-four-sensor strategy and hydraulic transient testing is illustrated in Figure 3.1. Two pairs of pressure transducers ( $T_A, T_B$  and  $T_C, T_D$ ) bracket the section of pipe under investigation. The distance between the two transducers in each pair,  $L_{AB}$  for the distance between  $T_A$  and  $T_B$ , and  $L_{CD}$  for that between  $T_C$  and  $T_D$ , are recommended to be short (recommended to be 2 m or less) in real pipelines, such that the transfer function of the short pipe reach can be calibrated or theoretically determined (Shi et al. 2017). Two transient pressure wave generators are used, with one on each side of the pipe section of interest.

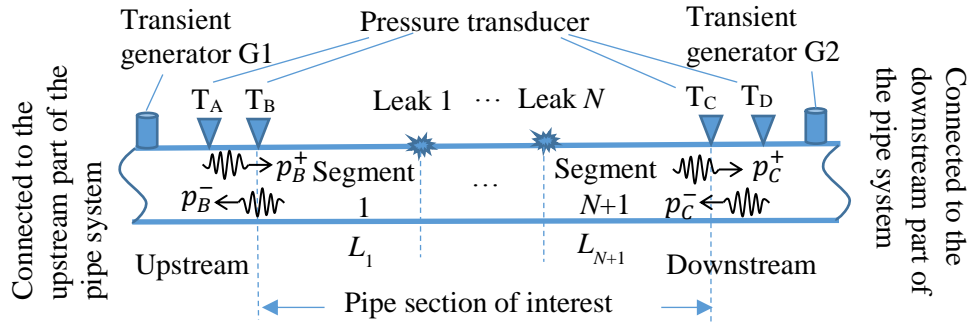


Figure 3.1 Test configuration for extracting the transfer matrix of a targeted pipe section with  $N$  leaks.

The pipe section between transducer  $T_B$  and  $T_C$  can be considered as a linear-time-invariant (LTI) system. The directional travelling waves  $p_B^+$  and  $p_C^-$  which are travelling into the pipe section are considered as the input to the LTI system; while the waves  $p_B^-$  and  $p_C^+$  that are travelling out of the section are taken as the output. A pair of directional travelling pressure waves (e.g.  $p_B^+$  and  $p_B^-$ ) can be determined from the pressure waves (pressure perturbations) as measured by two transducers in close proximity (e.g.  $p_A$  and  $p_B$  as the pressure perturbations measured by  $T_A$  and  $T_B$ ) and using a wave separation technique (Shi et al. 2017). Once the directional pressure waves at the two boundaries of a pipe section are obtained, the pipe section can be regarded as an independent system since the boundary conditions are entirely specified. As a result, two pairs of transducers enable the analysis of a specific section of pipe independently from the complexities of the rest of the pipeline system.

### 3.2.3 Determination of the transfer matrix using pressure measurements

For a pipe section with unknown conditions, the transfer matrix have four elements ( $U_{11}$ ,  $U_{12}$ ,  $U_{21}$  and  $U_{22}$ ) to be determined. Two independent transient tests are needed to establish four equations to solve these four unknowns. This can be achieved by generating transient excitation from the two sides of the pipe section one at a time, and measure the pressure responses by the four transducers in each test. Based on Equation (3.1), the flowing matrix can be established

$$\begin{bmatrix} Q_{C1} & Q_{C2} \\ H_{C1} & H_{C2} \end{bmatrix} = \begin{bmatrix} U_{11} & U_{12} \\ U_{21} & U_{22} \end{bmatrix} \begin{bmatrix} Q_{B1} & Q_{B2} \\ H_{B1} & H_{B2} \end{bmatrix} \quad (3.4)$$

where  $H_{B1}$ ,  $Q_{B1}$ ,  $H_{C1}$  and  $Q_{C1}$  are the complex pressure head and flow in the first transient test (using transient generator 1), and  $H_{B2}$ ,  $Q_{B2}$ ,  $H_{C2}$  and  $Q_{C2}$  are the parameters in the second test (using transient generator 2). The complex head parameters at the location of T<sub>B</sub> ( $H_{B1}$  and  $H_{B2}$ ) and those at the location of T<sub>C</sub> ( $H_{C1}$  and  $H_{C2}$ ) can be readily obtained by transforming the measured time-domain pressure perturbations ( $p_B$  and  $p_C$ ) into the frequency domain. The complex flow parameters ( $Q_{B1}$ ,  $Q_{B2}$ ,  $Q_{C1}$  and  $Q_{C2}$ ) are not directly measured but can be obtained from the directional pressure waves (Yamamoto et al. 2015).

The directional pressure waves (as in the frequency domain, represented by capital letters) at the location of  $T_B$ , for example, can be described by (Shi et al. 2017)

$$P_B^+ = \frac{P_A S_{AB} - P_B S_{AB}^2}{1 - S_{AB}^2} \quad (3.5)$$

$$P_B^- = \frac{P_B - P_A S_{AB}}{1 - S_{AB}^2} \quad (3.6)$$

where  $S_{AB}$  is the transfer function of the short pipe section between  $T_A$  and  $T_B$ , and its expression is

$$S_{AB}(i\omega) = e^{-\mu L_{AB}} \quad (3.7)$$

The complex flow can be calculated by (Yamamoto et al. 2015)

$$Q_B = \frac{P_B^+ - P_B^-}{Z_P} \quad (3.8)$$

As a result, the complex flow  $Q$  can be determined from the pressure measurements, the transfer function of the short pipe reach between the two pressure transducers, and the characteristic impedance of the pipeline, and the expression for  $Q_B$  is

$$Q_B = \frac{2P_A S_{AB} - P_B - P_B S_{AB}^2}{Z_P (1 - S_{AB}^2)} \quad (3.9)$$

Note that more information on pipe transient flow determination using multiple pressure measurements can be found in the literature (Washio et al. 1996b; Kashima et al. 2013). Once the head and flow are all known, elements in the transfer matrix can be obtained by solving the matrix in Equation (3.4).

### 3.3 Leak detection for a targeted pipe section using transfer matrix

#### 3.3.1 Transfer matrix for a pipe section with leaks

For a uniform pipe section with  $N$  leaks, as depicted in Figure 3.1, the relationship between the two sets of pressure and flow as observed at the two boundaries can be written as

$$\begin{Bmatrix} Q \\ H \end{Bmatrix}_D = \mathbf{U}_N \begin{Bmatrix} Q \\ H \end{Bmatrix}_U \quad (3.10)$$

where  $\mathbf{U}_N$  is the overall transfer matrix for the pipe section with  $N$  leaks. Considering the effect of pipe wall friction is small for large diameter water pipelines and to highlight the leak-induced effect, the effect of friction is neglected in the following derivation but discussed later. The field matrix  $\mathbf{F}_i$  for a frictionless and uniform pipe segment  $i$  is given as (Chaudhry 2014)

$$\mathbf{F}_i = \begin{bmatrix} \cos\left(\frac{\omega L_i}{a}\right) & -\frac{j}{Z_c} \sin\left(\frac{\omega L_i}{a}\right) \\ -jZ_c \sin\left(\frac{\omega L_i}{a}\right) & \cos\left(\frac{\omega L_i}{a}\right) \end{bmatrix} \quad (3.11)$$

where  $Z_c = a / gA$  and it is the characteristic impedance of the frictionless pipe; and  $L_i$  is the length of the  $i^{\text{th}}$  pipe segment.

The point matrix  $\mathbf{P}_i$  for the  $i^{\text{th}}$  leak is given as (Lee et al. 2005b; Gong et al. 2013a)

$$\mathbf{P}_i = \begin{bmatrix} 1 & -\frac{1}{Z_{Li}} \\ 0 & 1 \end{bmatrix} \quad (3.12)$$

where  $Z_{Li} = 2H_{Li} / Q_{Li}$  and it is the impedance of the  $i^{\text{th}}$  leak,  $H_{Li}$  is the steady-state head at the leak and  $Q_{Li}$  is the steady-state discharge out of the leak.

The overall transfer matrix  $\mathbf{U}_N$  for the pipe section with  $N$  leaks can be expressed by orderly multiplying the field matrices and point matrices from downstream to upstream and written as

$$\mathbf{U}_N = \begin{bmatrix} U_{11.N} & U_{12.N} \\ U_{21.N} & U_{22.N} \end{bmatrix} = \mathbf{F}_{N+1} \mathbf{P}_N \dots \mathbf{F}_2 \mathbf{P}_1 \mathbf{F}_1 \quad (3.13)$$

where the footnote  $N$  denotes the number of leaks in the pipe section.

Now considering a uniform pipe section with one leak, the overall transfer matrix  $\mathbf{U}_1$  is

$$\mathbf{U}_1 = \begin{bmatrix} U_{11.1} & U_{12.1} \\ U_{21.1} & U_{22.1} \end{bmatrix} = \mathbf{F}_2 \mathbf{P}_1 \mathbf{F}_1 \quad (3.14)$$

After substituting Equations (3.11) and (3.12) into Equation (3.14) and performing appropriate matrix operations, the analytical expressions of the transfer matrix elements are given as

$$U_{11.1} = \cos\left(\frac{\omega L}{a}\right) + \frac{jZ_c}{2Z_{L1}} \sin\left(\frac{\omega L}{a}\right) - \frac{jZ_c}{2Z_{L1}} \sin\left[\frac{(1-2x_{L1})\omega L}{a}\right] \quad (3.15)$$

$$U_{12.1} = -\frac{j}{Z_c} \sin\left(\frac{\omega L}{a}\right) - \frac{1}{2Z_{L1}} \cos\left(\frac{\omega L}{a}\right) - \frac{1}{2Z_{L1}} \cos\left[\frac{(1-2x_{L1})\omega L}{a}\right] \quad (3.16)$$

$$U_{21.1} = -jZ_c \sin\left(\frac{\omega L}{a}\right) - \frac{Z_c^2}{2Z_{L1}} \cos\left(\frac{\omega L}{a}\right) + \frac{Z_c^2}{2Z_{L1}} \cos\left[\frac{(1-2x_{L1})\omega L}{a}\right] \quad (3.17)$$

$$U_{22.1} = \cos\left(\frac{\omega L}{a}\right) + \frac{jZ_c}{2Z_{L1}} \sin\left(\frac{\omega L}{a}\right) + \frac{jZ_c}{2Z_{L1}} \sin\left[\frac{(1-2x_{L1})\omega L}{a}\right] \quad (3.18)$$

where  $x_{L1}$  is the dimensionless leak location, which is defined as the ratio of the distance from the leak to the upstream end of the pipe to the total length of the pipe  $L$ . For the  $i^{th}$  leak,  $x_{Li} = (L_1 + L_2 + \dots + L_i) / L$ . The transfer matrix  $\mathbf{U}_N$  for a pipe section with  $N$  leaks can be derived following the same procedure.

### 3.3.2 Extraction of the leak-induced feature

The impact of a leak on the transfer matrix can be seen through comparing the transfer matrix of the pipe section with one leak [Equations (3.15) to (3.18)] with that of an intact pipe [Equation (3.11)]. In this research, one of the leak-induced features, the imaginary part of  $U_{22} - U_{11}$ , is selected to determine the

leak location and size. When there is no leak,  $U_{22} - U_{11}$  is null since the two elements should be identical according to Equations (3.1) and (3.11).

For a pipe section with only one leak, the imaginary part of the difference between  $U_{22,1}$  [Equation (3.18)] and  $U_{11,1}$  [Equation (3.15)] is defined as  $T_1$  and given as

$$T_1 = \text{Im}\{U_{22,1} - U_{11,1}\} = \frac{Z_c}{Z_{L1}} \sin\left[\frac{(1-2x_{L1})L\omega}{a}\right] \quad (3.19)$$

where  $\text{Im}\{\}$  gives the imaginary part of the parameter in the bracket.

It can be seen from Equation (3.19) that  $T_1$  is a sinusoidal function that is related to the leak impedance (which relates to the leak size) and the leak location (except for a leak at a normalized location of 0.5). The leak locations defines the period of the sinusoidal pattern and the leak impedance defines the amplitude of the pattern. This finding is similar to that observed from the pressure response of a reservoir-pipeline-valve (R-P-V) system with a leak (Lee et al. 2005b), however this sinusoidal function is different from the one observed in the previous work. The expression in Equation (3.19) is much simpler and independent from any boundary conditions.

Using the same approach as outlined above, the leak-induced effects for a pipe system with two leaks,  $T_2$ , can be derived as



$$T_2 = \text{Im}\{U_{22.2} - U_{11.2}\} = \frac{Z_c}{Z_{L1}} \sin\left[\frac{(1-2x_{L1})L\omega}{a}\right] + \frac{Z_c}{Z_{L2}} \sin\left[\frac{(1-2x_{L2})L\omega}{a}\right] \quad (3.20)$$

Equation (3.20) indicates that two leaks will introduce two sinusoidal patterns with different periods.

For a pipe system with three leaks, the analytical expression of  $T_3$  is derived as

$$T_3 = \text{Im}\{U_{22.3} - U_{11.3}\} = \frac{Z_c}{Z_{L1}} \sin\left[\frac{(1-2x_{L1})L\omega}{a}\right] + \frac{Z_c}{Z_{L2}} \sin\left[\frac{(1-2x_{L2})L\omega}{a}\right] + \frac{Z_c}{Z_{L3}} \sin\left[\frac{(1-2x_{L3})L\omega}{a}\right] + T_h \quad (3.21)$$

where  $T_h$  is a higher order term

$$T_h = \frac{Z_c Z_c Z_c}{4Z_{L1} Z_{L2} Z_{L3}} \left\{ \begin{array}{l} \sin[(1-2x_{L1})L\omega/a] - \\ \sin[(1-2x_{L2})L\omega/a] + \\ \sin[(1-2x_{L3})L\omega/a] + \\ \sin[(1-2x_{L1} + 2x_{L2} - 2x_{L3})L\omega/a] \end{array} \right\} \quad (3.22)$$

The ratio of the characteristic impedance of pipe and the impedance of the  $i^{\text{th}}$  leak can be described as

$$\frac{Z_c}{Z_{Li}} = \frac{a}{\sqrt{2gH_L}} \frac{C_d A_L}{A} \quad (3.23)$$

where  $C_d A_L / A$  is the normalized leak size. For small leaks (which are difficult to detect by conventional techniques and are the focus of this research), the impedance of the leak is much larger than the characteristic impedance of the

pipe (i.e. the value of  $Z_c/Z_{Li}$  is much smaller than 1). Consequently, the value of the higher order term  $T_h$  will be significantly smaller than the values of the first three items in Equation (3.21) and negligible. For a pipe section with more than three leaks, the higher order term will be even smaller. As a result, the leak-induced effect on the transfer matrix of a pipe section with  $n$  leaks can be described as

$$T_N = \text{Im}\{U_{22,N} - U_{11,N}\} = \sum_{i=1}^N \frac{Z_c}{Z_{Li}} \sin\left[\frac{(1-2x_{Li})L\omega}{a}\right] \quad (3.24)$$

### 3.3.3 Determination of the leak location and size

$T_N$  in Equation (3.24) is a frequency domain signal with the x-axis being the frequency and in the unit of Hz. If assuming the x-axis to be a time axis, the leak-induced signal  $T_N$  has a wave form equivalent to a superposition of  $N$  sinusoidal waves. The period/frequency of each sinusoidal wave corresponds to the location of a leak, and the amplitude is related to the leak impedance. In other words, the frequency and amplitude of each sinusoidal wave in the  $T_N$  signal can be used to determine the location and impedance (size) of a leak.

The frequency and amplitude information of the  $N$  sinusoidal waves can be extracted by applying the Fourier transform to the  $T_N$  signal (i.e. treat it like a time-domain signal) and analysing the resultant signal  $T_N$ . Since the leak-induced signals in  $T_N$  are sinusoidal waves, based on the theory of the discrete Fourier transform (Oppenheim et al. 1997), each leak will be represented by a

spike in the imaginary part of  $T_N$ . If the normalized leak location is in the range of (0, 0.5), the corresponding spike in the imaginary part of  $T_N$  will be negative in value; if the normalized leak location is in the range of (0.5, 1), the corresponding spike will be positive in value. As a result, the location of the  $i^{\text{th}}$  leak is determined by

$$x_{Li} = \frac{1}{2} + \text{Sgn} \left\{ \text{Im} \left\{ T_N(F_{Pi}) \right\} \right\} \left( \frac{F_{Pi} a}{2L} \right) \quad (3.25)$$

where  $F_{Pi}$  is the “frequency” that corresponds to the  $i^{\text{th}}$  peak in the imaginary part of  $T_N$ ,  $T_N(F_{Pi})$  is the complex value at the peak frequency, and  $\text{Sgn} \{ \}$  assesses the sign of the parameter in the bracket.

The ratio of the pipe characteristic impedance to the impedance of the  $i^{\text{th}}$  leak is determined by

$$\frac{Z_c}{Z_{Li}} = 2 \text{Abs} \left\{ T_N(F_{Pi}) \right\} \quad (3.26)$$

where  $\text{Abs} \{ \}$  gives the absolute value of the parameter in the bracket. The effective leak size can be determined by substituting Equation (3.26) into Equation (3.23) and performing appropriate mathematical operations, with the final expression being

$$C_d A_L = 2 \text{Abs} \left\{ T_N(F_{Pi}) \right\} \frac{A \sqrt{2gH_L}}{a} \quad (3.27)$$

### 3.4 Numerical simulations

Two numerical case studies are conducted to validate the proposed targeted leak detection technique. The system in Case 1 is a transmission main and that in Case 2 is a water distribution network.

#### 3.4.1 Case 1: A single pipe with two leaks

##### *System information*

The layout of the pipeline system studied in Case 1 is given in Figure 3.2. The system is an R-P-V system with two leaks and two deteriorated pipe sections (e.g. sections with extended corrosion). The pipe deterioration is represented by a reduction in wave speed. The pipe section of interest (the targeted pipe section) is the section between  $T_B$  and  $T_C$ . The length information is given in Figure 3.2 and other system parameters are summarized in Table 3.1. The normalized leak locations are  $x_{L1} = 0.2$  and  $x_{L2} = 0.7$ , respectively. The ratios of the leak impedance to the characteristic impedance of pipe are  $Z_c/Z_{L1} = 0.00415$  and  $Z_c/Z_{L2} = 0.0116$ , respectively.

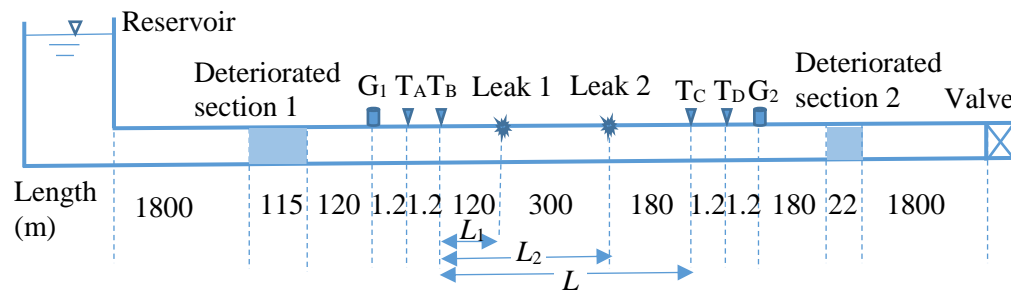


Figure 3.2 Layout of the single pipeline system in Case 1.

Table 3.1 System information for Case 1.

Parameter	Value
Reservoir head, $H_r$	60 m
Pipe internal diameter, $D$	500 mm
Effective opening area of Leak 1, $C_{d1}A_{L1}$	22 mm <sup>2</sup>
Effective opening area of Leak 2, $C_{d2}A_{L2}$	63 mm <sup>2</sup>
Steady-state flow through valve, $Q_0$	0.2 m <sup>3</sup> /s
Steady-state flow through Leak 1, $Q_{L1}$	0.75 L/s
Steady-state flow through Leak 2, $Q_{L2}$	2.08 L/s
Wave speed in intact pipe, $a_0$	1200 m/s
Wave speed in deteriorated section 1, $a_1$	1150 m/s
Wave speed in deteriorated section 2, $a_2$	1100 m/s
Darcy-Weisbach friction factor, $f$	0.015
Normalised location of Leak 1, $x_{L1}$	0.2
Normalised location of Leak 2, $x_{L2}$	0.7
Impedance ratio of pipe to Leak 1, $Z_c/Z_{L1}$	0.00415
Impedance ratio of pipe to Leak 2, $Z_c/Z_{L2}$	0.0116

### ***Pressure response***

The method of characteristics (MOC) (Wylie and Streeter 1993; Chaudhry 2014) is used to simulate the transient response of the pipeline system. Steady friction is considered to evaluate its impact on the leak detection. The time step used is 0.0001 s. Two transient tests are simulated: in the first test, a pulse pressure

wave with a duration of 10 ms and a peak size about 6 m is generated at  $G_1$  (by opening and then closing a side-discharge valve); and in the second test, a pulse pressure wave with the same characteristics is generated at  $G_2$ . The pressure traces at  $T_A$  and  $T_D$  as obtained from the first test are shown in Figure 3.3. The standing pressure at  $T_D$  is lower than that at  $T_A$  because of the effect of steady friction. The two large pulses in the  $T_A$  and  $T_D$  traces are the incident pulse wave, arriving at  $T_A$  and  $T_D$  in sequence. A number of small pulses can be seen in both traces, and they are reflections from the two leaks and the two deteriorated pipe sections. Due to the complexity introduced by the deteriorated pipe sections, it is difficult to identify the leaks from the pressure responses even if the reflections are clear.

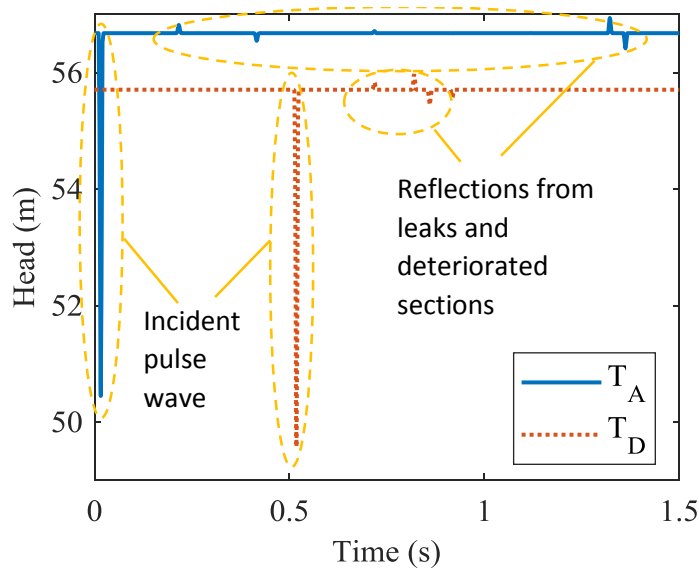


Figure 3.3 Pressure responses at  $T_A$  and  $T_D$  as obtained from transient test 1 (using generator  $G_1$ ) in Case 1.

### ***Transfer matrix extraction***

The pressure measurements at  $T_A$  to  $T_D$  are transformed to the frequency domain by the Fourier transform after the steady-state head being offset from

the original measurement. The calculations outlined in previous sections are then conducted to obtain the transfer matrix for the pipe section between  $T_B$  and  $T_C$ . The imaginary part of the numerically obtained transfer matrix element  $U_{22}$  is shown in Figure 3.4, together with the theoretical counterpart for the same pipe section with two leaks and that for the same pipe section without any leak (only the results up to 30 Hz are shown for clarity). The theoretical results are calculated using Equation (3.13) with the friction effect neglected.

It can be seen from Figure 3.4 that the numerically determined  $\text{Im}\{U_{22}\}$  (solid line) is highly consistent with the theoretical result for the same pipe section with two leaks (dotted line), except for the small error close to the zero frequency. In contrast, the theoretical  $\text{Im}\{U_{22}\}$  for the same pipe section but with no leaks is quite different because it only has one sinusoidal component that is related to the fundamental frequency of the pipe section [refer to Equation (3.11)].

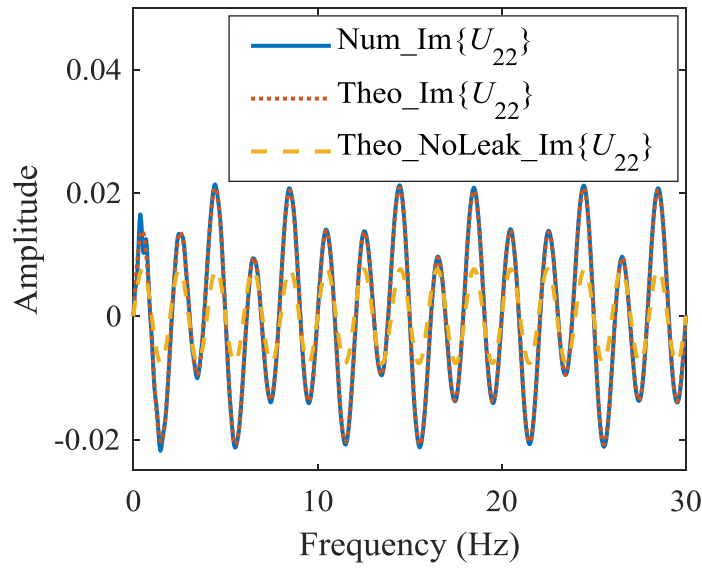


Figure 3.4 Imaginary part of transfer matrix element  $U_{22}$  as obtained from numerical simulations and the transfer matrix extraction technique for the pipe section with two leaks in Case 1 (solid line), compared with the theoretical result for the same pipe section with two leaks (dotted line), and the theoretical result for the pipe section when it is intact (dashed line).

The results of  $\text{Im}\{U_{22} - U_{11}\}$  are then obtained from the numerically derived transfer matrix and also from analytical calculations [using Equation (3.20)], and the results are compared in Figure 3.5 (only the results up to 30 Hz are shown for clarity). The result obtained from the numerical simulations is highly consistent with the theoretical result. Note that if there is no leak, the result of  $\text{Im}\{U_{22} - U_{11}\}$  should be zero across all the frequencies.



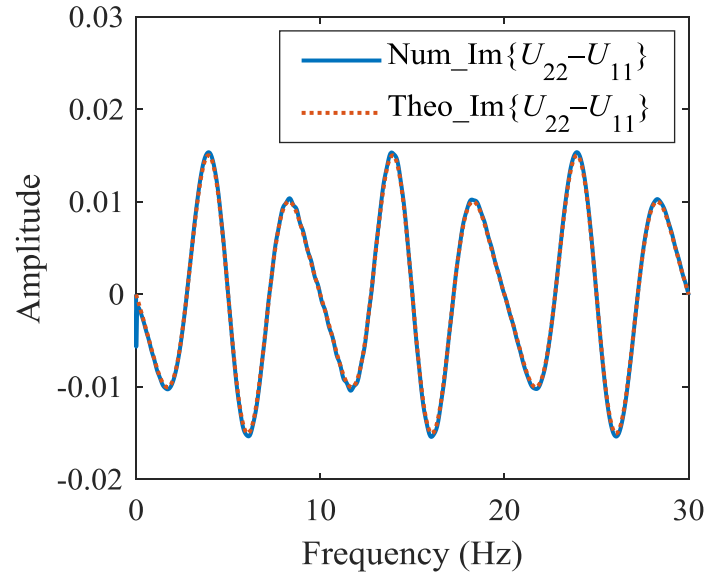


Figure 3.5 Imaginary part of  $(U_{22} - U_{11})$  as obtained from numerical simulations and the transfer matrix extraction technique for the pipe section with two leaks in Case 1 (solid line), and the theoretical result for the same pipe section with two leaks (dotted line).

### ***Leak detection***

Leak detection is conducted by analysing the numerically obtained  $\text{Im}\{U_{22} - U_{11}\}$  using the technique outline in Equations (3.25) and (3.26), and the results are shown in Figure 6. The two distinctive pikes indicate that there are two leaks in the pipe section of interest. The normalized locations are determined as  $x_{L1} = 0.20$  and  $x_{L2} = 0.70$ , respectively, as shown by the x-axis, and the values of the impedance ratio are  $Z_c/Z_{L1} = 0.00427$  and  $Z_c/Z_{L2} = 0.0119$ , respectively, according to the size of the two spikes. The results are highly consistent with the theoretical values as shown in Table 3.1. The successful detection has validated the effectiveness of the proposed targeted leak detection technique.

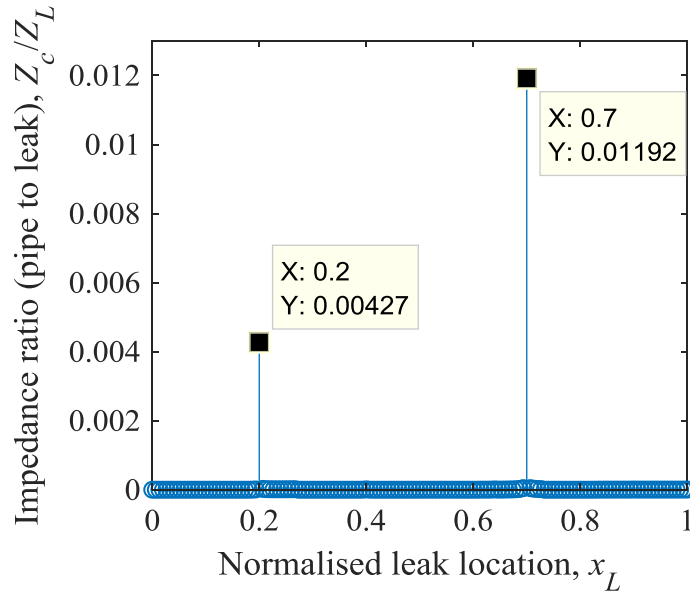


Figure 3.6 Results from the proposed leak detection technique showing the existence of two leaks (indicated by the two spikes), their normalised locations and the corresponding values of impedance ratio (pipe to leak).

### 3.4.2 Case 2: A pipe section in a pipe network

#### *System information*

The layout of the pipeline system studied in Case 2 is given in Figure 3.7. The system is a simple pipe network with two reservoirs. Four pressure transducers are used ( $T_A$  to  $T_D$ ). The pipe section of interest is the section between  $T_B$  and  $T_C$ , and one leak exists in this section. Two transient wave generators are used, which are placed on an upstream pipe section and a downstream pipe section, respectively. Key pipe system information is summarized in Table 3.2.

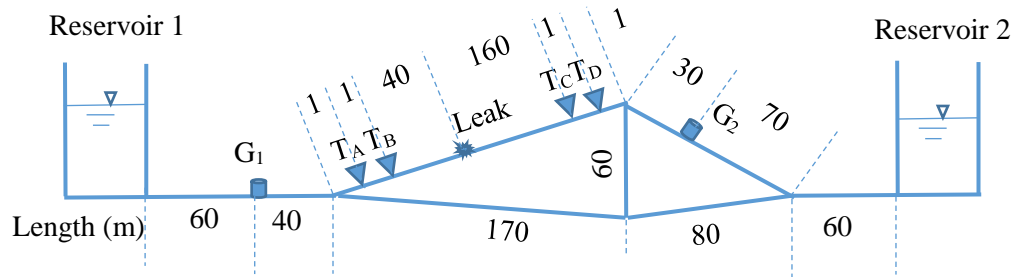


Figure 3.7 Layout of the simple pipe network in Case 2.

Table 3.2 System information for Case 2.

Parameter	Value
Head of Reservoir 1, $H_{r1}$	60 m
Head of Reservoir 2, $H_{r2}$	57 m
Internal diameter of all pipe sections, $D$	200 mm
Effective opening area of the leak, $C_d A_L$	47 mm <sup>2</sup>
Steady-state flow in the pipe directly downstream of the leak, $Q_0$	27 L/s
Steady-state flow through the leak, $Q_L$	1.6 L/s
Wave speed in all pipe sections, $a_0$	1000 m/s
Darcy-Weisbach friction factor, $f$	0.015
Normalised location of the leak, $x_L$	0.2
Impedance ratio of pipe to leak, $Z_c/Z_L$	0.0443

### ***Pressure response***

MOC (Wylie and Streeter 1993; Chaudhry 2014) is used to simulate the transient response of the simple pipe network system. Steady friction is considered to evaluate its impact on the leak detection. The time step used is 0.0002 s. Two transient tests are simulated using the generator  $G_1$  and  $G_2$ , respectively. Considering the complexity of the network, the excitation signal used in both tests is a special type of pseudo-random binary signal (PRBS) – the inverse repeat signal (IRS) instead of discrete pulse or step signals. The IRS is a periodic signal that is suitable for extracting the pipeline frequency response (Gong et al. 2013b), and it can be generated by continuously altering the opening area of a side-discharge valve between two levels (Gong et al. 2016b). The IRS signal used in this study is the same as that described in Gong et al. (2013b) (simulating 10 shift registers with a clock frequency of 100 Hz), and has a period of 20.46 s. Each numerical test has a simulated time duration of 20 mins, which is over 58 periods of the IRS. Spectrum analysis confirms that the pipe system reaches the steady-oscillatory condition after 200 s (about 10 periods). A section of the pressure traces at  $T_A$  as obtained from the first test is shown in Figure 3.8. Due to the pseudo-random nature of the excitation signal, the pressure response of the pipe system is complex and difficult to analysis directly in the time domain.

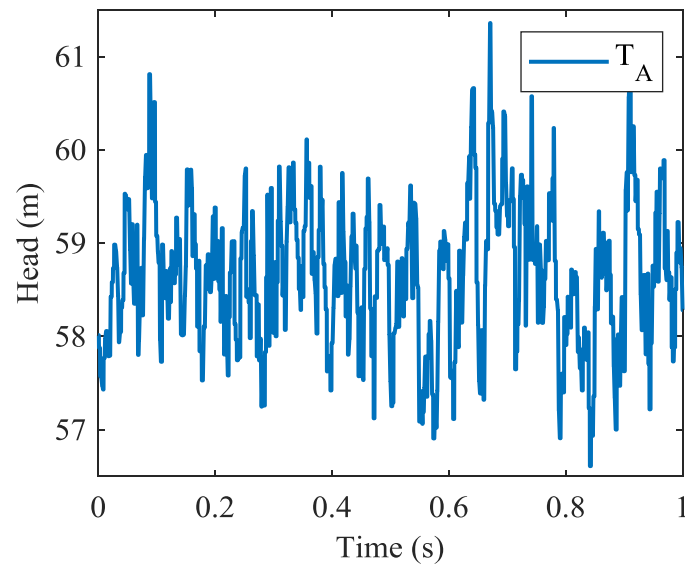


Figure 3.8 Pressure responses at  $T_A$  as obtained from transient test 1 (using generator G1) in Case 2.

### ***Transfer matrix extraction***

The same technique as outlined in previous sections can be used to extract the transfer matrix of the target pipe section. Since the excitation is a periodic signal, the pressure response should also be periodic once the pipe system is in the steady-oscillatory condition (Wylie and Streeter 1993; Chaudhry 2014). The analysis in this numerical study only focus on one period of the steady-oscillatory pressure response for each sensor in each test. Averaging of the results from multiple periods may be needed in real applications. The determined  $\text{Im}\{U_{22} - U_{11}\}$  is shown in Figure 3.9, together with the theoretical result for comparison [using Equation (3.19)]. It can be seen that the numerically determined result is highly consistent with the theoretical result.

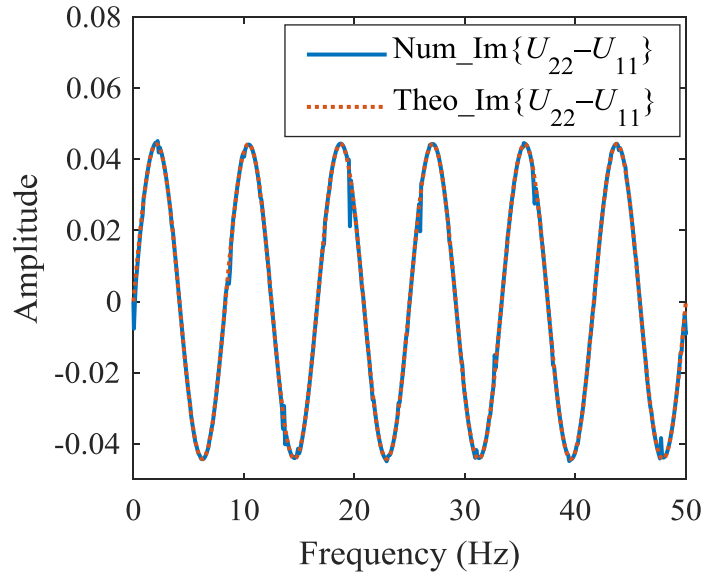


Figure 3.9 Imaginary part of  $(U_{22} - U_{11})$  as obtained from numerical simulations and the proposed transfer matrix extraction technique for the pipe section with one leak in Case 2 (solid line), and the theoretical result for the same pipe section with one leak (dotted line).

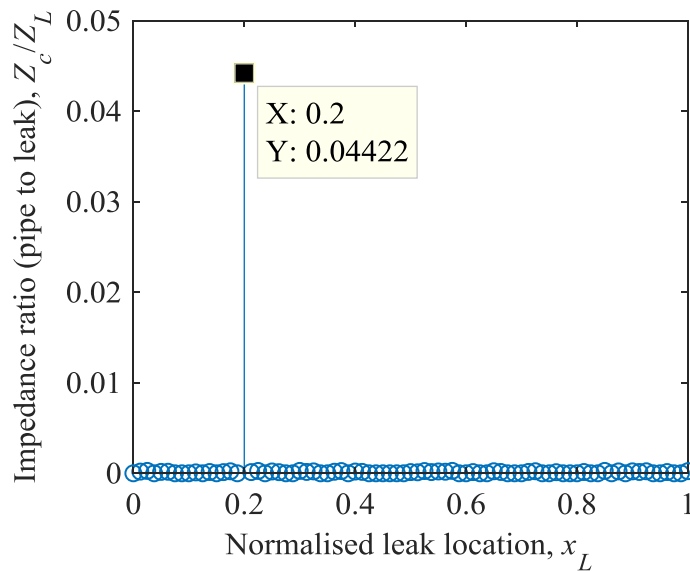


Figure 3.10 Results from the proposed leak detection technique showing the existence of one leaks (indicated by the single spike), the normalised leak location and the corresponding value of impedance ratio (pipe to leak).

### ***Leak detection***

Leak detection is conducted by analysing the numerically obtained  $\text{Im}\{U_{22} - U_{11}\}$  using the technique outline in Equations (3.25) and (3.26), and the results are shown in Figure 3.10. The distinctive pike indicates that there is one leak in the pipe section of interest. The normalized locations are determined as  $x_L = 0.20$  from the x-axis, and the value of the impedance ratio is  $Z_c/Z_L = 0.0442$  according to the size of the spike. The results are highly consistent with the theoretical values as shown in Table 3.2. The successful detection has once again validated the effectiveness of the proposed targeted leak detection technique.

## **3.5 Discussion**

### **3.5.1 Effect of friction**

Friction is neglected in the proposed leak detection algorithm. The effect of friction on the frequency response of pipeline systems has been investigated in detail by Lee et al. (2005b) for leak detection in R-P-V systems. It has been found that the effect of steady-friction is minor and approximately uniform across all the frequencies, therefore it should not affect the period of the sinusoidal waves in the  $T_N$  signal or the localization of the leak. The impact of steady friction on the amplitude of the sinusoidal waves is very limited for real water transmission pipelines, therefore the impact on the leak impedance/size determination is limited. The above has been confirmed by the two numerical case studies conducted in the current research, in which the locations of the

leaks are accurately determined despite that steady friction is included in the numerical simulations.

The unsteady friction, however, will induce a non-uniform dampening for the frequency responses, and a correction technique has been proposed in Lee et al. (2006). Recent research on the unsteady friction in water pipelines concludes that the effect of unsteady friction in large diameter water transmission pipelines is limited (Vardy et al. 2015), and it has been generally neglected in practice (Shucksmith et al. 2012; Meniconi et al. 2013; Stephens et al. 2013). If the pipe section of interest (the section in bracket of the two pairs of transducers) is relatively long such that the fundamental frequency is low, the excitation and the analysis only need to focus on the low frequencies [e.g. in Case 1, the periodic nature of  $\text{Im}\{U_{22} - U_{11}\}$  is already clear in the range of 0 to 30 Hz Figure(3.6)]. In the low frequency range, the effect of unsteady friction is limited and less non-uniform.

### **3.5.2 Challenges in field application**

Challenges are expected in real application of the proposed leak detection technique. Although the two-source-four-sensor testing configuration for water pipe transfer matrix extraction has been validated in the laboratory (Yamamoto et al. 2015), the implementation of this testing configuration in real pipe systems can be difficult. Transient generators (source) can be installed on existing access points such as fire hydrants or air valves. The transducers need to be installed in pairs and the distance between the two sensors in a pair needs to be short to enable the analysis. This is challenging since in real water



pipelines it is uncommon to have two accessible points in close proximity. Although live tapping can be done to create new fittings for the transducers, it is undesirable or expensive especially when the pipe is buried. Recent research on fibre optic pressure sensor arrays (Gong et al. 2018b) may provide a solution in the future. It is envisaged that a fibre optic pressure sensor array, as in the form of a flexible cable, can be inserted into a pipeline through a single access point. The same access point can also be used for transient wave generation. The fibre optic pressure sensors measure the transient response of the pipe system. The same configuration can be repeated at another access point to achieve the two-source-four-sensor testing configuration. Preliminary success has been achieved in the laboratory (Gong et al. 2018b), in which leak reflections are identifiable from the pressure measurement; however, several design challenges need to be resolved to enhance the accuracy and robustness of the measurements.

Another challenge is the effectiveness (e.g. bandwidth and tolerance to noise) of the excitation transient wave. Pressure measurements in real pipeline systems will suffer from noise and transient interference (e.g. generated from water users). It is expected that conventional discrete transient excitation (e.g. pulse and step waves) will not be effective, and the PRBS is needed to achieve accurate extraction of the transfer matrix. Averaging the results from multiple periods of the steady-oscillatory response will reduce the effect of noise. A side-discharge valve based PRBS transient generator has been developed and tested in the laboratory (Gong et al. 2016b); however, field applications may require a larger and more powerful transient wave generator. The challenge is how to

maintain the fast response of the valve for a consistent and wide bandwidth of the excitation.

The structure complexity of ageing pipelines can be another challenge. The proposed technique is a significant step forward to tackle complex pipe systems, and it enables a targeted pipe section to be visually isolated for independent analysis in any complex network. However, within the targeted pipe section, the condition of the pipe can still be complex, with the presence of not only leaks but non uniform pipe wall deterioration. Duan et al. (2011) demonstrated that FRF-based leak detection is applicable to complex series pipelines. Further research is needed to investigate the impact of pipe wall deterioration or other defects (e.g. blockages) in the targeted pipe section on leak detection.

### **3.6 Conclusions**

A new pipeline leak detection technique has been proposed in this research. The technique enables leak detection for a targeted pipe section independent from the complexities of the pipe system where the targeted section is embedded in. This is achieved by extracting the transfer matrix of the targeted pipe section using a two-source-four-sensor hydraulic transient testing strategy, and analysing the resultant transfer matrix by a newly developed algorithm. The proposed technique has been validated by two numerical case studies. In the first study (Case 1), the two leaks in a pipe section embedded in a reservoir-pipeline-valve system have been successfully determined using pulse excitation waves. In the second study (Case 2), the location and impedance of the leak in a pipe section embedded in a simple pipe network are successfully determined using pseudo-random binary signals as the excitation.

This research is a significant step towards the application of hydraulic transient-based leak detection techniques in real water distribution systems. The concept of “virtually” isolating a target pipe section out of a complex pipe system for independent analysis is useful for not only leak detection but also other applications such as blockage detection and pipe wall condition assessment. Practical challenges, however, are expected in the field, and they include the implementation of the two-source-four-sensor testing configuration in buried pipelines, the effectiveness of the excitation transient wave, and the structural uncertainties and complexities within the targeted pipe section. Further research, in particular experimental studies, is needed to solve these practical issues and enable a cost-effective application in the field.

This page is intentionally left blank

## Chapter 4

# Wave separation and pipeline condition assessment using in-pipe fibre optic pressure sensors

## (Journal Paper 3)

Publication details:

Shi, H., Gong, J., Cook, P. R., Arkwright, J. W., Png, G. M., Lambert, M. F., Zecchin, A. C., and Simpson, A. R. (2019). "Wave separation and pipeline condition assessment using in-pipe fibre optic pressure sensors." *Journal of Hydroinformatics*, 21(2), 371-379, 10.2166/hydro.2019.051.

This page is intentionally left blank

## Statement of Authorship

Title of Paper	Wave separation and pipeline condition assessment using in-pipe fibre optic pressure sensors
Publication Status	<input checked="" type="checkbox"/> Published <input type="checkbox"/> Accepted for Publication <input type="checkbox"/> Submitted for Publication <input type="checkbox"/> Unpublished and Unsubmitted work written in manuscript style
Publication Details	Shi, H., Gong, J., Cook, P. R., Arkwright, J. W., Png, G. M., Lambert, M. F., Zecchin, A. C., and Simpson, A. R. (2019). "Wave separation and pipeline condition assessment using in-pipe fibre optic pressure sensors." <i>Journal of Hydroinformatics</i> , 21(2), 371-379, <a href="https://doi.org/10.2166/hydro.2019.051">10.2166/hydro.2019.051</a> .

### Principal Author

Name of Principal Author (Candidate)	He Shi
Contribution to the Paper	Conception and design of the project; Analysis and interpretation of the research data; Drafting the manuscript.
Overall percentage (%)	60%
Certification:	This paper reports on original research I conducted during the period of my Higher Degree by Research candidature and is not subject to any obligations or contractual agreements with a third party that would constrain its inclusion in this thesis. I am the primary author of this paper.
Signature	Date 14/03/2019

### Co-Author Contributions

By signing the Statement of Authorship, each author certifies that:

- i. the candidate's stated contribution to the publication is accurate (as detailed above);
- ii. permission is granted for the candidate to include the publication in the thesis; and
- iii. the sum of all co-author contributions is equal to 100% less the candidate's stated contribution.

Name of Co-Author	Jinzhe Gong
Contribution to the Paper	Conception and design of the project; Analysis and interpretation of the research data; Critically reviewing the manuscript.
Signature	Date 15/3/2019

Name of Co-Author	Peter Cook		
Contribution to the Paper	Conception and design of the project; Analysis and interpretation of the research data; Critically reviewing the manuscript.		
Signature		Date	20/3/19

Name of Co-Author	John Arkwright		
Contribution to the Paper	Conception and design of the project; Analysis and interpretation of the research data; Critically reviewing the manuscript.		
Signature		Date	20/3/19

Name of Co-Author	Gretel Png		
Contribution to the Paper	Conception and design of the project; Analysis and interpretation of the research data; Critically reviewing the manuscript.		
Signature		Date	18 MAR 2019

Name of Co-Author	Martin Lambert		
Contribution to the Paper	Conception and design of the project; Analysis and interpretation of the research data; Critically reviewing the manuscript.		
Signature		Date	15/3/19

Name of Co-Author	Aaron Zecchin		
Contribution to the Paper	Conception and design of the project; Analysis and interpretation of the research data; Critically reviewing the manuscript.		
Signature		Date	15/3/19

Name of Co-Author	Angus Simpson		
Contribution to the Paper	Conception and design of the project; Analysis and interpretation of the research data; Critically reviewing the manuscript.		
Signature		Date	15/3/2019



## **Abstract**

The use of two pressure transducers in close proximity can enable the separation of the directional travelling pressure waves in pipelines. However, the implementation of this measurement strategy in real water pipes is difficult due to the lack of closely located access points. This paper reports the use of a customised in-pipe fibre optic pressure sensor array for hydraulic transient wave separation and pipeline condition assessment. The fibre optic pressure sensor array can be inserted into a pressurised pipeline through a single access point. The array consists of multiple fibre Bragg grating (FBG)-based pressure sensors in close proximity (~0.5 m apart). A previously developed wave separation algorithm is adapted to analyse the transient pressure measurement from the FBG sensors. The resultant directional pressure waves are then used to detect pipe sections with a thinner wall thickness. A challenge is the influence of the in-pipe fibre optic sensing cable on the transient pressure measurement. The impact is analysed and adjustments to the pipeline condition assessment algorithm are undertaken to resolve the issue. The successful experimental application verifies the usefulness of the in-pipe fibre optic sensor array, which can facilitate transient-based pipeline condition assessment for buried water pipes with limited access points.

This page is intentionally left blank

## 4.1 Introduction

Water utilities globally are facing the problem of ageing water distribution systems (WDSs), and the cost of maintenance and replacement is predicted to explode under current practice. For instance, it is estimated that more than US\$1 trillion will be required between 2011 to 2035 to replace ageing water mains and address projected growth (American Water Works Association 2012). Pipeline condition assessment has becoming increasingly important, because the actual condition of pipelines can help strategically prioritise investment and extend asset life.

Among many pipeline condition assessment techniques available, hydraulic transient-based methods are particularly attractive because they can achieve continuous pipe wall condition assessment for hundreds of metres up to kilometres of pipe in a single test (Stephens et al. 2013). The approach uses small controlled hydraulic transient pressure waves, which travel at about 1200 m/s in pressurised metallic water pipes, will induce wave reflections at pipe cross-sections with physical changes (e.g. leaks, blockages and wall thinning due to corrosion), and the reflections can be interpreted by appropriate algorithms to reveal the nature of the anomaly (Chaudhry 2014). In addition to pipe wall condition assessment (Zeng et al. 2018b; Zhang et al. 2018a), many transient-based techniques have been developed for the detection of leaks (Brunone and Ferrante 2001; Covas et al. 2005; Shamloo and Haghghi 2009; Soares et al. 2010; Gong et al. 2013a; Duan 2016a), blockages (Sattar et al. 2008; Meniconi et al. 2013; Massari et al. 2014), illegal branches (Meniconi et

al. 2011a), general anomaly screening (Meniconi et al. 2015) or system parameter identification (Zecchin et al. 2014a).

In operational pipe systems, pressure sensors are installed at existing access points (Ghazali et al. 2012; Gong et al. 2015), such as air valves or fire hydrants, which are typically hundreds of meters apart from each other, to avoid excavation or tapping. For any interior point along a pipe, the measurement from a single pressure sensor is always the superimposed amplitude of the pressure waves travelling upstream and downstream. As a result, it is difficult to tell whether a measured pressure reflection is from the upstream or downstream side of the transducer, or actually a combination of waves from both sides. The use of measurements from multiple access points (hundreds of metres apart) and a time-shifting technique (Gong et al. 2016c) is helpful in providing the directional information, but only when the reflected waves are simple in wave form and limited in number (i.e. the pipeline configuration and condition are not complex).

A wave separation technique recently developed for hydraulic transient pressure waves in pipelines has provided a robust solution to obtain the directional information of wave reflections (Shi et al. 2017). The wave separation technique uses two pressure sensors in close proximity along a pipe (in the scale of metres), and they are referred to as a “dual-sensor”. It was adapted to water pipe systems from the original technique for separating directional acoustic waves using multiple microphones (Chung and Blaser 1980). In the wave separation technique, the time-domain pressure reflection signals as measured by the dual-sensor are transformed into the frequency

domain, processed based on the fact that a directional wave arrives at the two sensors at different times but with a specific time delay, and then transformed back into the time domain. The results are two directional pressure waves with significantly reduced complexity, in which any major wave reflection can be attributed to its source by the principle of time-domain reflectometry. One practical challenge of this wave separation technique in buried water pipelines, however, is the difficulty in achieving the dual-sensor measurement configuration.

To address this challenge, the authors have developed in-pipe fibre optic transient pressure sensors, with the first generation tested in the laboratory for proof-of-concept (Shi et al. 2015) and the second generation tested and reported in this paper for wave separation and pipe condition assessment. The optic pressure sensors are based on fibre Bragg gratings (FBGs), and multiple sensors are placed in close proximity (~0.5 m) in a protective cable. The sensor cable, with a diameter of ~4 mm, can be inserted into a pipeline through a single access point. Laboratory experiments are conducted in a single copper pipeline with two short sections in thinner wall thicknesses, and the wave separation technique is applied to the measured transient pressure data for pipe wall condition assessment purpose. One particular challenge is the impact of the sensor cable on the transient response. The sensor design, the impact of the sensor cable, the wave separation and the application to pipe wall condition assessment are discussed in the following sections.

## **4.2 In-pipe fibre optic transient pressure sensor array**

The in-pipe fibre optic sensor array used in this research includes five FBG-based pressure sensors (FBG1 to FBG5) in a 5.37 m long cable, the schematic of which is given in Figure 4.1. It is a further development based on the FBG manometry catheter developed by Arkwright et al. (2012) for measuring muscular activity in the human gut. The distance between FBG1 and FBG2 is 0.725 m and that for the rest is 0.5 m. The cable that protects the optical fibre is made from plastic material, and has a diameter of approximately 4 mm. At each FBG pressure sensor, a 10 mm window is open in the protective cable, and a flexible elastomeric sleeve is used to cover the FBG, as illustrated in Figure 4.2. The FBG is designed to have a downward arc under atmosphere pressure and the flexible sleeve is in close contact with the sensor. As the pressure increases from atmosphere pressure, the sleeve presses the FBG further downwards, which causes a change in the strain and in turn a shift in the reflected wavelength of the FBG. This configuration, in particular the arc-shaped pre-load, is a new design compared with its predecessor reported in Shi et al. (2015), and it enables high sensitivity to pressure variations under high background pressure condition (as is the case in pressurised water pipes). This in-pipe fibre optic sensor array has recently been applied to measure leak-induced hydraulic noise in the steady state and wave reflections under transient events (Gong et al. 2018b).

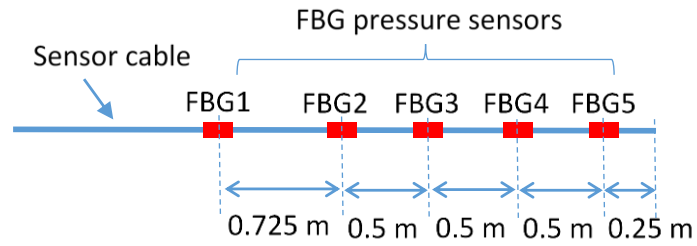


Figure 4.1 Schematic of the in-pipe fibre optic sensor cable.

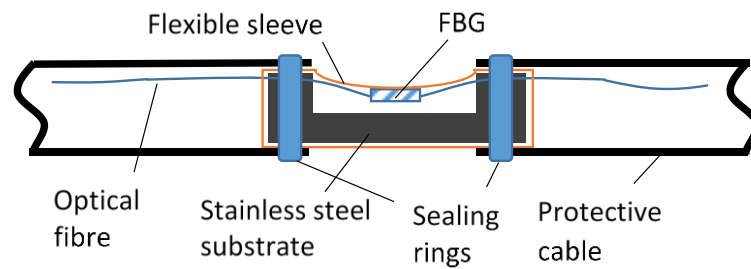


Figure 4.2 Schematic of the Fibre Bragg Grating (FBG) pressure sensor.

## 4.3 Laboratory experiments

### 4.3.1 Experimental apparatus

Laboratory experiments have been conducted to assess the usefulness of the in-pipe fibre optic sensor array in transient pressure wave separation and pipe wall condition assessment. The layout of the experimental pipeline systems is given in Figure 4.3.

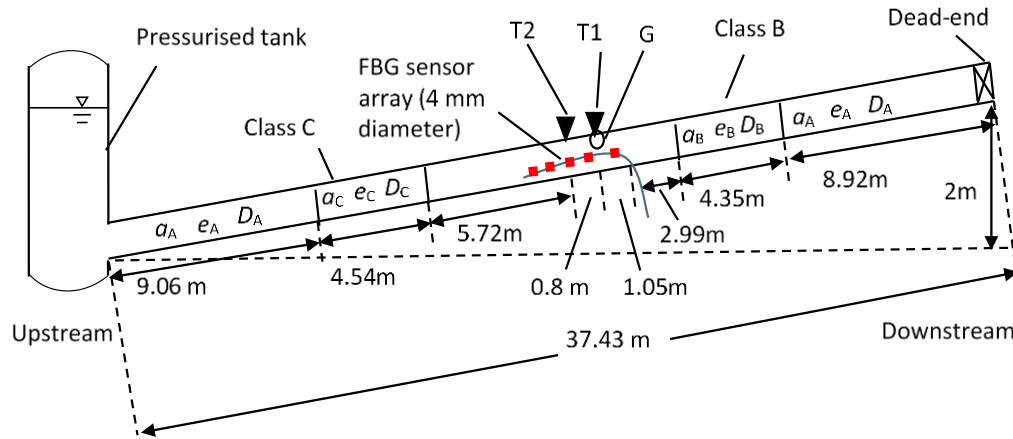


Figure 4.3 Layout of the experimental pipeline system.

The laboratory system was a copper pipe that consisted of mainly Class A pipe sections and two short sections in Class B and C respectively. The Class B and C sections have a thinner wall thickness and were used to simulate deteriorated pipe sections (e.g. extended corrosion). The length information of the pipeline system is shown in Figure 3.3 and the physical details of pipes in different classes are given in Table 4.1, where  $D$ ,  $e$ ,  $a$  and  $B$  represent internal diameter, wall thickness, wave speed and impedance, respectively, and the subscripts A, B, and C represent pipe Class A, B and C, respectively. Pipe impedance  $B$  is defined as

$$B = \frac{a}{gA} \quad (4.1)$$

in which  $g$  is the gravitational acceleration, and  $A$  is the cross-sectional area of the pipe section under consideration.



Table 4.1 Physical details of the pipeline system used in the laboratory experiments.

Pipe class	Internal diameter (mm)	Wall thickness (mm)	Wave speed (m/s)	Impedance (s/m <sup>2</sup> )
A	$D_A = 22.14$	$e_A = 1.63$	$a_A = 1,319$	$B_A = 349,000$
B	$D_B = 22.96$	$e_B = 1.22$	$a_B = 1,273$	$B_B = 314,000$
C	$D_C = 23.58$	$e_C = 0.91$	$a_C = 1,217$	$B_C = 284,000$

Two conventional pressure transducers (T1 and T2 in Figure 3, M5HB, Keller AG, Switzerland) were flush mounted on the pipe wall through small brass blocks encasing the pipe. A solenoid-controlled side-discharge valve was used as the transient wave generator (G), and it was installed at the same cross-section of the pipe where T1 was located. The solenoid valve was installed on the top of the pipe for water discharge and the release of any trapped air. The transducers were installed on the side and with an upward angle to prevent any air from being trapped at the sensor head. The fibre optic sensor cable was inserted into the pipeline through an angled tapping point and sealed with an O-ring gland. The insertion point is 1.05 m away from the transient generator G and transducer T1. The optical fibre was illuminated using a super-luminescent light emitting diode (DL-BP1-1501A, DenseLight, Singapore) and the reflected wavelengths from the sensor array were monitored using a solid-state spectrometer (I-MON 512 HS, Ibsen Photonics, Denmark). Transducer T2 and FBG3 were placed at the same location, and as a result, the overall length of the

fibre optic cable inside the pipeline is 3.1 m. The sampling rate for the FBG sensors was 12.376 kHz and that for the conventional sensors was 20 kHz.

### 4.3.2 Pressure measurements and simulations

In the initial steady-state condition, the pipeline system was pressurised at 3 bar by the pressurised tank, and the solenoid valve was fully open to discharge water. The solenoid valve was then abruptly closed, which resulted in two identical incident step waves propagating along the pipe in two directions.

The pressure measurements from T2 and FBG3 are shown in Figure 4.4, together with the measurement from T2 when no fibre optic cable was present, and with the numerical pressure response at T2 obtained by the method of characteristics (MOC). In the MOC simulation, a pipe model is established based on the information in Figure 4.3 and Table 4.1 for the scenario that the fibre optic sensor cable is present. The wave speed in the pipe section where the fibre cable is enclosed is 1,230 m/s as determined from the laboratory measurements, and this is used in the numerical model. The time step used in the simulation is 0.5 ms. Steady friction with a Darcy-Weisbach frictional factor of 0.02 is considered.

The incident wave and the major wave reflections from key features are highlighted in Figure 4.4. According to the principle of time-domain reflectometry (TDR), once a wave front encounters a physical discontinuity (e.g. a wall thickness change), reflections occur and propagate backwards. Reflections from features closer to the generator will arrive at the transducer (at the same or close location of the generator) sooner. The short duration of the

wave front ensures a high spatial resolution. Based on the analysis in Gong et al. (2013c), for a step wave with an effective rise time of  $T_r$  and a wave speed of  $a$ , reflections from two discontinuities with a distance of  $T_r a / 2$  or larger are distinguishable from each other. The effective rise time of the incident step wave in this study is about 2 ms as shown in Figure 4.4. Considering the highest wave speed of 1,319 m/s as in Table 4.1, the spatial resolution is about 1.32 m. The distance between any two major physical discontinuities is larger than this threshold in the experimental system (Figure 4.3), therefore the major reflections can be identified with confidence, especially after the wave separation as discussed later.

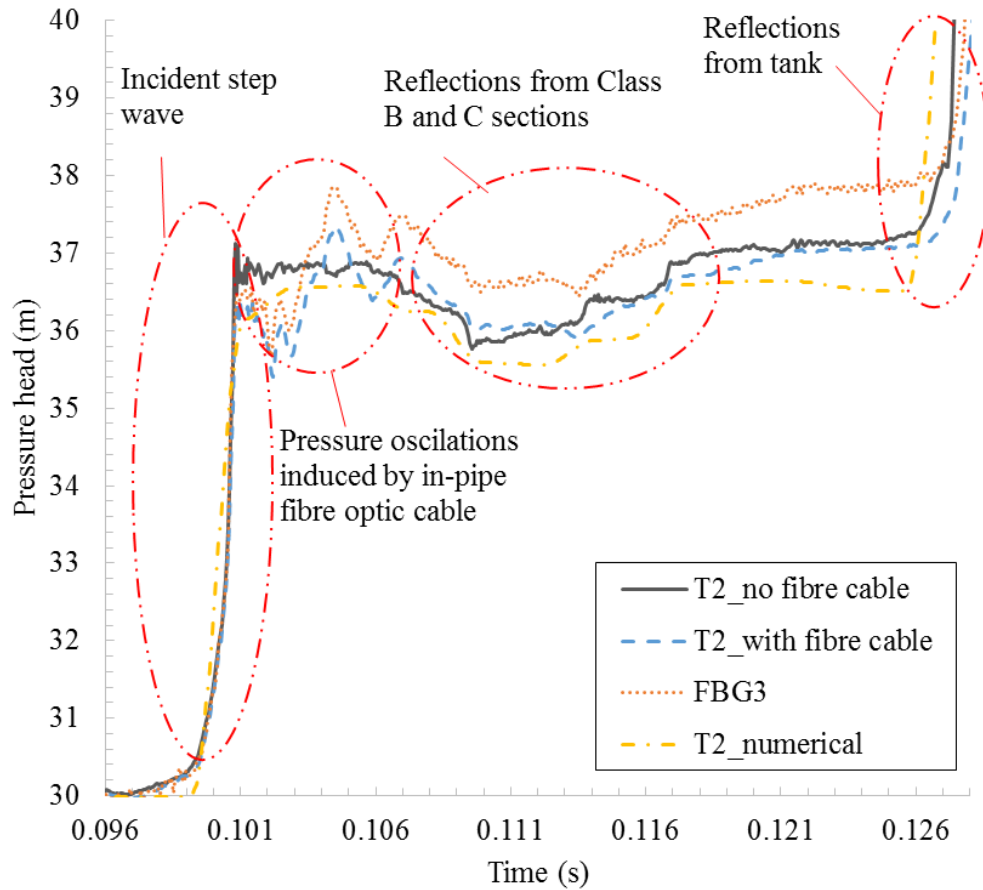


Figure 4.4 Transient pressure responses from conventional sensor T2 (laboratory results with and without the present of fibre sensor cable, and numerical results) and from fibre optic sensor FBG3 (fibre sensor cable in pipe).

It can be seen from Figure 4.4 that the presence of the in-pipe fibre optic sensor cable changes the transient pressure response of the pipeline system. The impact of the cable mainly manifests as pressure oscillations in a short time period after the generation of the incident wave. The pressure oscillations are attributed to the in-pipe cable together with the tapping point for cable insertion, which change the local impedance of the pipeline. Using the experimentally determined wave speed of 1,230 m/s and Equation (3.1), and considering the

small change in the pipe cross-sectional area (the cross-sectional area of cable is about 3% that of the pipe, but the cable area may be compressed to be even smaller under pressure), the impedance of the pipe section with the in-pipe fibre optic cable is calculated as  $337,000 \text{ s/m}^2$ , which is smaller than the impedance of normal Class A pipe. The pressure signal seems complex in the original measurement as shown in Figure 3.4 but will become clearer after the wave separation as discussed later.

Combined pressure wave reflections from the Class B and C sections are also recorded in the traces in Figure 4.4. The laboratory measurements from both T2 and FBG3 when the in-pipe cable was present are slightly smoother than that from T2 when no cable was in the pipe. The effect of signal smoothness is most likely due to the viscoelasticity of the plastic material.

Overall, those three experimental traces are generally consistent, and they are also consistent with the numerical results. Since the length of the cable inside the pipe is short (3.1 m), the pressure oscillations induced by the cable is confined in a very short time period ( $\sim 5 \text{ ms}$ ) after the generation of the incident wave and the effect of signal smoothness is insignificant.

## **4.4 Wave Separation**

### **4.4.1 Directional pressure waves**

The pressure measurements from FBG2 and FBG3, as shown in Figure 4.5, are used for wave separation. They are close to the transient generator and the results can be compared with those obtained from the conventional sensors (T1

and T2). The procedure of the wave separation follows that outlined in Shi et al. (2017). The short-duration wave fronts of the incident step wave as measured by FBG2 and FBG3 (as shown in Figure 4.5) are extracted and used to empirically calibrate the transfer function for the short pipe section between the two sensors. The transfer function describes how the wave evolves over propagation, and includes information about the wave speed and wave attenuation. The wave reflections before the arrival of the tank-induced reflection are extracted and put into the wave separation algorithm. The results of the directional pressure reflection waves experimentally extracted from the FBG sensors and the conventional sensors are given in Figure 4.6. The wave separation algorithm is also applied to the numerically simulated pressure responses and the results are shown in Figure 4.6 for comparison. Note that the directional pressure waves are normalised by the size of the incident wave for ease of comparison.

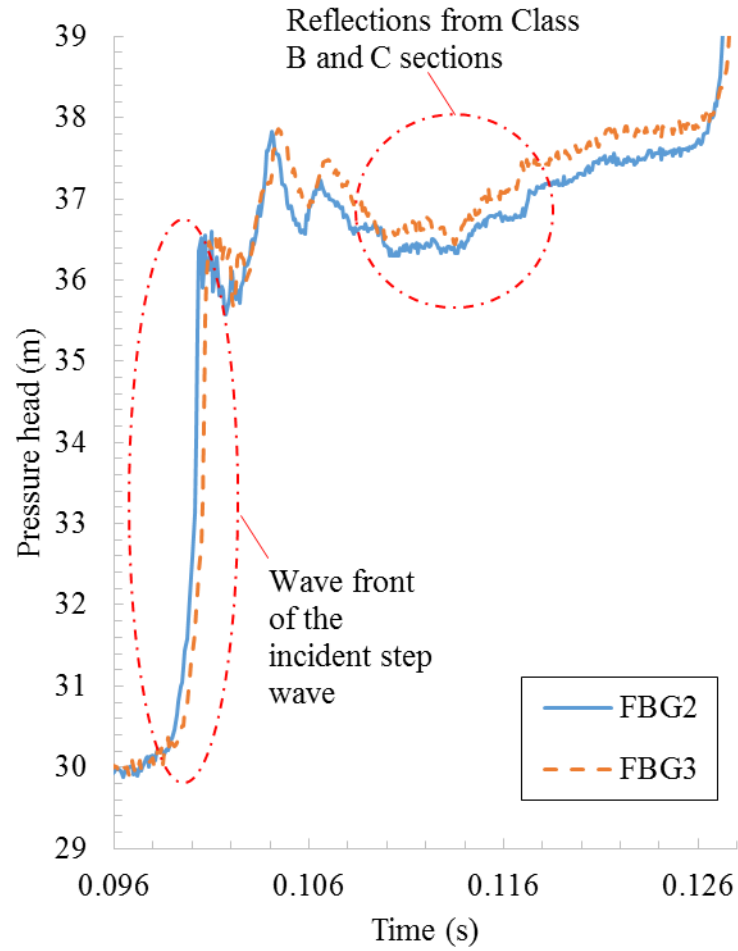


Figure 4.5 Transient pressure measurements from FBG2 and FBG3.

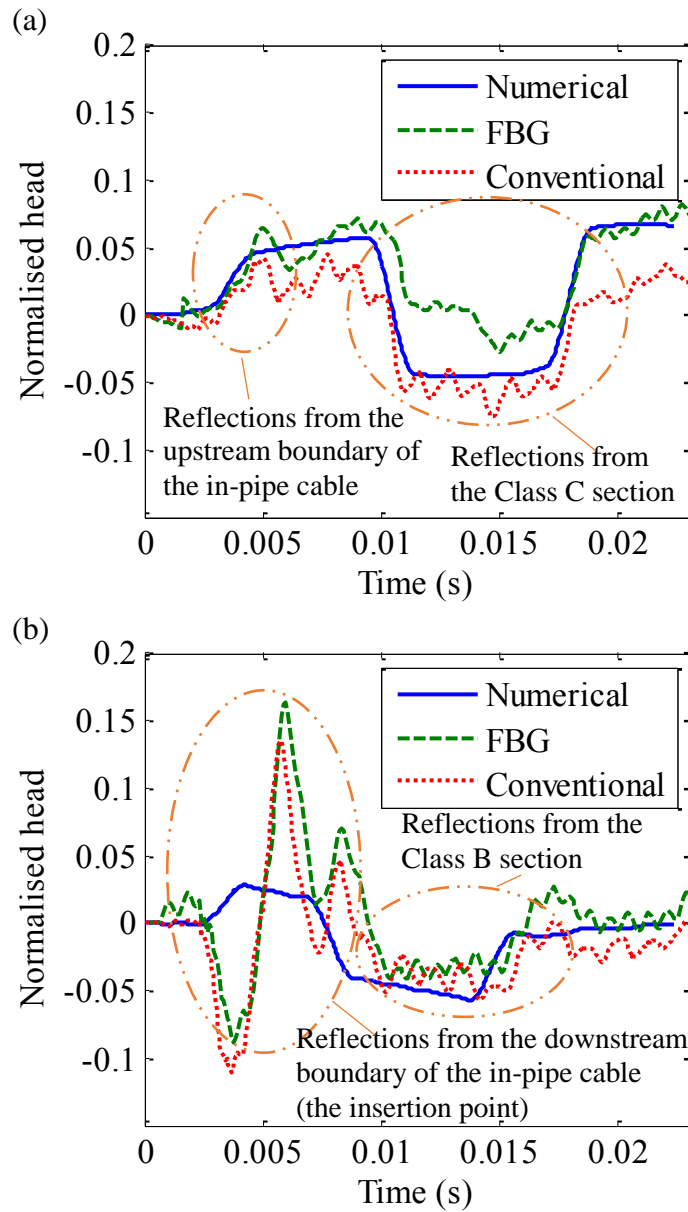


Figure 4.6 Wave separation results obtained from numerical simulations, fibre optic sensors (FBG2 and FBG3) and conventional sensors (T1 and T2): (a) wave reflections from the upstream side of the dual-sensor and propagating towards the dead-end; and (b) wave reflections from the downstream side of the dual-sensor and propagating towards the tank.

Figure 4.6 demonstrates that the major reflections from the Class B and Class C sections have been separated using the experimental data from either the FBG sensors or the conventional sensors, and the experimental results are consistent



with the numerical results. The wave separation decomposes the superimposed raw pressure measurement into directional pressure waves, simplifies the complexity of the signal, and enables better understanding of the source of reflections. Discrepancies exist and are discussed in the following sub-section.

#### **4.4.2 Discussion**

The experimentally determined directional waves using the FRB sensors and the conventional sensors are highly consistent in the wave form. For the wave reflections from the upstream side of the dual-sensor and propagating towards the dead-end [Figure 4.6(a)], the experimental results are also highly consistent with the numerical results. The first step rise is the reflection from the upstream boundary of the in-pipe cable, and it is because that the pipe section (Class A) with the cable has a lower impedance than that in normal Class A pipe sections. The cable is made from plastic material, which is much lower in strength compared to the material of the pipe wall (copper), and it results in a lower wave speed and therefore a lower impedance for the pipe section hosting the cable. When a positive wave propagating from a lower impedance pipe section to a higher impedance one, a positive pressure wave reflection will occur (Wylie 1983). The following step drop and then step rise are reflections from the Class C pipe section, which has an impedance lower than the Class A pipe. Detailed explanation of the wave reflection mechanism from a short pipe section with a different impedance can be found in Gong et al. (2013c). The experimental results have some small oscillations in addition to the major reflections. The oscillations can be resulted from the transient interference induced by the vibration of the solenoid valve at the sudden closure, and the uncertainty in the

empirical determination of the transfer function. The numerical results are smooth and clearly show the expected reflections, which confirms the effectiveness and accuracy of the wave separation algorithm itself.

For the wave reflections from the downstream side of the dual-sensor and propagating towards the tank [Figure 4.6(b)], the reflections from the Class B section (as highlighted in the figure) are generally consistent for the three sets of results; however, discrepancies are observed between the experimental and the numerical results for the reflections from the downstream boundary of the in-pipe cable (which was the cable insertion point). The experimental results show a negative reflection followed by a positive reflection and some wave oscillations, while the numerical results show a step response similar to the upstream-boundary reflection as seen in Figure 4.6(a). The insertion tapping point (an angled conduit in a brass block) was sealed by an O-ring gland with a “finger-tight” condition. The conduit and the O-ring seal are likely to respond to pressure transients like a small accumulator, thus producing the signature of a negative reflection followed by a positive reflection as observed in the experimental results. The numerical model did not include this complexity, therefore the numerical result only shows the step reflection as induced by an impedance change at the downstream-boundary of the in-pipe cable.

## **4.5 Pipe wall condition assessment**

### **4.5.1 Methodology**

The original direct-reflection-analysis-based condition assessment technique (Gong et al. 2013c) needs to be further developed for the directional waves

obtained from the in-pipe fibre optic sensor array. The original condition assessment algorithm assumes that the incident wave is generated and the pressure responses are measured in an intact pipe section, and the deteriorated sections are limited in number and mild in deterioration. In the case of using the in-pipe fibre optic sensor cable, the generation of the incident wave and the pressure measurement are undertaken in the section that encloses the cable, and the impedance of this section is considerably lower than that in normal intact pipe sections. However, the same principle still applies. That is, when a pressure wave propagates from the  $i$ th pipe section to the  $(i+1)$ th pipe section where the impedance changes, the sign-sensitive amplitude of the normalised wave reflection (equivalent to the reflection coefficient) and that of the normalised transmitted wave (equivalent to the transmission coefficient) are related to the impedance of the two sections (Wylie 1983; Gong et al. 2013c), as given in Equations (4.2) and (4.3), respectively.

$$R_{i,i+1} = \frac{B_{i+1} - B_i}{B_{i+1} + B_i} \quad (4.2)$$

$$T_{i,i+1} = \frac{2B_{i+1}}{B_{i+1} + B_i} = 1 + R_{i,i+1} \quad (4.3)$$

where  $R_{i,i+1}$  and  $T_{i,i+1}$  are the reflection and transmission coefficient, respectively, for a wave propagating from the  $i$ th to the  $(i+1)$ th pipe section.

The relationships shown in Equations (4.2) and (4.3) are the same as the reflection and transmission coefficients defined in acoustic reflectometry (Sharp 1996), where typically acoustic waves propagating in air and in a wave

guide are considered. Considering an incident wave generated at section 1 and only propagating towards one direction (as in the case of directional waves as previously discussed), the normalised initial reflection from the  $n$ th section as would be measured in the 1st section can be derived as

$$R_{1,n} = R_{n-1,n} \prod_{i=1}^{n-2} (1 - R_{i,i+1}^2) \quad (4.4)$$

### 4.5.2 Application and verification

To verify the modified condition assessment algorithm as discussed in the previous section, Equation (4.4) is applied to the directional pressure wave coming from the upstream side of the dual-sensor and propagating towards the dead-end [Figure 4.6(a)]. Rearranging Equation (4.2), the impedance of the  $(i+1)$ th section can be calculated by

$$B_{i+1} = B_i \frac{1 + R_{i,i+1}}{1 - R_{i,i+1}} \quad (4.5)$$

The pipe section with the FBG sensor cable inside can be considered as the 1st section, the normal Class A section on the upstream side is the 2nd section, and the Class C section is the 3rd section. The reflection coefficients  $R_{1,2}$  and  $R_{1,3}$  can be determined from the sign-sensitive amplitude of the major wave reflections in the directional wave shown in Figure 4.6(a). The reflection coefficient  $R_{2,3}$  can then be calculated by Equation (4.4). Finally Equation (4.5) can be used to calculate  $B_3$ , which, in this case, is the impedance of the Class

C section  $B_C$ . Table 4.2 summarises the results. Note that, although three significant figures are used for the values, the reflection coefficients (i.e. the amplitude of the normalised reflections) are determined manually and uncertainties are involved.

Table 4.2 Pipe impedance determined from the directional pressure wave coming from the upstream side of the dual-sensor and propagating towards the dead-end [Figure 4.6(a)].

Cases	Reflection coefficient $R_{1,2}$	Reflection coefficient $R_{1,3}$	Reflection coefficient $R_{2,3}$	Determined impedance $B_C$ (s/m <sup>2</sup> )
Numerical	0.040	-0.10	-0.10	285,000
FBG	0.0588	-0.0962	-0.0965	287,000
Conventional	0.0497	-0.110	-0.110	280,000

It can be seen from Table 4.2 that the determined impedance values for the Class C section are consistent with the calculated theoretical value of  $B_C$  as given in Table 4.1 (284,000 s/m<sup>2</sup>), which verifies that pipeline condition assessment can be conducted using the in-pipe fibre optic sensors with the methodology presented. The values of  $R_{2,3}$  are very close to those of  $R_{1,3}$ , which demonstrates that the local impedance change induced by the in-pipe sensor cable has an insignificant impact on the pipeline condition assessment. The discrepancies between the determined impedance values and the theoretical value are mainly due to the error associated with the wave separation,

uncertainties in the determined amplitude of wave reflections and uncertainties in the pipeline parameters used to calculate the theoretical value.

## **4.6 Conclusions**

A customised in-pipe fibre optic pressure sensor array has been used in the laboratory for hydraulic transient wave separation and pipeline condition assessment. The in-pipe fibre optic sensor array consists of five FBG-based pressure sensors in close proximity. The optic fibre is protected by a plastic cable with a diameter ~4 mm and the cable can be inserted into a pressurised pipeline through a single tapping point. With empirical calibration of the transfer function of the short pipe section between two sensors, a previously developed wave separation technique is successfully implemented on the transient pressure data measured from the fibre optic sensors, and the resultant directional waves are consistent with those obtained from conventional pressure sensors.

The impact of the in-pipe fibre optic sensor cable to the transient pressure response of the pipeline system has been assessed and discussed based on the directional pressure waves. The in-pipe sensor cable, as made from a plastic material, reduces the local pipe impedance and therefore introduces wave reflections. It also slightly smoothen the transient pressure signal. The entrance point of the cable acts like a small accumulator and introduces pressure oscillations. However, overall the impact of the in-pipe cable is moderate because of its short length, and it does not impede the application of transient pressure measurement for pipeline condition assessment.

A direct wave-reflection-analysis-based pipeline condition assessment algorithm has been further developed to incorporate the impact of the local impedance change induced by the in-pipe cable. The impedance of a Class C pipe section, which has a thinner wall thickness to simulate a deteriorated section, has been determined from the previously obtained directional waves, and the results are consistent with the theoretical value.

The results have verified the usefulness of the in-pipe fibre optic sensor array for hydraulic transient wave separation and pipeline condition assessment. The in-pipe sensor cable provides the ability to have multiple pressure measurements through one access point.

This page is intentionally left blank



# Chapter 5

## Conclusions

### 5.1 Research outcomes

This PhD research has focused on the development of new transient pressure measurement strategies and associated new signal processing algorithms for pipeline leak detection and wall condition assessment in complex pipe systems.

The main outcomes of this research are summarised as follows:

(1) A practical wave separation technique has been developed (Chapter 2), which uses two pressure sensors in close proximity (a dual-sensor unit) and enables the extraction of directional pressure waves travelling towards both the upstream and downstream ends of a pipeline. Both a pulse wave and a step wave can be used as the transient excitation. A technique has been developed for estimating the transfer function between the two sensors, which is essential information for wave separation. This approach is more practical than using an analytical estimation for real pipelines with parametric uncertainties. The effectiveness of this wave separation technique has been demonstrated through numerical simulations and laboratory experiments.

(2) A new transient pressure generation and measurement strategy has been proposed for the purpose of condition assessment of targeted pipe sections embedded in complex pipe systems (Chapter 3). The strategy, termed as the *two-generator-four-sensor* strategy, uses two dual-sensor units to bracket a pipe section to be analysed, and the two transient pressure generators to bracket the two dual-sensor units (and the pipe section in-between). The configuration enables an extraction of the transfer matrix of the in-bracket pipe section through the virtual isolation. The characterisation of the transfer matrix properties of this section (upon which the following leak detection methods are based) would remain unresolvable without the *two-generator-four-sensor* strategy.

(3) A new pipeline leak detection algorithm has been developed based on the analysis of the transfer function of a pipe section “virtually” isolated by the *two-generator-four-sensor* configuration, as explained above. It has been found that the imaginary part of the difference between two elements in the transfer matrix is sensitive to leaks. The result should be zero if no leak is present, while a leak will introduce a sinusoidal pattern on this imaginary part of the transfer function. The period and the magnitude of the pattern are related to the location and impedance of the leak, respectively. The algorithm determines the location and size of the leak based on this information, and is applicable to the analysis of multiple leaks.

(4) A technique has been developed for realising distributed pressure measurement along a pipe through only a single access point (Chapter 4). This is achieved by a customised in-pipe fibre optic pressure sensor array. The fibre

optic array is encased in a flexible cable with a diameter of 4 mm. The sensor cable can be inserted into a pipeline through a small opening on the pipe wall. The optical fibre based pressure sensors can measure transient pressure fluctuations at a high sampling rate (up to 20 kHz) and a high background pressure (up to 10 bar). The in-pipe fibre optic sensor array has been tested in the laboratory for pipe wall condition assessment. It has found that the presence of the in-pipe sensor cable, as made from a plastic material, reduces the local pipe impedance and therefore introduces wave reflections. It also slightly smooths the transient pressure signal, as the high frequency components dissipate at a faster rate. However, the overall the impact of the in-pipe cable is moderate because of its short length, and it does not impede the application of transient pressure measurement for pipeline condition assessment. A TDR-based pipeline condition assessment algorithm has been further developed to incorporate the impact of the local impedance change induced by the in-pipe cable.

## **5.2 Research contributions**

The key contributions of the aforementioned research outcomes have been summarised as follows:

(1) The wave separation reduces the complexities associated with wave superposition and provides the directional information of the measured wave reflections. This unprecedented directional information creates opportunities to develop more advanced pipeline leak detection and condition assessment techniques. The proposed technique provides a model free wave separation

approach, thereby overcoming past limitations associated with parametric uncertainties in model-based approaches.

(2) The *two-generator-four-sensor* configuration, combined with custom developed signal processing algorithms, can “virtually” break any complex pipeline systems down to its simplest form – a single pipe section. The extracted transfer matrix is a full representation of the characteristics of the “virtually” isolated pipe section, and is independent from any complexities of the rest of the pipe system (e.g. boundary conditions and other network connectivity). As a result, the extracted transfer matrix is much simpler than the transfer matrix of the overall pipe system, and the analysis is more straightforward, and amenable to analytic investigation. By focusing on the isolation of the dynamics of single pipes through the use of the *two-generator-four-sensor* configuration, the proposed approach represents a significant departure from the conventional research approach of gradually adapting the transient-based techniques developed for single pipeline systems (e.g. reservoir-pipeline-valve or reservoir-pipeline-reservoir systems) to more complex pipe systems and networks.

(3) The new leak detection technique, as combined with the *two-generator-four-sensor* configuration, enables the detection and location of multiple leaks in targeted pipe sections embedded in complex pipe systems (including pipe networks). This research represents a significant step towards the application of hydraulic transient-based leak detection techniques in real water distribution systems. It is envisaged that other defects, such as blockages and extended pipe

wall deterioration, can also be detected using the extracted transfer matrix of the “virtually” isolated pipe section.

(4) The in-pipe sensor cable provides the ability to have multiple pressure measurements through one access point. This is important since most water pipes in the field are buried underground, and access is only obtainable through sparsely available existing hydraulic devices such as air valves and fire hydrants. Successful laboratory verification has proven the concept and provided useful information for future developments.

### **5.3 Future work**

Specific topics for future work have been identified based on the findings of this PhD research, these include:

(1) *To further develop the wave separation technique for persistent transient excitation.*

Recent research has shown that persistent transient excitation, such as pseudo random binary sequences, can enhance the robustness and accuracy of system identification, either in the time domain (Nguyen et al. 2018) or in the frequency domain (Gong et al. 2016b). The current generation wave separation technique has been developed for and validated by discrete transient excitation only, including pulse and step waves.

(2) *To conduct experimental verification of the two-generator-four-sensor configuration and the associated leak detection technique for targeted pipe sections in complex pipe systems.*

Extensive numerical simulations have been conducted to validate the two-generator-four-sensor-based transfer matrix extraction and the associated leak detection for the “virtually” isolated pipe sections. Experimental studies are needed to further enhance the practicality of the techniques.

(3) *To develop next generation in-pipe fibre optic pressure sensor cables for field applications.*

This research validated the in-pipe fibre optic pressure sensor cable in a single copper pipeline with 25 mm diameter in the laboratory only. It is envisaged that the distributed pressure measurement will be equally effective in larger field pipes, but challenges exist in the insertion of the sensor cable. Field water pipes, as buried underground, are typically only accessible through a stand pipe with a length about one metre and perpendicular to the main pipe. To avoid disruptions to service, the insertion needs to be conducted in the normal system operating condition and against the back pressure, which is typically in the range of 3 to 8 bars.

---

# References

- American Water Works Association. (2012). "Buried No Longer: Confronting America's Water Infrastructure Challenge." Denver, CO.
- Arkwright, J. W., Blenman, N. G., Underhill, I. D., Maunder, S. A., Spencer, N. J., Costa, M., Brookes, S. J., Szczesniak, M. M., and Dinning, P. G. (2012). "Measurement of muscular activity associated with peristalsis in the human gut using fiber bragg grating arrays." *IEEE Sensors J.*, 12(1), 113-117, 10.1109/JSEN.2011.2123883.
- Beech, I. B., and Sunner, J. (2004). "Biocorrosion: towards understanding interactions between biofilms and metals." *Current Opinion in Biotechnology*, 15(3), 181-186, 10.1016/j.copbio.2004.05.001.
- Beuken, R. H. S., Lavooij, C. S. W., Bosch, A., and Schaap, P. G. (2006). "Low leakage in the Netherlands confirmed." *Proceedings of the Water Distribution Systems Analysis Symposium 2006*, American Society of Civil Engineers, Reston, VA, 10.1061/40941(247)174.
- Bracken, M., Johnston, D., and Coleman, M. (2010). "Acoustic based condition assessment of asbestos cement water transmission laterals." *Proceedings of the Pipelines 2010 Conference*, American Society of Civil Engineers, Reston, VA, 815-825, 10.1061/41138(386)78.
- Brunone, B. (1999). "Transient test-based technique for leak detection in outfall pipes." *J. Water Resour. Plan. Manage.*, 125(5), 302-306, 10.1061/(ASCE)0733-9496(1999)125:5(302).

- Brunone, B., and Ferrante, M. (2001). "Detecting leaks in pressurised pipes by means of transients." *J. Hydraulic Res.*, 39(5), 539-547, 10.1080/00221686.2001.9628278.
- Brunone, B., Ferrante, M., and Meniconi, S. (2008). "Portable pressure wave-maker for leak detection and pipe system characterization." *J. Am. Water Works Assn.*, 100(4), 108-116, 10.1002/j.1551-8833.2008.tb09607.x.
- Bureau of Meteorology. (2016). "National Performance Report 2014-2015: Urban Water Utilities." Melbourne, Australia.
- Butterfield, J. D., Collins, R. P., and Beck, S. B. M. (2018). "Influence of pipe material on the transmission of vibroacoustic leak signals in real complex water distribution systems: case study." *J. Pipeline Syst. Eng. Prac.*, 9(3), 05018003, 10.1061/(ASCE)PS.1949-1204.0000321.
- Capponi, C., Ferrante, M., Zecchin, A. C., and Gong, J. (2017). "Leak detection in a branched system by inverse transient analysis with the admittance matrix method." *Water Resour. Manage.*, 31(13), 4075-4089, 10.1007/s11269-017-1730-6.
- Chaudhry, M. H. (2014). *Applied Hydraulic Transients*, 3rd Ed., Springer, New York, NY.
- Chung, J. Y., and Blaser, D. A. (1980). "Transfer function method of measuring in - duct acoustic properties. I. Theory." *J. Acoust. Soc. Am.*, 68(3), 907-913, 10.1121/1.384778.
- Colombo, A. F., and Karney, B. W. (2002). "Energy and costs of leaky pipes toward comprehensive picture." *J. Water Resour. Plan. Manage.*, 128(6), 441-450, 10.1061/(ASCE)0733-9496(2002)128:6(441).



- Colombo, A. F., Lee, P., and Karney, B. W. (2009). "A selective literature review of transient-based leak detection methods." *J. Hydro. Environ. Res.*, 2(4), 212-227, 10.1016/j.jher.2009.02.003.
- Costello, S. B., Chapman, D. N., Rogers, C. D. F., and Metje, N. (2007). "Underground asset location and condition assessment technologies." *Tunnelling and Underground Space Technology*, 22(5–6), 524-542, 10.1016/j.tust.2007.06.001.
- Covas, D., Ramos, H., and De Almeida, A. B. (2005). "Standing wave difference method for leak detection in pipeline systems." *J. Hydraulic Eng.*, 131(12), 1106-1116, 10.1061/(ASCE)0733-9429(2005)131:12(1106).
- Covas, D., and Ramos, H. (2010). "Case studies of leak detection and location in water pipe systems by inverse transient analysis." *J. Water Resour. Plan. Manage.*, 136(2), 248-257, 10.1061/(asce)0733-9496(2010)136:2(248).
- De Sanctis, G., and Van Walstijn, M. (2009). "A frequency domain adaptive algorithm for wave separation." *Proceedings of the 12th International Conference on Digital Audio Effects (DAFx-09)*, Politecnico di Milano, Como, Italy, 498-505.
- Demma, A., Cawley, P., Lowe, M., Roosenbrand, A. G., and Pavlakovic, B. (2004). "The reflection of guided waves from notches in pipes: a guide for interpreting corrosion measurements." *NDT & E International*, 37(3), 167-180, 10.1016/j.ndteint.2003.09.004.
- Donazzolo, V., and Yelf, R. (2010). "Determination of wall thickness and condition of Asbestos Cement pipes in sewer rising mains using Surface

- Penetrating Radar." IEEE Computer Society, Piscataway, NJ, 10.1109/ICGPR.2010.5550183.
- Duan, H.-F., Lee, P. J., Ghidaoui, M. S., and Tung, Y.-K. (2011). "Leak detection in complex series pipelines by using the system frequency response method." *J. Hydraulic Res.*, 49(2), 213-221, 10.1080/00221686.2011.553486.
- Duan, H.-F., Lee, P. J., Ghidaoui, M. S., and Tung, Y.-K. (2012). "Extended blockage detection in pipelines by using the system frequency response analysis." *J. Water Resour. Plan. Manage.*, 138(1), 55-62, 10.1061/(asce)wr.1943-5452.0000145.
- Duan, H.-F., Lee, P. J., Kashima, A., Lu, J., Ghidaoui, M. S., and Tung, Y.-K. (2013). "Extended blockage detection in pipes using the system frequency response: analytical analysis and experimental verification." *J. Hydraulic Eng.*, 139(7), 763-771, 10.1061/(asce)hy.1943-7900.0000736.
- Duan, H.-F. (2016a). "Transient frequency response based leak detection in water supply pipeline systems with branched and looped junctions." *J. Hydroinform.*, 19(1), 17, 10.2166/hydro.2016.008.
- Duan, H. F. (2016b). "Sensitivity analysis of a transient-based frequency domain method for extended blockage detection in water pipeline systems." *J. Water Resour. Plan. Manage.*, 142(4), 10.1061/(ASCE)WR.1943-5452.0000625.
- Duran, O., Althoefer, K., and Seneviratne, L. D. (2003). "Pipe inspection using a laser-based transducer and automated analysis techniques."

- 
- IEEE/ASME Transactions on Mechatronics*, 8(3), 401-9, 10.1109/TMECH.2003.816809.
- Ferrante, M., and Brunone, B. (2003). "Pipe system diagnosis and leak detection by unsteady-state tests. 1. Harmonic analysis." *Adv. Water Resour.*, 26(1), 95-105, 10.1016/S0309-1708(02)00101-X.
- Ferrante, M., Massari, C., Todini, E., Brunone, B., and Meniconi, S. (2012). "Experimental investigation of leak hydraulics." *J. Hydroinform.*, 15(3), 666-675, 10.2166/hydro.2012.034.
- Fuchs, H. V., and Riehle, R. (1991). "Ten years of experience with leak detection by acoustic signal analysis." *Appl. Acoust.*, 33(1), 1-19, 10.1016/0003-682X(91)90062-J.
- Gaewski, P. E., and Blaha, F. J. (2007). "Analysis of total cost of large diameter pipe failures." Water Research Foundation, Denver, CO.
- Ghazali, M. F., Beck, S. B. M., Shucksmith, J. D., Boxall, J. B., and Staszewski, W. J. (2012). "Comparative study of instantaneous frequency based methods for leak detection in pipeline networks." *Mech. Syst. Signal Pr.*, 29, 187-200, 10.1016/j.ymsp.2011.10.011.
- Gong, J., Lambert, M. F., Simpson, A. R., and Zecchin, A. C. (2012a). "Distributed deterioration detection in single pipelines using transient measurements from pressure transducer pairs." *Proceedings of the 11th International Conference on Pressure Surges*, BHR Group, Cranfield, UK, 127-140.
- Gong, J., Zecchin, A. C., Lambert, M. F., and Simpson, A. R. (2012b). "Signal separation for transient wave reflections in single pipelines using inverse filters." *Proceedings of the World Environmental & Water*

- Resources Congress 2012*, ASCE, Reston, VA, 3275-3284, 10.1061/9780784412312.329.
- Gong, J., Lambert, M. F., Simpson, A. R., and Zecchin, A. C. (2013a). "Single-event leak detection in pipeline using first three resonant responses." *J. Hydraulic Eng.*, 139(6), 645-655, 10.1061/(ASCE)HY.1943-7900.0000720.
- Gong, J., Simpson, A. R., Lambert, M. F., and Zecchin, A. C. (2013b). "Determination of the linear frequency response of single pipelines using persistent transient excitation: a numerical investigation." *J. Hydraulic Res.*, 51(6), 728-734, 10.1080/00221686.2013.818582.
- Gong, J., Simpson, A. R., Lambert, M. F., Zecchin, A. C., Kim, Y.-I., and Tijsseling, A. S. (2013c). "Detection of distributed deterioration in single pipes using transient reflections." *J. Pipeline Syst. Eng. Prac.*, 4(1), 32-40, 10.1061/(ASCE)PS.1949-1204.0000111.
- Gong, J., Zecchin, A. C., Simpson, A. R., and Lambert, M. F. (2014a). "Frequency response diagram for pipeline leak detection: comparing the odd and the even harmonics." *J. Water Resour. Plan. Manage.*, 140(1), 65-74, 10.1061/(ASCE)WR.1943-5452.0000298.
- Gong, J., Lambert, M. F., Simpson, A. R., and Zecchin, A. C. (2014b). "Detection of localized deterioration distributed along single pipelines by reconstructive MOC analysis." *J. Hydraulic Eng.*, 140(2), 190-198, 10.1061/(ASCE)HY.1943-7900.0000806.
- Gong, J., Stephens, M. L., Arbon, N. S., Zecchin, A. C., Lambert, M. F., and Simpson, A. R. (2015). "On-site non-invasive condition assessment for cement mortar-lined metallic pipelines by time-domain fluid transient

- analysis." *Struct. Health Monit.*, 14(5), 426-438, 10.1177/1475921715591875.
- Gong, J., Zecchin, A. C., Lambert, M. F., and Simpson, A. R. (2016a). "Determination of the creep function of viscoelastic pipelines using system resonant frequencies with hydraulic transient analysis." *J. Hydraulic Eng.*, 142(9), 04016023, 10.1061/(ASCE)HY.1943-7900.0001149.
- Gong, J., Lambert, M. F., Zecchin, A. C., and Simpson, A. R. (2016b). "Experimental verification of pipeline frequency response extraction and leak detection using the inverse repeat signal." *J. Hydraulic Res.*, 54(2), 210-219, 10.1080/00221686.2015.1116115.
- Gong, J., Lambert, M. F., Zecchin, A. C., Simpson, A. R., Arbon, N. S., and Kim, Y.-I. (2016c). "Field study on non-invasive and non-destructive condition assessment for asbestos cement pipelines by time-domain fluid transient analysis." *Struct. Health Monit.*, 15(1), 113-124, 10.1177/1475921715624505.
- Gong, J., Lambert, M. F., Nguyen, S. T. N., Zecchin, A. C., and Simpson, A. R. (2018a). "Detecting thinner-walled pipe sections using a spark transient pressure wave generator." *J. Hydraulic Eng.*, 144(2), 06017027, 10.1061/(ASCE)HY.1943-7900.0001409.
- Gong, J., Png, G. M., Arkwright, J. W., Papageorgiou, A. W., Cook, P. R., Lambert, M. F., Simpson, A. R., and Zecchin, A. C. (2018b). "In-pipe fibre optic pressure sensor array for hydraulic transient measurement with application to leak detection." *Measurement*, 126, 309-317, 10.1016/j.measurement.2018.05.072.

- Gould, S. J. F., Davis, P., and Marlow, D. R. (2016). "Importance of installation practices for corrosion protection of ductile iron pipe." *Urban Water J.*, 13(2), 198-211, 10.1080/1573062X.2014.955858.
- Hachem, F. E., and Schleiss, A. J. (2012). "Effect of drop in pipe wall stiffness on water-hammer speed and attenuation." *J. Hydraulic Res.*, 50(2), 218-227, 10.1080/00221686.2012.656838.
- Jo, B. Y., Laven, K., and Jacob, B. (2010). "Advances in CCTV technology for in-service water mains." *Proceedings of the Pipelines 2010 Conference*, American Society of Civil Engineers, Reston, VA, 538-547, 10.1061/41138(386)52.
- Jönsson, L., and Larson, M. (1992). "Leak detection through hydraulic transient analysis." In *Pipeline Systems*, B. Coulbeck and E. P. Evans, eds., Kluwer Academic Publishers, Dordrecht, the Netherlands 273-286.
- Jung, B. S., and Karney, B. W. (2008). "Systematic exploration of pipeline network calibration using transients." *J. Hydraulic Res.*, 46(SUPPL. 1), 129-137, 10.1080/00221686.2008.9521947.
- Kapelan, Z., Savic, D. A., and Walters, G. A. (2004). "Incorporation of prior information on parameters in inverse transient analysis for leak detection and roughness calibration." *Urban Water J.*, 1(2), 129-143, 10.1080/15730620412331290029.
- Kapelan, Z. S., Savic, D. A., and Walters, G. A. (2003). "A hybrid inverse transient model for leakage detection and roughness calibration in pipe networks." *J. Hydraulic Res.*, 41(5), 481-492, 10.1080/00221680309499993.

- Karim, M. R., Abbaszadegan, M., and Lechevallier, M. (2003). "Potential for pathogen intrusion during pressure transients." *J. Am. Water Works Assn.*, 95(5), 134-146, 10.1002/j.1551-8833.2003.tb10368.x.
- Kashima, A., Lee, P. J., Ghidaoui, M. S., and Davidson, M. (2013). "Experimental verification of the kinetic differential pressure method for flow measurements." *J. Hydraulic Res.*, 51(6), 634-644, 10.1080/00221686.2013.818583.
- Kemp, J. A., Bilbao, S., McMaster, J., and Smith, R. A. (2013). "Wave separation in the trumpet under playing conditions and comparison with time domain finite difference simulation." *J. Acoust. Soc. Am.*, 134(2), 1395-1406, 10.1121/1.4812254.
- Kim, S. (2014). "Inverse transient analysis for a branched pipeline system with leakage and blockage using impedance method." *Procedia Eng.*, 89, 1350-1357, 10.1016/j.proeng.2014.11.456.
- Kim, S. H. (2005). "Extensive development of leak detection algorithm by impulse response method." *J. Hydraulic Eng.*, 131(3), 201-208, 10.1061/(ASCE)0733-9429(2005)131:3(201).
- Lee, P. J., Vítkovský, J. P., Lambert, M. F., Simpson, A. R., and Liggett, J. A. (2005a). "Frequency domain analysis for detecting pipeline leaks." *J. Hydraulic Eng.*, 131(7), 596-604, 10.1061/(ASCE)0733-9429(2005)131:7(596).
- Lee, P. J., Vítkovský, J. P., Lambert, M. F., Simpson, A. R., and Liggett, J. A. (2005b). "Leak location using the pattern of the frequency response diagram in pipelines: a numerical study." *J. Sound Vib.*, 284(3-5), 1051-1073, 10.1016/j.jsv.2004.07.023.

- Lee, P. J., Lambert, M. F., Simpson, A. R., Vítkovský, J. P., and Liggett, J. A. (2006). "Experimental verification of the frequency response method for pipeline leak detection." *J. Hydraulic Res.*, 44(5), 693–707, 10.1080/00221686.2006.9521718.
- Lee, P. J., Lambert, M. F., Simpson, A. R., Vítkovský, J. P., and Misiunas, D. (2007a). "Leak location in single pipelines using transient reflections." *Aust. J. Water Resour.*, 11(1), 53-65, 10.1080/13241583.2007.11465311.
- Lee, P. J., Vítkovský, J. P., Lambert, M. F., Simpson, A. R., and Liggett, J. A. (2007b). "Leak location in pipelines using the impulse response function." *J. Hydraulic Res.*, 45(5), 643-652, 10.1080/00221686.2007.9521800.
- Lee, P. J., and Vitkovsky, J. P. (2010). "Quantifying linearization error when modeling fluid pipeline transients using the frequency response method." *J. Hydraulic Eng.*, 136(10), 831-836, 10.1061/(asce)hy.1943-7900.0000246.
- Lee, P. J., Duan, H. F., Ghidaoui, M., and Karney, B. (2013). "Frequency domain analysis of pipe fluid transient behaviour." *J. Hydraulic Res.*, 51(6), 609-622, 10.1080/00221686.2013.814597.
- Li, R., Huang, H., Xin, K., and Tao, T. (2015). "A review of methods for burst/leakage detection and location in water distribution systems." *Water Sci. Technol.*, 15(3), 429-441, 10.2166/ws.2014.131.
- Liggett, J. A., and Chen, L.-C. (1994). "Inverse transient analysis in pipe networks." *J. Hydraulic Eng.*, 120(8), 934-955, 10.1061/(ASCE)0733-9429(1994)120:8(934).



- Liou, C. P. (1998). "Pipeline leak detection by impulse response extraction." *J. Fluids Eng.*, 120(4), 833-838, 10.1115/1.2820746.
- Liu, Z., and Kleiner, Y. (2012). "State-of-the-art review of technologies for pipe structural health monitoring." *IEEE Sensors J.*, 12(6), 1987-1992, 10.1109/jsen.2011.2181161.
- Liu, Z., and Kleiner, Y. (2013). "State of the art review of inspection technologies for condition assessment of water pipes." *Measurement*, 46(1), 1-15, 10.1016/j.measurement.2012.05.032.
- Lowe, M. J. S., Alleyne, D. N., and Cawley, P. (1998). "Defect detection in pipes using guided waves." *Ultrasonics*, 36(1-5), 147-154, 10.1016/s0041-624x(97)00038-3.
- Massari, C., Yeh, T. C. J., Ferrante, M., Brunone, B., and Meniconi, S. (2014). "Detection and sizing of extended partial blockages in pipelines by means of a stochastic successive linear estimator." *J. Hydroinform.*, 16(2), 248-258, 10.2166/hydro.2013.172.
- Meniconi, S., Brunone, B., Ferrante, M., and Massari, C. (2011a). "Transient tests for locating and sizing illegal branches in pipe systems." *J. Hydroinform.*, 13(3), 334-345, 10.2166/hydro.2011.012.
- Meniconi, S., Brunone, B., and Ferrante, M. (2011b). "In-line pipe device checking by short-period analysis of transient tests." *J. Hydraulic Eng.*, 137(7), 713-722, 10.1061/(asce)hy.1943-7900.0000309.
- Meniconi, S., Duan, H. F., Lee, P. J., Brunone, B., Ghidaoui, M. S., and Ferrante, M. (2013). "Experimental investigation of coupled frequency and time-domain transient test-based techniques for partial blockage detection in

- pipelines." *J. Hydraulic Eng.*, 139(10), 1033-1044, 10.1061/(ASCE)HY.1943-7900.0000768.
- Meniconi, S., Brunone, B., Ferrante, M., Capponi, C., Carrettini, C. A., Chiesa, C., Segalini, D., and Lanfranchi, E. A. (2015). "Anomaly pre-localization in distribution–transmission mains by pump trip: preliminary field tests in the Milan pipe system." *J. Hydroinform.*, 17(3), 377-389, 10.2166/hydro.2014.038.
- Mora-Rodríguez, J., Delgado-Galván, X., Ramos, H. M., and López-Jiménez, P. A. (2014). "An overview of leaks and intrusion for different pipe materials and failures." *Urban Water J.*, 11(1), 1-10, 10.1080/1573062X.2012.739630.
- Mpesha, W., Gassman, S. L., and Chaudhry, M. H. (2001). "Leak detection in pipes by frequency response method." *J. Hydraulic Eng.*, 127(2), 134-147, 10.1061/(ASCE)0733-9429(2001)127:2(134).
- Mpesha, W., Chaudhry, M. H., and Gassman, S. L. (2002). "Leak detection in pipes by frequency response method using a step excitation." *J. Hydraulic Res.*, 40(1), 55-62, 10.1080/00221680209499873.
- Muggleton, J. M., and Brennan, M. J. (2004). "Leak noise propagation and attenuation in submerged plastic water pipes." *J. Sound Vib.*, 278(3), 527-537, 10.1016/j.jsv.2003.10.052.
- Muggleton, J. M., Brennan, M. J., Pinnington, R. J., and Gao, Y. (2006). "A novel sensor for measuring the acoustic pressure in buried plastic water pipes." *J. Sound Vib.*, 295(3-5), 1085-98, 10.1016/j.jsv.2006.01.032.
- Munjaj, M. L., and Doige, A. G. (1990). "Theory of a two source-location method for direct experimental evaluation of the four-pole parameters

- of an aeroacoustic element." *J. Sound Vib.*, 141(2), 323-333, 10.1016/0022-460X(90)90843-O.
- Mutikanga, H. E., Sharma, S., and Vairavamoorthy, K. (2009). "Water loss management in developing countries: Challenges and prospects." *J. Am. Water Works Assn.*, 101(12), 57-68, 10.1002/j.1551-8833.2009.tb10010.x.
- Nguyen, S. T. N., Gong, J., Lambert, M. F., Zecchin, A. C., and Simpson, A. R. (2018). "Least squares deconvolution for leak detection with a pseudo random binary sequence excitation." *Mech. Syst. Signal Pr.*, 99, 846-858, 10.1016/j.ymsp.2017.07.003.
- Nixon, W., and Ghidaoui, M. S. (2006). "Range of validity of the transient damping leakage detection method." *J. Hydraulic Eng.*, 132(9), 944-957, 10.1061/(ASCE)0733-9429(2006)132:9(944).
- Oppenheim, A. V., Willsky, A. S., and Nawab, S. H. (1997). *Signals and Systems*, 2nd Ed., Prentice Hall, Upper Saddle River, N.J.
- Pudar, R. S., and Liggett, J. A. (1992). "Leaks in pipe networks." *J. Hydraulic Eng.*, 118(7), 1031-1046, 10.1061/(ASCE)0733-9429(1992)118:7(1031).
- Puust, R., Kapelan, Z., Savic, D. A., and Koppel, T. (2010). "A review of methods for leakage management in pipe networks." *Urban Water J.*, 7(1), 25 - 45, 10.1080/15730621003610878.
- Rakitin, B., and Xu, M. (2015). "Centrifuge testing to simulate buried reinforced concrete pipe joints subjected to traffic loading." *Canadian Geotechnical Journal*, 52(11), 1762-1774, 10.1139/cgj-2014-0483.

- Rezaei, H., Ryan, B., and Stoianov, I. (2015). "Pipe failure analysis and impact of dynamic hydraulic conditions in water supply networks." *Procedia Eng.*, 119, 253-262, 10.1016/j.proeng.2015.08.883.
- Salissou, Y., and Panneton, R. (2010). "Wideband characterization of the complex wave number and characteristic impedance of sound absorbers." *J. Acoust. Soc. Am.*, 128(5), 2868-2876, 10.1121/1.3488307.
- Sattar, A. M., Chaudhry, M. H., and Kassem, A. A. (2008). "Partial blockage detection in pipelines by frequency response method." *J. Hydraulic Eng.*, 134(1), 76-89, 10.1061/(ASCE)0733-9429(2008)134:1(76).
- Sattar, A. M., and Chaudhry, M. H. (2008). "Leak detection in pipelines by frequency response method." *J. Hydraulic Res.*, 46(sup 1), 138-151, 10.1080/00221686.2008.9521948.
- Shamloo, H., and Haghghi, A. (2009). "Leak detection in pipelines by inverse backward transient analysis." *J. Hydraulic Res.*, 47(3), 311-318, 10.1080/00221686.2009.9522002.
- Shamloo, H., and Haghghi, A. (2010). "Optimum leak detection and calibration of pipe networks by inverse transient analysis." *J. Hydraulic Res.*, 48(3), 371-376, 10.1080/00221681003726304.
- Sharp, D. B. (1996). "Acoustic pulse reflectometry for the measurement of musical wind instruments." PhD Dissertation, University of Edinburgh, Edinburgh, UK.
- Shi, H., Gong, J., Arkwright, J. W., Papageorgiou, A. W., Lambert, M. F., Simpson, A. R., and Zecchin, A. C. (2015). "Transient pressure measurement in pipelines using optical fibre sensor." *Proceedings of the*

*40th Australian Conference on Optical Fibre Technology*, Engineers Australia, Barton, ACT, Australia.

Shi, H., Gong, J., Zecchin, A. C., Lambert, M. F., and Simpson, A. R. (2017). "Hydraulic transient wave separation algorithm using a dual-sensor with applications to pipeline condition assessment." *J. Hydroinform.*, 19(5), 752-765, 10.2166/hydro.2017.146.

Shucksmith, J. D., Boxall, J. B., Staszewski, W. J., Seth, A., and Beck, S. B. M. (2012). "Onsite leak location in a pipe network by cepstrum analysis of pressure transients." *J. Am. Water Works Assn.*, 104(8), E457-E465, 10.5942/jawwa.2012.104.0108.

Soares, A. K., Covas, D. I. C., and Reis, L. F. R. (2010). "Leak detection by inverse transient analysis in an experimental PVC pipe system." *J. Hydroinform.*, 13(2), 153, 10.2166/hydro.2010.012.

Stephens, M. L., Simpson, A. R., and Lambert, M. F. (2008). "Internal wall condition assessment for water pipelines using inverse transient analysis." *Proceedings of the 10th Annual Symposium on Water Distribution Systems Analysis*, ASCE, Reston, VA, 10.1061/41024(340)80.

Stephens, M. L., Lambert, M. F., and Simpson, A. R. (2013). "Determining the internal wall condition of a water pipeline in the field using an inverse transient model." *J. Hydraulic Eng.*, 139(3), 310–324, 10.1061/(ASCE)HY.1943-7900.0000665.

Świetlik, J., Raczyk-Stanisławiak, U., Piszora, P., and Nawrocki, J. (2012). "Corrosion in drinking water pipes: The importance of green rusts." *Water Research*, 46(1), 1-10, 10.1016/j.watres.2011.10.006.

- Tucker, M. S. (2010). "Performance of ductile-iron pipe in earthquake/seismic zones." *J. Am. Water Works Assn.*, 102(5), 98-103, 10.1002/j.1551-8833.2010.tb10112.x.
- Tur, J. M. M., and Garthwaite, W. (2010). "Robotic devices for water main in-pipe inspection: A survey." *Journal of Field Robotics*, 27(4), 491-508, 10.1002/rob.20347.
- Vardy, A. E., Brown, J. M. B., He, S., Ariyaratne, C., and Gorji, S. (2015). "Applicability of Frozen-Viscosity Models of Unsteady Wall Shear Stress." *J. Hydraulic Eng.*, 141(1), 04014064, 10.1061/(ASCE)HY.1943-7900.0000930.
- Vítkovský, J. P., Simpson, A. R., and Lambert, M. F. (2000). "Leak detection and calibration using transients and genetic algorithms." *J. Water Resour. Plan. Manage.*, 126(4), 262-265, 10.1061/(ASCE)0733-9496(2000)126:4(262).
- Vítkovský, J. P., Lee, P. J., Stephens, M. L., Lambert, M. F., Simpson, A. R., and Liggett, J. A. (2003). "Leak and blockage detection in pipelines via an impulse response method." *Pumps, Electromechanical Devices and Systems Applied to Urban Water Management: Proceedings of the International Conference*, A. A. Balkema Publishers, Lisse, The Netherlands, 423–430.
- Vítkovský, J. P., Lambert, M. F., Simpson, A. R., and Liggett, J. A. (2007). "Experimental observation and analysis of inverse transients for pipeline leak detection." *J. Water Resour. Plan. Manage.*, 133(6), 519-530, 10.1061/(ASCE)0733-9496(2007)133:6(519).

- Wang, X. J., Lambert, M. F., Simpson, A. R., Liggett, J. A., and Vítkovský, J. P. (2002). "Leak detection in pipelines using the damping of fluid transients." *J. Hydraulic Eng.*, 128(7), 697-711, 10.1061/(ASCE)0733-9429(2002)128:7(697).
- Washio, S., Takahashi, S., and Yamaguchi, S. (1996a). "Measurement of transiently changing flow rates in oil hydraulic column separation." *JSME International Journal, Series B: Fluids and Thermal Engineering*, 39(1), 51-56, 10.1299/jsmeb.39.51.
- Washio, S., Takahashi, S., Yu, Y., and Yamaguchi, S. (1996b). "Study of unsteady orifice flow characteristics in hydraulic oil lines." *J. Fluids Eng.*, 118(4), 743-748, 10.1115/1.2835504.
- Water Corporation WA. (2014). "Water Corporation: Management of Water Pipes." Perth, Australia.
- Wylie, E. B. (1983). "The microcomputer and pipeline transients." *J. Hydraulic Eng.*, 109(12), 1723-1739, 10.1061/(ASCE)0733-9429(1983)109:12(1723).
- Wylie, E. B., and Streeter, V. L. (1993). *Fluid Transients in Systems*, Prentice Hall Inc., Englewood Cliffs, New Jersey, USA.
- Yamamoto, K., Müller, A., Ashida, T., Yonezawa, K., Avellan, F., and Tsujimoto, Y. (2015). "Experimental method for the evaluation of the dynamic transfer matrix using pressure transducers." *J. Hydraulic Res.*, 53(4), 466-477, 10.1080/00221686.2015.1050076.
- Zecchin, A., Lambert, M., Simpson, A., and White, L. (2014a). "Parameter identification in pipeline networks: transient-based expectation-maximization approach for systems containing unknown boundary

- conditions." *J. Hydraulic Eng.*, 140(6), 04014020, 10.1061/(ASCE)HY.1943-7900.0000849.
- Zecchin, A. C., Simpson, A. R., Lambert, M. F., White, L. B., and Vítkovský, J. P. (2009). "Transient modeling of arbitrary pipe networks by a laplace-domain admittance matrix." *J. Eng. Mech.*, 135(6), 538-547, 10.1061/(ASCE)0733-9399(2009)135:6(538).
- Zecchin, A. C. (2010). "Laplace-domain analysis of fluid line networks with application to time-domain simulation and system parameter identification." PhD Dissertation, The University of Adelaide, Adelaide, SA, Australia.
- Zecchin, A. C., White, L. B., Lambert, M. F., and Simpson, A. R. (2013). "Parameter identification of fluid line networks by frequency-domain maximum likelihood estimation." *Mech. Syst. Signal Pr.*, 37(1-2), 370-387, 10.1016/j.ymsp.2013.01.003.
- Zecchin, A. C., Gong, J., Simpson, A. R., and Lambert, M. F. (2014b). "Condition assessment in hydraulically noisy pipeline systems using a pressure wave splitting method." *Procedia Eng.*, 89, 1336-1342, 10.1016/j.proeng.2014.11.452.
- Zeng, W., Gong, J., Lambert, M., Simpson, A., Cazzolato, B., and Zecchin, A. (2018a). "Detection of extended blockages in pressurised pipelines using hydraulic transients with a layer-peeling method." *Proceedings of the 29th IAHR Symposium on Hydraulic Machinery and Systems*, International Association for Hydro-Environment Engineering and Research (IAHR), Madrid, Spain.



- Zeng, W., Gong, J., Zecchin, A. C., Lambert, M. F., Simpson, A. R., and Cazzolato, B. S. (2018b). "Condition assessment of water pipelines using a modified layer peeling method." *J. Hydraulic Eng.*, 144(12), 04018076, 10.1061/(ASCE)HY.1943-7900.0001547.
- Zhang, C., Zecchin, A. C., Lambert, M. F., Gong, J., and Simpson, A. R. (2018a). "Multi-stage parameter-constraining inverse transient analysis for pipeline condition assessment." *J. Hydroinform.*, 20(2), 10.2166/hydro.2018.154.
- Zhang, C., Gong, J., Zecchin, A. C., Lambert, M. F., and Simpson, A. R. (2018b). "Faster inverse transient analysis with a head based method of characteristics and a flexible computational grid for pipeline condition assessment." *J. Hydraulic Eng.*, 144(4), 04018007, 10.1061/(ASCE)HY.1943-7900.0001438.
- Zhang, C., Gong, J., Simpson, A., Zecchin, A., and Lambert, M. (2019). "Impedance estimation along pipelines by generalized reconstructive Method of Characteristics for pipeline condition assessment." *J. Hydraulic Eng.*, 145(4), 04019010, 10.1061/(ASCE)HY.1943-7900.0001580.